PERFORMANCE PREDICTION OF AXIALLY LOADED PILES AND PILE GROUPS BY LOAD TRANSFER METHOD

Mr. Qui Van Lai

A Dissertation Submitted in Partial Fulfillment of the Requirements
for the Degree of Doctor of Philosophy Program in Civil Engineering
Department of Civil Engineering
Faculty of Engineering
Chulalongkorn University
Academic Year 2016

การทำนายพฤติกรรมของเสาเข็มและเสาเข็มกลุ่มภายใต้แรงกระทำตามแกนด้วยการคำนวณจากสมการส่งถ่ายแรง

นายชิว วัน ลาย

วิทยานิพนธ์นี้เป็นส่วนหนึ่งของการศึกษาตามหลักสูตรปริญญาวิศวกรรมศาสตรดุษฎีบัณฑิต
สาขาวิชาวิศวกรรมโยธา ภาควิชาวิศวกรรมโยธา
คณะวิศวกรรมศาสตร์ จุฬาลงกรณ์มหาวิทยาลัย
ปีการศึกษา 2559

Thesis Title	PERFORMANCE PREDICTION OF AXIALLY LOADED PILES AND PILE GROUPS BY LOAD TRANSFER METHOD
By	Mr. Qui Van Lai
Field of Study	Civil Engineering
Thesis Advisor	Associate Professor Tirawat Boonyatee, D.Eng.

Accepted by the Faculty of Engineering, Chulalongkorn University in Partial Fulfillment of the Requirements for the Doctoral Degree

.....Dean of the Faculty of Engineering
(Associate Professor Supot Teachavorasinskun, D.Eng.)

THESIS COMMITTEE

.....Chairman
(Associate Professor Supot Teachavorasinskun, D.Eng.)
.....Thesis Advisor
(Associate Professor Tirawat Boonyatee, D.Eng.)
.....Examiner
(Assistant Professor Tanate Srisirirojanakorn, Ph.D.)
.....Examiner
(Associate Professor Boonchai Ukritchon, Sc.D)
.....Examiner
(Professor Suched Likitlersuang, D.Phil)
.....External Examiner
(Dr. Boonlert Siribumrungwong, D.Eng.)

ชิว วัน ลาย : การทำนายพฤติกรรมของเสาเข็มและเสาเข็มกลุ่มภายใต้แรงกระทำตามแกนด้วยการคำนวณจากสมการส่งถ่ายแรง (PERFORMANCE PREDICTION OF AXIALLY LOADED PILES AND PILE GROUPS BY LOAD TRANSFER METHOD) อ.ที่ปรึกษาวิทยานิพนธ์หลัก: รศ. ดร. ฐิรวัตร บุญญะฐี, 102 หน้า.

การเจริญเติบโตทางเศรษฐกิจและสังคมทำให้เกิดการขยายตัวของเมืองอย่างรวดเร็วและเกิดการก่อสร้างอาคารสูงเพิ่มขึ้น ในขณะที่เทคโนโลยีการก่อสร้างอาคารสูงด้านต่างๆ มีการพัฒนามากขึ้นนั้น การออกแบบฐานรากอาคารให้ได้ประหยัดและปลอดภัยก็ทวีความสำคัญมากขึ้น โดยเฉพาะการประมาณอัตราการทรุดตัวของเสาเข็มซึ่งเป็นระบบฐานรากที่นิยมใช้กันมากที่สุด วิธีส่งถ่ายแรงเป็นวิธีการหนึ่งที่สามารถใช้ในการประมาณอัตราการทรุดตัวของเสาเข็มได้ ซึ่งถึงแม้ว่าจะให้ผลการคำนวณได้ไม่ละเอียดเท่ากับวิธีการอื่นๆ เช่น ระเบียบวิธีไฟไนต์อิลิเมนต์ หรือ ระเบียบวิธีบาวน์ดะรีเอลิเมนต์ แต่ก็สามารถคำนวณได้ง่ายและรวดเร็วกว่ามาก จึงน่าจะเหมาะสำหรับการออกแบบเบื้องต้นหรือการออกแบบอาคารทั่วไปที่มีเงื่อนไขไม่ซับซ้อน

วิธีการส่งถ่ายแรงที่ถูกพัฒนาขึ้นในช่วงแรกๆ จะประมาณค่าการทรุดตัวจากความสัมพันธ์ระหว่างแรงและการเคลื่อนที่สัมพันธ์ที่ผิวด้านข้างและปลายเสาเข็ม ซึ่งนิยมเรียกว่ากราฟ *t-z* อย่างไรก็ตาม ความสัมพันธ์ดังกล่าวสร้างขึ้นจากผลการทดสอบกำลังรับน้ำหนักของเสาเข็มโดยไม่ได้คำนึงถึงรูปแบบการทรุดตัวของชั้นดินที่อยู่โดยรอบ ดังนั้นจะไม่สามารถคำนวณหาปฏิสัมพันธ์กับเสาเข็มอื่นๆ ที่อยู่โดยรอบได้

ในการศึกษานี้ ผู้วิจัยได้เสนอวิธีการคำนวณแบบไม่เชิงเส้นชนิดใหม่ซึ่งพัฒนาตามแนวทางของวิธีส่งถ่ายแรงเพื่อใช้ในการประมาณการทรุดตัวของเสาเข็มเดี่ยวและเสาเข็มกลุ่ม และได้สอบเทียบกับผลการทดสอบกำลังรับน้ำหนักของเสาเข็มจริงและเสาเข็มจำลอง ในการคำนวณได้กำหนดให้การทรุดของดินประกอบด้วยส่วนที่เป็นอิลาสติกและส่วนที่ไม่เป็นอิลาสติกซึ่งเกิดขึ้นในลักษณะของการเลื่อนไถลบริเวณผิวด้านข้างของเสาเข็ม สำหรับการทรุดตัวแบบอิลาสติกนั้นได้คำนวณตามวิธีของแรนดอล์ฟและโรทธ์ (1978 & 1979) สำหรับเสาเข็มกลุ่มนั้นได้คำนวณตามแนวคิดเรื่องตัวประกอบปฏิสัมพันธ์ของโพโลส (1968) โดยคำนึงถึงการทรุดตัวที่ลดลงเนื่องจากอิทธพลของเสาเข็มที่อยู่รอบข้างด้วย จากการเปรียบเทียบกับข้อมูลตรวจวัดพบว่าวิธีการที่เสนอขึ้นใหม่นี้ให้ค่าที่สอดคล้องกันดีและสามารถใช้ได้กับแป้นเสาเข็มที่มีสภาพแข็งเกร็งและแบบหยืดหยุ่นได้ นอกจากวิธีการคำนวณในรูปทั่วไปแล้ว ผู้วิจัยยังได้จัดทำวิธีการคำนวณอย่างง่ายซึ่งสะดวกต่อการคำนวณภายใต้เงื่อนไขเฉพาะซึ่งอาจพบได้บ่อยในงานออกแบบทั่วไป

ภาควิชา วิศวกรรมโยธา ลายมือชื่อนิสิต .....

สาขาวิชา วิศวกรรมโยธา ลายมือชื่อ อ.ที่ปรึกษาหลัก .....

ปีการศึกษา 2559

5771449921 : MAJOR CIVIL ENGINEERING
KEYWORDS:

QUI VAN LAI: PERFORMANCE PREDICTION OF AXIALLY LOADED PILES AND PILE GROUPS BY LOAD TRANSFER METHOD. ADVISOR: ASSOC. PROF. DR. TIRAWAT BOONYATEE, D.Eng., 102 pp.

Nowadays, economic and population growth around the world increase the speed of urbanization, making skyscrapers become popular. Together with the development of high-rise buildings, the requirements of capacity and settlement of foundations become complex and demanding. In particular, the accurate estimation of pile settlements becomes essential in pile design. The load transfer method (Seed and Reese, 1957) is practical for routine design because of its less computational effort. In the early days, the load transfer methods were based on relationships between the resistance and relative displacement at pile-soil boundaries which are usually referred to as t-z curves. Since these techniques did not consider the deformation of soil around piles, they cannot be applied to the settlement analysis of pile groups.

In this study, a new nonlinear approach for axially loaded piles and pile groups is proposed and validated with field tests and model tests. The proposed method divides the settlement of soil into elastic and inelastic (slippage) components. The inelastic deformation is assumed to occur in a narrow zone around piles while the deformation in the outer zone is determined by an elastic solution proposed by Randolph and Wroth (1978 & 1979). The extension from single pile analysis to pile group analysis is carried out based on the interaction factor concept (Poulos, 1968) together with the reconsideration of the pile-soil-pile interaction by taking the stiffening effect of nearby piles into account. Predictions by the proposed method are well agreed with the validation data, under both of rigid and flexible cap conditions. In addition to the general procedure, a simplify solution is also provided for typical conditions which usually encountered in routine designs.

Department:	Civil Engineering	Student's Signature	.....
Field of Study:	Civil Engineering	Advisor's Signature	.....
Academic Year:	2016		

ACKNOWLEDGEMENTS

First and foremost, I would like to give big thank to my supervisor Assoc. Prof. Dr Tirawat Boonyatee for his advice, support and, in particular, his patient. My research and my thesis would not be completed without him. Three year ago, I firstly came his office to say “I am the new student under your advice” and at that time, I was really the freshman in the research. With his patient, friendly teaching style, I have learned a great knowledge from him. Throughout the last three years, his door was always open to me. I am happy with this thing and I, sometime, think I am so lucky to be his student. With the further plan is to be the lecturer, his teaching style look the standard of my style.

I would like to thank my co-advisors Prof. Dr. Makoto Kimura for the big support to my research. Although he is the super busy person but he always to give me best care and best condition to do research when I was in Japan. Besides, I also appreciate Asst. Prof. Dr Yasuo Sawamura who give me the motivation in experiment works.

I appreciate to the kindly helping of my classmates in the Department of Civil Engineering, Chulalongkorn University, Thailand and Department of Civil and Earth Resources Engineering, Kyoto University, Japan. In particular, Mr. Nguyen Thanh Son, Mr. Lingdung Mase, Mr. Ryunosuke Kido, Mr. Yuma Daito are the unforgettable names in my mind.

I would like to thank the AUN/SEED-Net and Jica group. My research was supported by the scholarship of AUN/SEED-Net and Jica group. I wish to express my gratitude to the their financial support

Finally, I would like to thank my parent. They always the give me their encouragements and endless supports. Words do not express my gratitude to them. I am proud of them.

CONTENTS

Page

Page

Page

LIST OF TABLE

LIST OF FIGURE

LIST OF NOTATIONS

α_{kj} is the interaction factor determine from induced settlement of pile k due to the settlement of pile j

α_{skj} is α_{kj} at the pile shaft

α_{bkj} is α_{kj} at the pile base

$\alpha_{,i}$, $\beta_{,i}$ are the factors for determining the maximum unit shear stress at the shaft of segment i

a_b, b_b are the empirical parameters for the t-z curve at the base of a pile

a_b^h, b_b^h are the empirical parameters for the hyperbolic t-z curve at the base of a pile

$a_{,i}$, $b_{,i}$ are the empirical parameters for the t-z curve at the shaft of segment i

$a_{,i}^h$, $b_{,i}^h$ are the empirical parameters for the hyperbolic t-z curve at the shaft of segment i

$a'_{j,i}$, $b'_{j,i}$ are the empirical parameters for the t-z curve at the shaft of segment i of pile j considering effects from all piles in group

A_p is the section area of pile

$C_{,i}$ is the initial flexibility for the t-z curve at the shaft of segment i without considering effects from all piles in group

C'_j is the initial flexibility for the t-z curve at the shaft of pile j considering effects from all piles in group

$C'_{j,i}$ is the initial flexibility for the t-z curve at the shaft of segment i of pile j considering effects from all piles in group

D is the diameter of pile

$d_{w,i}$ is the depth from ground water level to the middle of soil layer i

E_p is the Young modulus of pile

E_s	is the Young modulus of soils
$E_{s,i}$	is the Young modulus of soil layer i
E_{sb}	is the Young modulus of soil below pile base
$\phi'_{,i}$	is the frictional angle of soil layer i
$\gamma_{s,i}$	is the unit weight of soil layer i
$G_{s,i}$	is the shear modulus of soil layer i
G_{sb}	is the shear modulus of the soil below pile base
GWL	is ground water level
$\varphi(r)$	is the attenuation function for ground settlement
L	is the length of pile
l	is the length of pile segment
$l_{,i}$	is the length of segment i
k_j	is the combined stiffness at the shaft of pile j
k_{jj}	is the original stiffness at the shaft of pile j
k_{jk}	is the contribution of the settlement at the shaft of pile k on pile j
k'_{jk}	is the stiffening effect due to pile k on pile j
n	is the number of segments in a pile
N_q^*	is the bearing capacity factor at pile base
n_p	is the number of piles in a group
ν_s	is the average of Poisson's ratio of soils over the length of pile
$\nu_{s,i}$	is the Poisson's ratio of soil layer i
ν_{sb}	is the Poisson's ratio of soil below pile base
$N_{SPT,i}$	is the uncorrected SPT value of soil layer i

$N'_{SPT,i}$ is the corrected SPT value of soil layer i

$P^b_{,i}$ is the resistance at the base of segment i

$P^b_{j,i}$ is the resistance at the base of segment i of pile j

P^{bf} is the maximum resistance at the base of a pile

$P^s_{,i}$ is the resistance at the shaft of segment i

$P^s_{j,i}$ is the resistance at the shaft of segment i of pile j

$P^t_{,i}$ is the resistance at the top of segment i

$P^t_{j,i}$ is the resistance at the top of segment i of pile j

Q is the load at the head of a pile

Q_g is the load at the head of a pile group

Q_j is the load at the head of pile j

Q_{ult} is the ultimate capacity of single pile

$Q_{ult,j}$ is the ultimate capacity of pile *j*

R is the reduction factor for the ultimate unit shear stress at pile shaft, $R \in$ [0.80-0.95]

R_b is the reduction factor for ultimate resistance at pile base, $R_b \in$ [0.80-0.95]

r_m is the radial distance from the pile center to a point at which the shear stress induced by the pile can be ignored.

r_{ms} is the r_m corrected for the stiffening effect

r_o is the radius of pile

r_{kj} Is the distance between pile k and j

$Su_{,i}$ is the undrained shear strength of soil layer i

σ_v	is the total overburden stress of soils
σ'_v	is the effective overburden stress of soils
σ_{vb}	is the total overburden stress of soil at the base of a pile
σ'_{vb}	is the effective overburden stress of soil at the base of a pile
$\sigma_{v,i}$	is the total overburden stress of soil at the middle of soil layer i
$\sigma'_{v,i}$	is the effective overburden stress of soil at the middle of soil layer i
τ	is the mobilized shear stress
$\tau^f_{,i}$	is the maximum unit shear stress at the shaft of segment i
$t_{,i}$	is the thickness of soil layer i
$u_{,i}$	is the water pressure at the middle of soil layer i
$U(r)$	is the settlement field at the radial distance r
$U_b(r)$	is the settlement field at the pile base level and radial distance r
$U(r,z)$	is the settlement field at the radial distance r and the depth z
$U_{kj,i}$	is the settlement field at the middle of soil layer i of pile k which induced pile settlement of pile j
$w^{sh}_{,i}$	is the settlement at the shaft of segment i
$w^{sh}_{j,i}$	is the settlement at the shaft of segment i of pile j
w^{sh}_{jk}	is the induced settlement at the shaft of pile j due to settlement at the shaft of pile k
w^{sh}_{jj}	is the settlement at the shaft of pile j in pile group induced by its own load
$w^b_{,i}$	is the settlement at the base of segment i
$w^b_{j,i}$	is the settlement at the base of segment i of pile j

w^{b}_{jk} is the induced settlement at the base of pile j due to settlement at the base of pile k

w^{b}_{jj} is the settlement at the base of pile j in pile group induced by its own load

$w^{t}_{,i}$ is the settlement at the top of segment i

$w^{t}_{j,i}$ is the settlement at the top of segment i of pile j

$w_{,z}$ is the settlement at depth z of a pile

$w_{j,z}$ is the settlement at depth z of pile j

$w_{,i}$ is the settlement at the middle of segment i

$w_{j,i}$ is the settlement at the middle of segment i of pile j

$w^{e}_{,i}$ is the elastic ground deformation at the middle of segment i

$w^{e}_{j,i}$ is the elastic ground deformation at the middle of segment i of pile j

$w^{e}_{j,z}$ is the elastic ground deformation at depth z of pile j

$w^{s}_{,i}$ is the slippage or the relative settlement at the middle of segment i

$w^{s}_{j,i}$ is the slippage or the relative settlement at the middle of segment i of pile j

$w^{s}_{j,z}$ is the slippage or the relative settlement at depth z of pile j

ζ_j is the stiffening factor of pile j

$Su_{,i}$ is the undrained shear strength of soil layer i

S is the settlement at the head of a pile

S_j is the settlement at the head of pile j considering effects from all piles in group

S_1^{ult} is S_1 at Q_{ult}

$\overline{S}$ is the settlement under unit load

s'_j is the settlement at the head of pile j considering stiffening effect from all piles in group

s'_{ju} is the settlement under unit load at the head of pile j considering stiffening effect from all piles in group

s_{kj} is the settlement at the head of pile k induced by the settlement of pile j

Δw_b is the step of the settlement at pile base for load-settlement algorithm

CHAPTER 1: INTRODUCTION

1.1 Background

Nowadays, the growth of economic and population around the world increase the speed of urbanization and make the skyscraper building become popular. Together with development of skyscraper building, the requirements about capacity and settlement for pile foundation of these building, become complex. Example, the allowable settlement is 10 mm followed by Eurocodes 7 standards or long-term serviced settlement is 15 mm followed the Canadian code. Thus, predicting load-settlement of pile foundation is very necessary. Until now, there have many approaches to predict load-settlement of pile foundation from simply to complex. In that, FEM and BEM are the best tool but they are complex and take computational effort. Analytical methods have been developed to reduce the disadvantage of FEM and BEM.

Although not as powerful as the finite element method or the boundary element method, the load transfer method firstly introduced by Seed and Reese (1957) requires less operation and is more practical for routine design. The early works were based on relationships between resistances at pile-soil boundaries which usually referred to as t-z curves determined from field static load test. Since these techniques did not consider the deformation of soil around piles, they cannot be applied to the settlement analysis of pile groups.

In the currently load-transfer approach, based on the closed-from solution of Randolph and Wroth (1978 & 1979), the t-z curves parameters and the soil profile can be determined more easily by elastic parameters of soil. By using soil profile, the concept of pile-soil-pile interaction (or in other words is interaction factor concept) firstly proposed Poulos (1968) was adopted in extension from the single analysis to pile group analysis. However, in current stage, there have two kind of assumption in load-transfer model.

Firstly, it is proposed that the response of pile was divided into elastic and inelastic (slippage) parts. The inelastic deformation was assumed to occur in a narrow zone around a pile, and the elastic part (or soil deformation in the outer zone) can also be

determined by closed-form solution of Randolph and Wroth (1978 & 1979). In extension form single pile analysis to pile group analysis, the induced settlement due to pile-soil-pile interaction was applied on elastic part. (Lee & Xiao, 2001; Wang et al, 2012).

Secondly, it is proposed that no slip occurred at pile soil interface and stiffening effect need to consider in using the pile-soil-pile interaction concept (Mylonakis & Gazetas, 1998; Zhang et al, 2015; Zhang et al, 2014)

It is seen that considering the slippage at pile soil interface is more realistic than no considering. Besides, considering stiffening effect is also necessary for making the calculation approach suitable with real behavior. It is vital to propose the developed load-transfer approach which can be accounted the slippage phenomenon and stiffening effect in pile-soil-pile interaction.

In addition, in the review process, it is seen that (1) The proposed approach of Wang et al. (2014) used the tangent stiffness for predicting nonlinear settlement of pile group (or in other word, explicit prediction). However, this kind of explicit prediction can be depended on the step-size calculation. (2) The meaning of stiffening effect mentioned in works of Mylonakis and Gazetas (1998) and Zhang et al. (2014) is difference. Mylonakis and Gazetas (1998) focused on response of passive pile to modify the interaction factor of Randolph and Wroth (1978) whereas Zhang et al. (2014) considered influence of other pile on the response of a pile. Thus, this two issue were also figured out in this thesis.

1.2 Objective

Based on the issues of the currently load-transfer method, this thesis has some objectives, as follows;

1. Propose a new nonlinear analytical method for single pile analysis by extension based on the works of Wang et al. (2012)
2. Investigate the stiffening effect in pile-soil-pile interaction by experiments

3. Propose a new linear analytical method for pile group considering stiffening effect by combining the works of Mylonakis and Gazetas (1998) and Zhang et al. (2014).
4. Proposed a new nonlinear analytical method for pile group by extensions based on the proposed linear analytical method for pile group

1.3 The scope of this research

In the limited time and money, this study is implemented in scopes, as follows;

1. Slippage can occur at pile-soil interface
2. Settlement of the pile can be computed by slippage deformation plus elastic
3. The pile-soil-pile interaction is only effected by far field settlement of the ground
4. Do not considering the installing effect.
5. Settlement prediction have not considered for long-term condition

1.4 Thesis outline

Following the proposed objectives, this thesis is divided including 6 chapters, as follows;

Chapter 1: Introduction

Chapter 2: Literate review

Chapter 3: Nonlinear analytical method for single pile

Chapter 4: Linear analytical method for pile group considering stiffening effect

Chapter 5: Nonlinear analytical method for pile group considering stiffening effect

Chapter 6: Conclusion and recommendations

In that, chapter 2 is implemented to obtain the back ground about the current load-transfer method. Besides, the chapter 3 is the solution for objective 1, chapter 4 is the solution for objective 2 and 3 and chapter 5 is the solution for the final objective.

1.5 Research benefit

In the progress of studying, the following papers have been published or are in press:

1. Lai-Van Qui and Tirawat Boonyatee (2015), Pile settlement prediction by load-transfer method: A case study in Bangkok, *The Twenty-Eighth KKHTCNN Symposium on Civil Engineering, November 16-18, 2015, Bangkok, Thailand*
2. Lai-Van Qui and Tirawat Boonyatee (2015), A revisit to the interaction factor of group piles considering stiffening effect, *The Twenty-Ninth KKHTCNN Symposium on Civil Engineering, December 3-5, 2016, Hong Kong, China*

CHAPTER 2: LITERATURE REVIEW

2.1 Introduction

Since a new proposed analytical method is the extension from currently load-transfer method by considering the combination of slippage at pile-soil interface and stiffening effect on pile-soil-pile interaction. Whereas, the currently load-transfer method was proposed by adopting the works from interaction factor method (Poulos, 1968), closed-form solution of Randolph and Wroth (1978 & 1979). Thus, for obtaining the current knowledge of load-transfer method, this chapter is sequentially reviewed the previous works, as follows;

1. Original load-transfer method (Seed & Reese, 1957)
2. Original interaction factor method (Poulos, 1968)
3. Original closed-form solution (Lee, 1993; Randolph & Wroth, 1979; Randolph & Wroth, 1978)
4. Modification of closed-form solution considering stiffening effect (Mylonakis and Gazetas, 1998)
5. Original modification of closed-form solution in term 1D FEM (Chow, 1986)
6. Modification of load-transfer methods considering slippage (Lee & Xiao, 2001; Wang et al, 2012)
7. Modification of load-transfer method considering stiffening effect (Zhang et al, 2014)

2.2 Review

2.2.1 Original load-transfer method

The load-transfer method was firstly proposed by **Seed and Reese (1957).** In this method, a pile was divided into segments which interact with surrounding soil layers by simplified load-displacement relationships (usually known as t-z curves) (Figure 2.1). In the early works, the parameter of t-z curves were determined from the field

static load test. (Armaleh & Desai, 1987; Coyle & Reese, 1966; HIRAYAMA, 1990; Kezdi, 1975; Reese et al, 1900; Vijayvergiya, 1977)

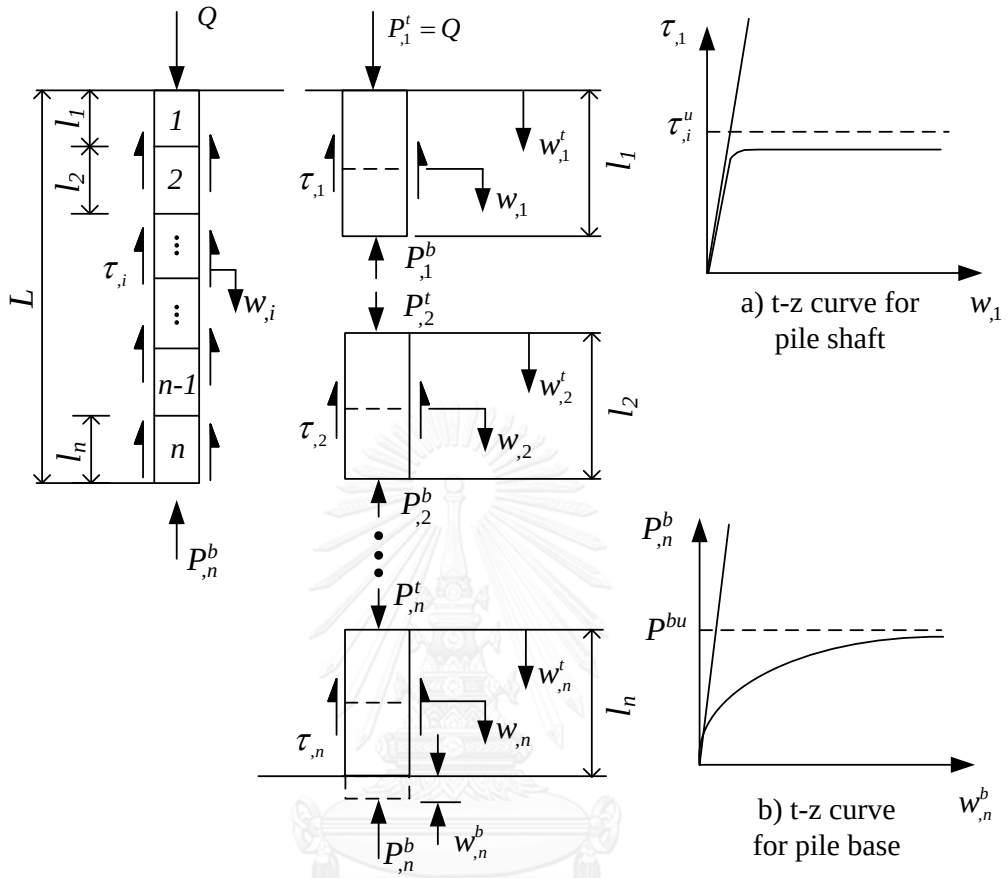

Figure 2.1 The concept of load-transfer approach (After Poulos, 1980)

To predict the settlement of pile, the standard iterative calculation procedure, in Figure 2.2, was used. At the beginning, a pile is divided into several segments. The settlement at pile base was assumed to be $w_{,n}^{b} = \Delta w^{b} = 0.001D$ for determining the mobilized resistance at pile base, $P_{,n}^{b}$, based on the t-z curve at pile base.

Starting from the bottommost segment i=n, and assuming the settlement at the middle of bottommost segment $w_{,i} = w_{,n}^{b}$. Based on the t-z curve at pile shaft, the mobilized resistance at pile shaft, $P_{,i}^{s}$, was determined. After that, the settlement at the middle of bottommost segment was recalculated, $w_{,i}^{re}$,by the summation of base settlement and compression of a lower half segment, as shown in Equation (2.1)

$$w_{,i}^{re} = w_{,i}^{b} + \frac{\left(P_{,i}^{t} + P_{,i}^{b}\right)/2 + P_{,i}^{b}}{2E_pA_p}\frac{l_i}{2} = w_{,i}^{b} + \frac{P_{,i}^{t} + 3P_{,i}^{b}}{8E_pA_p}l_i = w_{,i}^{b} + \frac{P_{,i}^{s} + 4P_{,i}^{b}}{8E_pA_p}l_i \qquad (2.1)$$

Compared to its assumed value, if the assumed and recalculated value of $w_{,i}$ did not equal, the routine calculation would be implemented by reassume $w_{,i}$, $w_{,i} = \left(w_{,i}^{re} + w_{,i}\right)/2$

After getting the satisfaction between assumed and recalculated value of $w_{,i}$, the mobilized resistance at pile shaft, $P_{,i}^{s}$, was corrected. The load and settlement at the top of bottom segment was calculate by

$$P_{,i}^{t} = P_{,i}^{s} + P_{,i}^{b}$$
$$w_{,i}^{t} = w_{,i}^{b} + \frac{P_{,i}^{t} + P_{,i}^{b}}{2E_pA_p}l_i \qquad (2.2)$$

Next, the load and settlement at the bottommost segment were transferred to the next segment followed continue of force and settlement between two segments.

$$w_{,i-1}^{b} = w_{,i}^{t}; \qquad P_{,i-1}^{b} = P_{,i}^{t} \qquad (2.3)$$

The same procedure was repeated from segment i=n-1 to segment i=1 until obtain the load-settlement at pile head.

After storing the recently predicted load-settlement at pile head, the value of $w_{,n}^{b}$, $w_{,n}^{b} = w_{,n}^{b} + \Delta w^{b}$ was increased. The whole procedure was repeated until the value of $w_{,n}^{b}$ larger than 10% of pile diameter.

Finally, plot the load-settlement curve from storing data

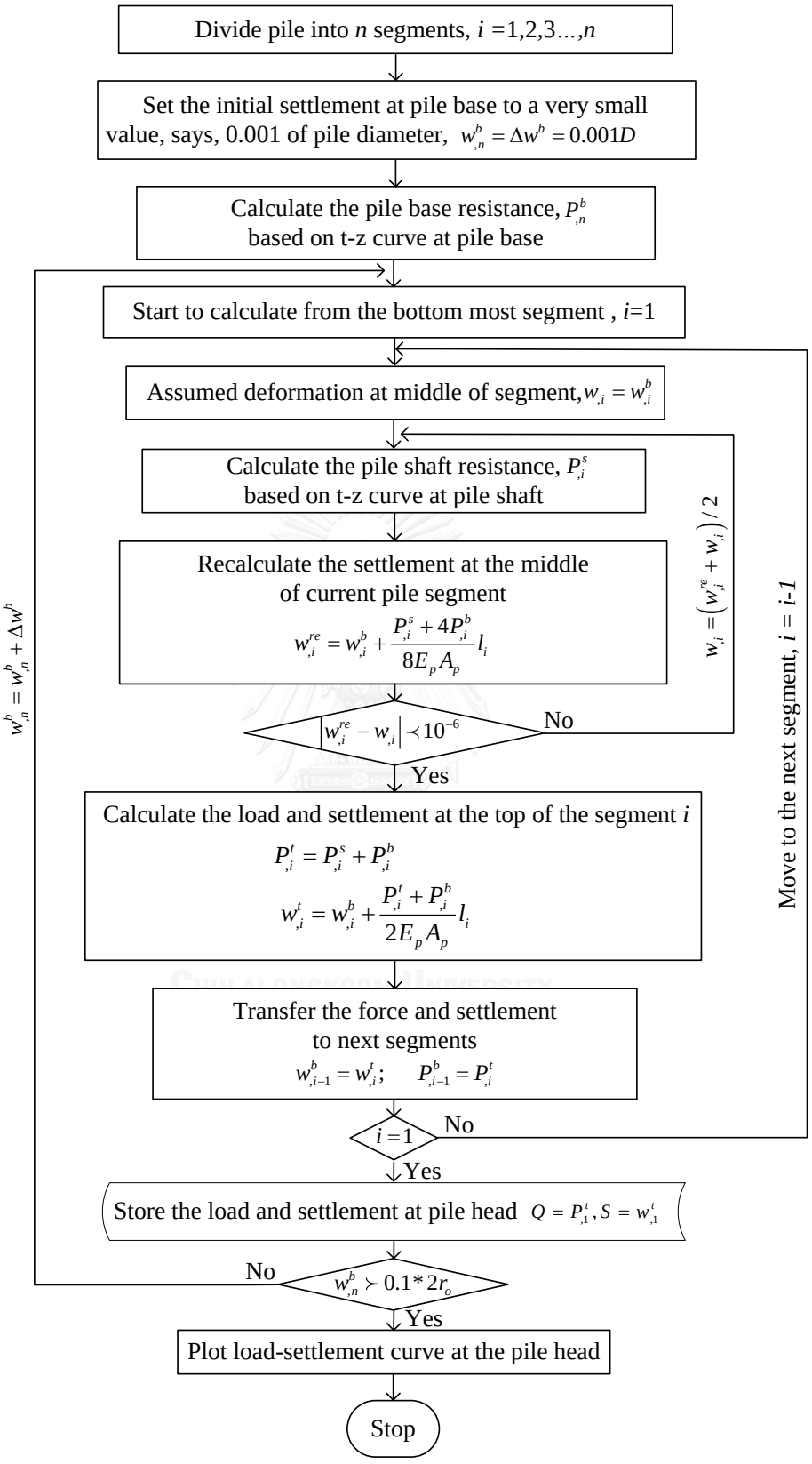

Figure 2.2 The standard algorithm of load-transfer method

2.2.2 Original interaction factor method

Poulos (1968) was firstly proposed interaction factor method. This approach is the simplifier practical approach based on the boundary element method (BEM). The interaction factor was simply described by the two-piles model in Figure 2.3. In this model with the same applied load *Q* on two piles, the settlement of pile #1 will be larger than its value in single pile having the same condition. The induced settlement was occurred by the pile-soil-pile interaction between piles. Based on the induced settlement and the settlement under own load of a pile #1, the interaction factor can be determined by Equation (2.4).

$$\alpha_{21} = {}^{s_{21}}\!/_{s_1} \qquad (2.4)$$

This factor depended on the stiffness ratio of pile and soil, the length of pile, the distance between two piles. For the practical purpose, the interaction factor was parametrically studied by BEM and prepared in graph as shown in Figure 2.4 (Poulos & Davis, 1980)

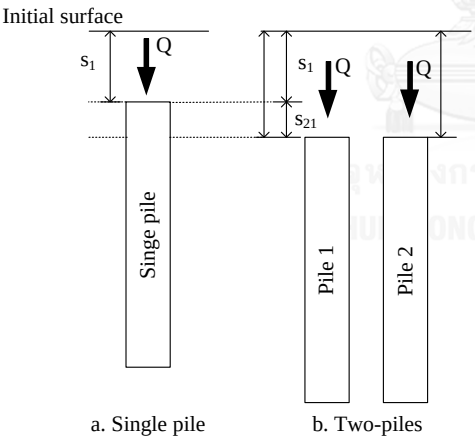

Figure 2.3 Model for determining interaction factor method (Poulos, 1968)

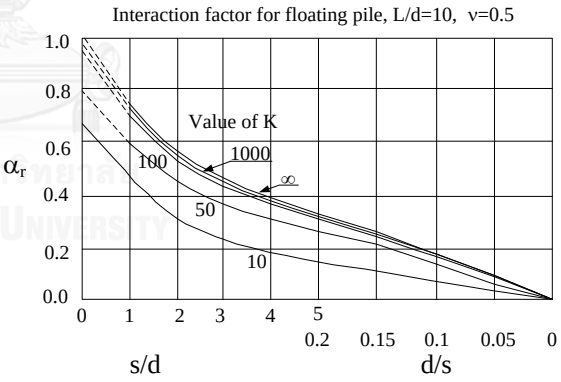

Figure 2.4 Interaction factor in case L/d=10 (After Poulos and David (1980))

In the elastic stage, by using the superposition rule, the settlement of each pile in group was calculated by summation of the settlements induced by its own load and the induced settlement due to settlement of other piles in group, as shown in Equation (2.5) . The adding settlement induced by another pile in group is presented by interaction factor

$$S_j = \bar{s}\left(P_j + \sum_{k=1,k\neq j}^{n_p} P_k \alpha_{jk} \right) \tag{2.5}$$

The settlement under unit load, $\bar{s}$, was determined from single pile analysis. In the works of Poulos (1968), the settlement of single pile can be calculated by Equation (2.6)

$$S = \frac{QI_p}{E_s D} \tag{2.6}$$

I_p was the settlement influence parameter. The settlement influence parameter was depended on some parameter length of pile and diameter of pile, L_p/d, Poisson ratio and condition below pile tip. I_p can be determined by

$$I_p = I_o R_k R_h R_v , \tag{2.7}$$

where I_0 is settlement influence parameter for the incompressible pile in semi-finite mass with Poisson's ratio 0.5; R_k is correction factor for pile compressible; R_h is correction factor for the finite layer depth below pile tip; R_v is correction factor for the Poisson's ratio of soil. Determination of $I_{0,} R_{k,} R_{h,} R_v$ is explained in detailed in the works of Poulos (19680).

The response of pile group was determined by multi-equation combining the equations for settlement prediction of piles (Equation (2.5)) and constrain equation presenting for the condition of pile cap. In particular, the load-settlement of pile group can be determined by multi-equation (2.8) for the flexible cap pile group and multi-equation (2.9) for rigid cap condition, respectively

$$\begin{cases} S_1 = \bar{s}\left(Q_1 + \sum_{k=1,k\neq 1}^{n_p} Q_k \alpha_{k1} \right) \\ \vdots \\ S_{n_p} = \bar{s}\left(Q_{n_p} + \sum_{k=1,k\neq 1}^{n_p} Q_k \alpha_{kn_p} \right) \\ Q_1 = Q_2 = \ldots = Q_j = Q_{n_p} \end{cases} \tag{2.8}$$

$$\begin{cases} S_1 = \bar{s}\left(Q_1 + \sum_{k=1,k\neq 1}^{n_p} Q_k \alpha_{k1}\right) \\ \vdots \\ S_{n_p} = \bar{s}\left(Q_{n_p} + \sum_{k=1,k\neq 1}^{n_p} Q_k \alpha_{kn_p}\right) \\ S_1 = S_2 = \ldots = S_j = S_{n_p} \end{cases} \tag{2.9}$$

2.2.3 Original closed-form solution

Randolph and Wroth (1978) proposed the close-form solution for predicting the settlement of a pile. This method considered surrounding soils of pile were the concentric cylinders having the shear stress reduced inversely with the surface of the cylinders (Figure 2.5). The settlement of the soils along the radius of pile which was described in Equation (2.10), decreased in logarithmic shape.

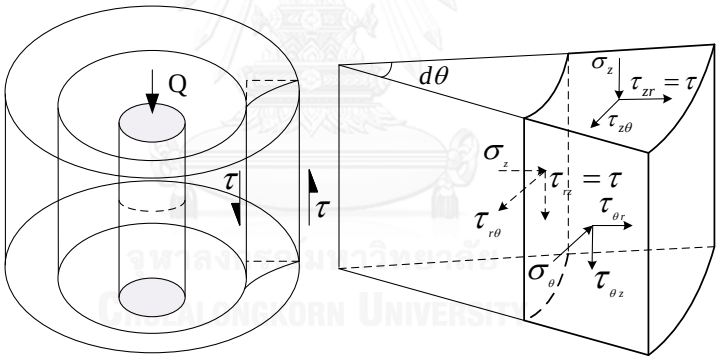

a. Concentrically cylinder soil model

b. Stress of concentrically cylinder soil model

Figure 2.5 Concentric cylinders ground model (Randolph & Wroth, 1978)

$$U(r) = \frac{\tau_o r_o}{G_s} \ln\left(\frac{r_m}{r}\right) = C\tau_o \tag{2.10}$$

r_m is the radial distance from the pile center to a point at which the shear stress induced by the pile can be ignored. The value of r_m can be approximated by

$$r_m \approx 2.5L(1-\nu_s) \tag{2.11}$$

The settlement of axially loaded pile was assumed by the couple of settlements at the pile shaft and base. Assuming no slip at pile-soil interface, the settlement of pile

shaft was compatible with the settlement of soil at pile-soil interface and was calculated by

$$w^{sh} = \frac{\tau_o r_o}{G_s} \ln\left(\frac{r_m}{r_0}\right) = U(r = r_o), \tag{2.12}$$

and the settlement at the pile base was calculated following the punching failure and showed in Equation (2.13)

$$w^b = \frac{P^b\left(1-\nu_b\right)}{4 \cdot r_o \cdot G_{sb}}, \tag{2.13}$$

The settlement at the pile head can be determined by Equation (2.14)

$$w^t = \frac{P^t / r_o G_s}{\left(\frac{4}{(1-\upsilon)} + \frac{2\pi}{\ln\left(r_m / r_o\right)} \frac{L}{r_o} \frac{\tanh\left(\mu L\right)}{\mu L}\right)} \tag{2.14}$$

$$\mu L = 2\left(L / ro\right)^2 \Big/ \left[ln\left(r_m / r_o\right)\left(E_p / G_s\right)\right]$$

Randolph and Wroth (1979) extended settlement prediction method for of single pile to pile group. In their approach, they assumed the neighbor unloaded pile can be settle as the same rate with the settlement of ground induced by settlement of loaded pile. The settlement of the ground can be determined by Eq.(2.15), (2.16).

$$U(r) = \frac{\tau_o r_o}{G_s} \ln\left(\frac{r_m}{r}\right) \tag{2.15}$$

$$U_b(r) = \frac{P^b\left(1-\nu_b\right)}{4 r_o G_{sb}} \frac{2 r_o}{\pi r} \tag{2.16}$$

Therefore, the interaction factor at pile shaft which shown by Eq. (2.17), can be determined from Equations (2.4), (2.12) and (2.15). In the same manner, the interaction factors at the pile base and pile head can be derived as shown in Equation (2.18) and (2.19).

$$\alpha_{skj} = \frac{\ln\left(r_m / r_{kj}\right)}{\ln(r_m / r_o)} \tag{2.17}$$

$$\alpha_{bkj} = \frac{2}{\pi}\frac{r_o}{r_{kj}} \tag{2.18}$$

$$\alpha_{kj} = \frac{\dfrac{4}{1-\nu} + \dfrac{2\pi\rho}{\zeta}\dfrac{l}{r_o}}{\dfrac{4}{1-\nu}\dfrac{s}{r_o c + s} + \dfrac{2\pi\rho}{\zeta + \ln\left(r_m / r_{kj}\right)}\dfrac{l}{r_o}} - 1 \tag{2.19}$$

$$\rho = \frac{G_{L/2}}{G_L};\ \zeta = \ln\left(r_m / r_o\right)\ ;\ \zeta_s = \ln\left(r_m / s\right)$$

Based on the interaction factor concept, the settlements at the shaft and the base of each pile in group can be determined accounting the effect on other piles in group by Equation (2.20) and (2.21), respectively.

$$w_j^{sh} = w_{jj}^{sh} + \sum_{k=1,k\neq j}^{n_p} w_{jk}^{sh} = \frac{\tau_o r_o}{G_s}\ln\left(\frac{r_m}{r_o}\right)\left[1 + \sum_{k=1,k\neq j}^{n_p}\alpha_{sjk}\right] \tag{2.20}$$

$$w_j^{b} = w_{jj}^{b} + \sum_{k=1,j\neq k}^{n_p} w_{jk}^{b} = \frac{P^b\left(1-\nu_b\right)}{4 r_o G_{sb}}\left[1 + \sum_{k=1,j\neq k}^{n_p}\alpha_{bjk}\right] \tag{2.21}$$

Lee (1993) modified the works of Randolph and Wroth (1979) by proposing the new formula for settlement at the pile shaft considering the compressible behavior of pile, as shown in Equation (2.22)

$$w_j^{sh} = w_j^{sh} + \sum_{k=1,k\neq j}^{n_p} w_{jk}^{sh} = \frac{\tau_o r_o}{G_s}\frac{\tanh\left(\mu L\right)}{\mu L}\ln\left(\frac{r_m}{r_o}\right)\left[1 + \sum_{k=1,k\neq j}^{n_p}\alpha_{sjk}\right] \tag{2.22}$$

In addition, the former equation for determining interaction factor was also revised by Equation (2.23)

$$\alpha = \frac{\frac{4}{1-\nu} + \frac{2\pi\rho}{\zeta}\frac{L}{r_o}\frac{\tanh(\bar{\mu}L)}{\bar{\mu}L}}{\frac{4}{1-\nu}\frac{1}{1+\zeta_b} + \frac{2\pi\rho L}{r_0}\frac{\tanh(\mu L)}{\mu L}\frac{1}{\zeta_g+\zeta_s}} - 1 \qquad (2.23)$$

$$\zeta_g = \ln\left(r_{mg}/r_o\right); \zeta = \ln\left(r_m/r_o\right); \ \zeta_b = \frac{2r_o}{\pi s}; \zeta_s = \ln\left(r_m/s\right); \bar{\mu} = 1.15\mu$$

The method (Lee, 1993) was verified with the BEM (Butterfield & Banerjee, 1971) and got the satisfaction up to 16 pile groups.

2.2.4 Modification of closed-form solution considering the stiffening effect

Mylonakis and Gazetas (1998) modified the interaction factor of Randolph and Wroth (1979) using the model shown in Figure 2.6.

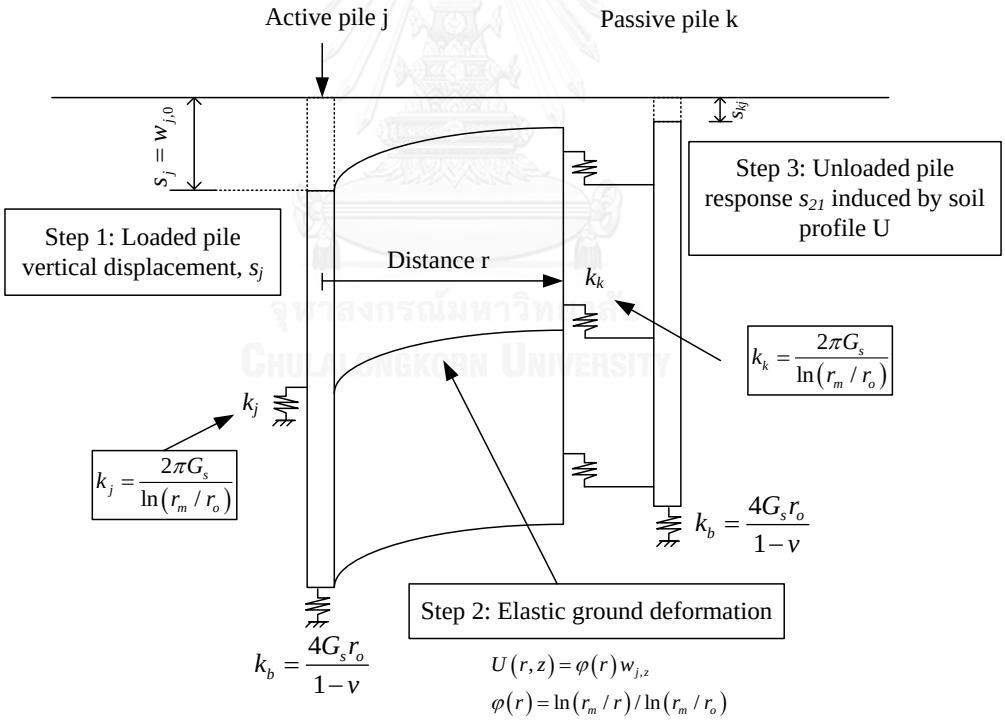

Figure 2.6 The proposed model for determination of interaction factor considering the response of passive pile (Mylonakis & Gazetas, 1998)

As the loaded pile (active pile) settles (step 1), the surrounding ground will also settle (step 2) and induce the settlement on the unloaded pile (or in another words, the

passive pile). However, the settlement of passive pile should be less than the surrounding ground because of the incompatibility of their stiffness (step 3). Therefore, the interaction factor will be smaller than the one determined by Equation (4.8). They defined this phenomenon as the stiffening effect (Fleming et al, 2008).

Besides that, it was claimed that the interaction factor between 2 piles was mainly controlled the pile shafts interaction and proposed the new equation for determination of interaction factor considering the response of passive pile. That equation was shown in Eq.(2.24)

$$\alpha_{21} = \frac{s_{21}}{s_1} = \xi \frac{\ln\left(r_m / r_{21}\right)}{\ln(r_m / r_o)} \tag{2.24}$$

where ξ is the diffraction factor which smaller than 1. The determination of ξ is explained in detailed in thesis of Mylonakis (1998).

2.2.5 Modification of the closed-form solution in term of 1D FEM

Chow (1986) proposed semi-analytical approach called the "hybrid approach" or 1D FEM approach based on the closed-form solution of Randolph and Wroth (1979). In this approach, piles in group divided in to many segments presented by nodes (Figure 2.7). The response of nodes was described by the flexibility factors determined from the work of Randolph and Wroth (1978). In particular, the flexibilities were determined by Eq.(2.25) for nodes at the shaft and (2.26) for nodes at the base, respectively.

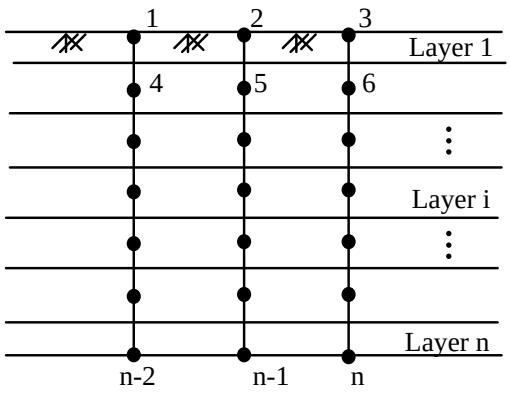

Figure 2.7 The model of pile group (Chow, 1986)

$$f_{k,i} = \ln\left(r_m / r_o\right) / \left(2\pi l_{,i} \cdot G_{s,i}\right) \tag{2.25}$$

$$f_k = \left(1-\nu\right) / \left(4G_{sb} r_o\right) \tag{2.26}$$

where $f_{k,i}$ is the flexibility for the node *k* at the shaft at soil layer i

The pile-soil-pile interaction in group pile was described by the interaction between nodes. By assuming the pile shaft resistance of each segment and pile base resistance were presented by the point load applying on nodes, the interaction between 2 nodes can be described by flexibility factor determined by Equation (2.27) (Mindlin, 1936).

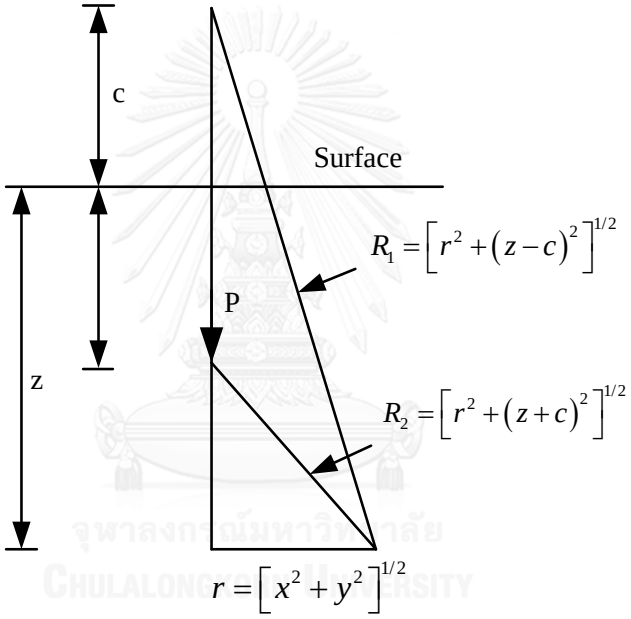

Figure 2.8 Solution for a vertical point load in a homogeneous, isotropic elastic half-space (Mindlin, 1936)

$$f_{kh} = \frac{1}{16\pi G(1-\nu)}\left\{\frac{3-4\nu}{R_1} + \frac{8(1-\nu)^2 - (3-4\nu)}{R_2} + \frac{(r-c)^2}{R_1^3} + \frac{(3-4\nu)(z+c)^2 - 2cz}{R_2^3} + \frac{6zc(z+c)^2}{R_2^5}\right\} \tag{2.27}$$

$$R_1 = \left[r^2 + (z-c)^2\right]^{1/2};\quad R_2 = \left[r^2 + (z+c)^2\right]^{1/2};\quad r = \left[x^2 + y^2\right]^{1/2} \tag{2.28}$$

Following Figure 2.7, z is the depth of node k; c the depth which the unit load is applied; x is the distance in x direction of node k as measured from node h; y is the distance in y direction of node k as measured from node h. The hybrid approach can be briefly described as follows,

Firstly, the piles in group were divided in to many segments respected with the sub-layer of ground and presented by nodes (Figure 2.7)

Secondly, governing equation of nodes system, described for response of pile group, would be determined by Eq.(2.29)

$$\left[[K_p]+\left[K_s\right]\right][s_i]=[P_i], \tag{2.29}$$

$[K_p]$ is n x n stiffness matrix of pile

$$[K_p]=\begin{bmatrix} k_{p1} & 0 & . & 0 \\ 0 & k_{p2} & . & . \\ . & . & . & . \\ 0 & . & . & k_{pn} \end{bmatrix} \tag{2.30}$$

$[K_s]=[F_s]^{-1}$ is n x n stiffness matrix of soil, $[F_s]$ is n x n flexibility matrix of soil

$$[F_s]=\begin{bmatrix} f_1 & f_{12} & . & f_{1n} \\ f_{21} & f_2 & . & . \\ . & . & . & . \\ f_{n1} & . & . & f_n \end{bmatrix} \tag{2.31}$$

$[s_i]$ is n x 1 matrix representing for settlement along depth of piles.

$[P_i]$ is n x 1 matrix representing loads on each node.

For the sub-element of $[K_p]$

$k_{pk,i}=\dfrac{E_p A_p}{l_{,i}}$ - for the node k at soil layer *i*

For the sub-element of $[F_s]$

$f_{k,i} = \ln(r_m / r_o) / (2\pi l_{,i} \cdot G_{s,i})$ - for the node k at the shaft at soil layer *i*

$f_k = (1-\nu) / (4G_{sb} r_o)$ - for the base node *k*

$$f_{kh} = \frac{P}{16\pi G_{kh}(1-\nu_{kh})}\left\{\frac{3-4\nu}{R_1} + \frac{8(1-\nu)^2 - (3-4\nu)}{R_2} + \frac{(r-c)^2}{R_1^3} + \frac{(3-4\nu)(z+c)^2 - 2cz}{R_2^3} + \frac{6zc(z+c)^2}{R_2^5}\right\}$$ - for the interaction between 2 nodes.

The sub-elements of [s_i] and [P_i] were variables and would be partly determined by constrains condition about load and settlement at the pile head.

In the final, the governing equation (2.29) was prepared by number of unknown variables respected with the number of equation. After solving the governing equation, the unknown variables of [s_i] and [P_i] presenting for the response of pile group, were determined.

2.2.6 Modification of load-transfer method considering slippage

Lee and Xiao (2001) modified the original load-transfer approach by considering the response of pile segment *i* decomposed into inelastic (slippage), $w_{,i}^s$, and elastic part (elastic ground deformation), $w_{,i}^e$, as shown in Equation (2.32).

$$w_{,i} = w_{,i}^s + w_{,i}^e \qquad (2.32)$$

The relationship between the slippage and mobilized shear stress at pile-soil interface can be described by hyperbolic Equation (2.33) and t-z curve in Figure 2.10.a

$$\tau_{,i} = \frac{w_{,i}^s}{a_{,i}^h + b_{,i}^h w_{,i}^s} \qquad (2.33)$$

In another way, the Equation (2.33) can be rewritten by Equation (2.34)

$$w_{,i}^{s} = \frac{a_{,i}^{h}\tau_{,i}}{1 - b_{,i}^{h} w_{,i}^{s}} \tag{2.34}$$

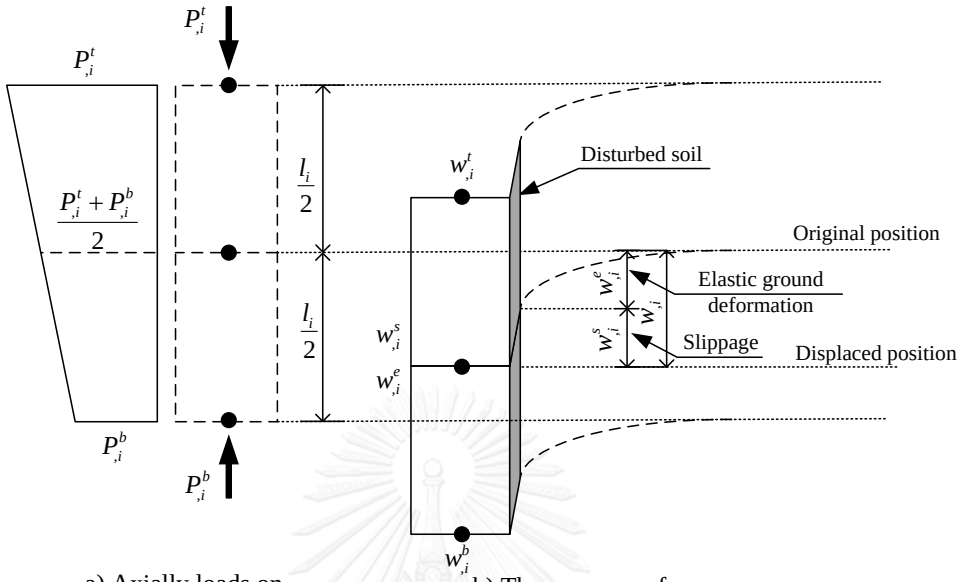

a) Axially loads on the segment i

b) The response of segment i

Figure 2.9 The response of pile segment i by applied axial loading

The physical meaning of $a_{,i}^{h}, b_{,i}^{h}$ are shown in Figure 2.10. In that, $1/a_{,i}^{h}$ is the initial stiffness and $1/b_{,i}^{h}$ is the ultimate stress

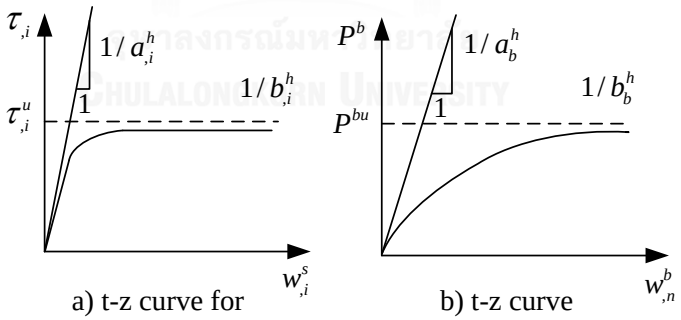

a) t-z curve for pile shaft

b) t-z curve for pile base

Figure 2.10 Hyperbolic t-z curves (Lee & Xiao, 2001)

The elastic ground deformation is determined following Randolph and Wroth (1978)

$$w_{,i}^{e} = \frac{r_o}{G_{s,i}} \ln\left(\frac{r_m}{r_o}\right) \cdot \tau_{,i} = C_{,i} \cdot \tau_{,i} \tag{2.35}$$

By substitute Equation (2.34) and (2.35) into (2.32), the response of pile segment *i* can be rewritten by Equation (2.36)

$$w_{,i} = \frac{a_{,i}^{h}\tau_{,i}}{1-b_{,i}^{h}w_{,i}^{s}} + C_{,i}\tau_{,i} \tag{2.36}$$

Or

$$\tau_{,i} = \frac{a_{,i}^{h} + C_{,i} + b_{,i}^{h}w_{,i}^{s} - \sqrt{\left(a_{,i}^{h} + C_{,i} + b_{,i}^{h}w_{,i}^{s}\right)^{2} - 4b_{,i}^{h}w_{,i}^{s}}}{2b_{,i}^{h}C_{,i}} \tag{2.37}$$

The settlement at pile tip, w^b, related to the mobilized tip resistance, P^b, was described by hyperbolic Equation (2.38) and t-z curve in Figure 2.10.b

$$P_{,n}^{b} = \frac{w_{,n}^{b}}{a_{b}^{h} + b_{b}^{h}w_{,n}^{b}} \tag{2.38}$$

For extend to pile group, the effects of all piles in group on pile *j* can be considered by modification of the elastic ground deformation, as shown in Equation (2.39)

$$w_{j,i}^{e} = w_{jj,i}^{e} + \sum_{k=1,k\neq j}^{n_p} w_{jk,i}^{e} = \frac{r_o}{G_{s,i}}\ln\left(\frac{r_m}{r_o}\right)\cdot\tau_{,i} + \sum_{k=1,k\neq j}^{n_p}\frac{r_o}{G_{s,i}}\ln\left(\frac{r_m}{r_{jk}}\right)\cdot\tau_{,i} \tag{2.39}$$

Thus, Equation (2.37) was changed to Equation (2.40) for pile group analysis

$$\tau_{j,i} = \frac{a_{,i}^{h} + \overline{C_{j,i}} + b_{,i}^{h}w_{j,i}^{s} - \sqrt{\left(a_{,i}^{h} + \overline{C_{j,i}} + b_{,i}^{h}w_{j,i}^{s}\right)^{2} - 4b_{,i}^{h}w_{j,i}^{s}}}{2b_{,i}^{h}\overline{C_{j,i}}} \tag{2.40}$$

$$\overline{C_{j,i}} = \frac{r_o}{G_{s,i}}\ln\left(\frac{r_m}{r_o}\right) + \sum_{k=1,k\neq j}^{n_p}\frac{r_o}{G_{s,i}}\ln\left(\frac{r_m}{r_{kj}}\right) \tag{2.41}$$

As the same manner, the response at the base of pile *j* considering the effects from all piles in group can be expressed by

$$P_{j,n}^{b} = \frac{a_{b}^{h} + \overline{C_{jb}} + b_{b}^{h}w_{j,n}^{b} - \sqrt{\left(a_{b}^{h} + \overline{C_{jb}} + b_{b}^{h}w_{j,n}^{b}\right)^{2} - 4b_{b}^{h}w_{j,n}^{b}}}{2b_{b}^{h}\overline{C_{jb,i}}} \tag{2.42}$$

$$\overline{C_{jb}} = \sum_{k=1,k\neq j}^{n_p} \frac{1-\nu_{sb}}{2r_{jk}G_{sb}} \tag{2.43}$$

For predicting the load-settlement curve of each pile in group, determination of parameters, $a_{jb}^{h}, b_{jb}^{h}, \overline{C_{jb}}$, for pile base and ($a_{j,i}^{h}, b_{j,i}^{h}, \overline{C_{j,i}}$) for all pile segment i were implemented. After that, the load-settlement curve of each pile in group would be determined by iterative calculation. The detail of the determination of the parameters and the iterative calculation were found in Lee and Xiao (2001)

After obtain the load-settlement curve of each pile in group, the performance of pile group is determined by the condition at pile cap, as shown in Figure 2.11

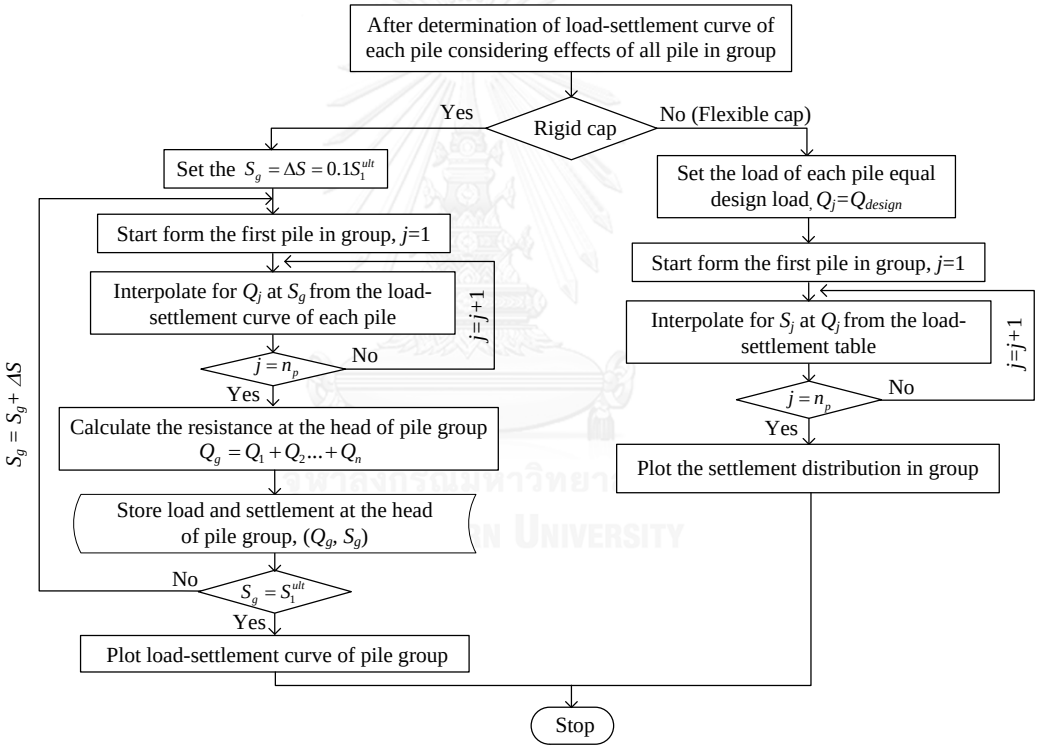

Figure 2.11 Flow chart to determine the response of pile group under rigid cap and flexible cap condition

For rigid cap condition which all piles displace at the same rate, by assuming the settlement of pile group, $S_g = \Delta S = 0.1S_1^{ult}$, the corresponding resistance of each pile with the assuming settlement, is interpolated from its load-settlement curve. The resistance of pile group is the summation of resistance of each pile. Increase routinely the settlement of pile group, $S_g = S_g + \Delta S$, and repeat the procedure to determine the

resistance of pile group until $S_g = S_1^{ult}$, the load-settlement curve of pile group is obtained.

For flexible cap which all piles were loaded under same load, by assuming the same design applied load on each pile, Q_j=Q_{design}, the corresponding settlement of each pile with the design applied load, is also interpolated from its load-settlement curve. After that, the settlement distribution in pile group is determined.

Wang et al. (2012) also proposed the new load-transfer method by adopting the work of Lee and Xiao (2001). In this work, the response of pile segment i was adopted from the work of Lee and Xiao (2001) and decomposed into inelastic (slippage), $w_{,i}^s$, and elastic part (elastic ground deformation), $w_{,i}^e$, as shown in (2.32) where $w_{,i} = w_{,i}^s + w_{,i}^e$

However, t-z curve at pile shaft segment and pile base was described by exponential Equation (2.44) and (2.45), respectively.

$$\tau_{,i} = a_{,i}\left(1-e^{-b_{,i}w_{,i}^s}\right) \tag{2.44}$$

$$P_{,n}^b = a_b(1-e^{-b_b w_{,n}^b}) \tag{2.45}$$

The meaning of $a_{,i}, b_{,i}, a_b, b_b$ can be described in Figure 2.12. The determination of $a_{,i}, b_{,i}, a_b, b_b$ parameters were detailed in work of Wang et al. (2012).

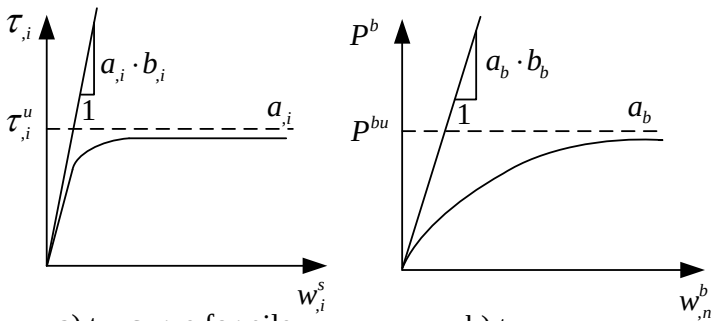

a) t-z curve for pile shaft segment i

b) t-z curve for pile base

Figure 2.12 t-z curves (Wang et al, 2012)

In addition, nonlinear behavior of concrete material of pile, described in Figure 2.13, was also considered following Equation (2.46)

$$\sigma_c = \begin{cases} f_c\left[2\frac{\varepsilon_c}{\varepsilon_o} - \left(\frac{\varepsilon_c}{\varepsilon_o}\right)^2\right] & ;\varepsilon_c \le \varepsilon_o \\ f_c\left[1 - 0.15\frac{\varepsilon_c - \varepsilon_o}{\varepsilon_{cu} - \varepsilon_o}\right] & ;\varepsilon_o \le \varepsilon_c \le \varepsilon_{cu} \end{cases}, \qquad (2.46)$$

Where σ_c and ε_c are the stress and the strain of concrete, respectively; f_c and ε_0 are the peak stress and the corresponding strain, respectively; and ε_{cu} is the ultimate strain of concrete.

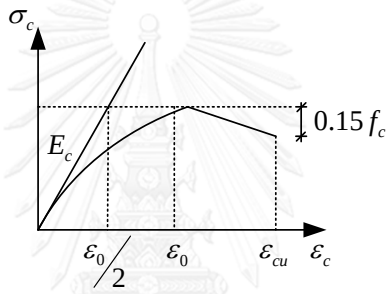

Figure 2.13 The Hognestad model of concrete material (Hognestad, 1951)

In single pile analysis, a pile model was proposed as shown in Figure 2.14

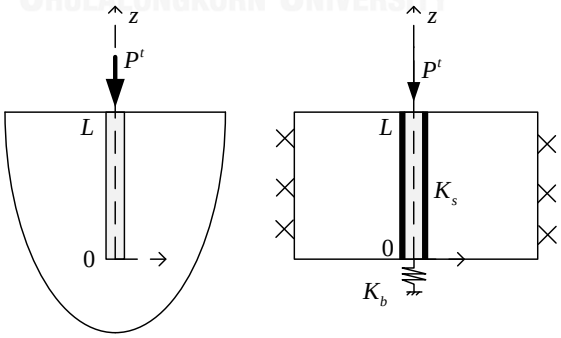

Figure 2.14 The pile model (Wang et al, 2012)

Wang et al. (2012) proposed that the total settlement at depth *z* can be determined by Equation (2.47) as well as Equation (2.48)

$$w_{,z} = \int_0^z \frac{P_z}{E_p A_p} dz + w^b \tag{2.47}$$

$$w_{,z} = w_{,z}^s + w_{,z}^e$$

(2.48)

Besides, they firstly proposed new second-order differential equation described for response of a pile, as shown in Equation (2.49)

$$\left(1 + C \cdot K_s\right) y^{"} = K_s w^b + \frac{K_s}{E_p A_p} y \tag{2.49}$$

where $y = \int_0^z P_z dz$; $y^{'} = P_z$; $y^{"} = P_z^{'}$ and K_s is the tangent stiffness of pile shaft response

$$K_s = a \cdot b \cdot e^{-bw^s} \tag{2.50}$$

The solution to Equation (2.49) can be obtain in the following form:

$$y = C_1 e^{hz} + C_2 e^{-hz} - E_p A_p w^b \tag{2.51}$$

By substituting the boundary condition $y_0 = 0$ and $y_0^{'} = K_b w^b$ in to Equation (2.51) , the value of C_1 and C_2 can be obtain by:

$$C_1 = \frac{E_p A_p + K_b / h}{2} w^b = c_1 w^b$$

$$C_2 = \frac{E_p A_p - K_b / h}{2} w^b = c_2 w^b$$

$$h = \sqrt{\frac{K_s}{E_p A_p (1 + C K_s)}}$$

(2.52)

K_b is the tangent stiffness of pile base response which can be determined by Equation (2.53)

$$K_b = a_b \cdot b_b \cdot e^{-bw^b} \tag{2.53}$$

By substituting Equation (2.52) and (2.51) into Equation (2.47), the pile base settlement can be obtained by:

$$w^b = \frac{P^t}{h(c_1 e^{hL} - c_2 e^{-hL})} \quad , \tag{2.54}$$

and the pile head settlement can be determined by

$$w^t = \frac{P^t}{E_p A_p h} \cdot \frac{(c_1 e^{hz} + c_2 e^{-hz})}{(c_1 e^{hL} - c_2 e^{-hL})} \tag{2.55}$$

The slippage along pile shaft and elastic ground deformation at depth *z* can be determined by

$$w^s_{,z} = \frac{P^t \cdot h}{K_s} \cdot \frac{(c_1 e^{hz} + c_2 e^{-hz})}{(c_1 e^{hL} - c_2 e^{-hL})} \tag{2.56}$$

$$w^e_{,z} = C \cdot P^t \cdot h \cdot \frac{(c_1 e^{hz} + c_2 e^{-hz})}{(c_1 e^{hL} - c_2 e^{-hL})} \tag{2.57}$$

In addition, the axial force P_z at the depth can be determined by

$$P_{,z} = P^t \cdot \frac{(c_1 e^{hz} + c_2 e^{-hz})}{(c_1 e^{hL} - c_2 e^{-hL})} \tag{2.58}$$

The determination of settlement of single pile can be following the flowchart showed in Figure 2.15.

Pile is divided into many segments *i*, (*i=1-n*). Assume the iterative calculation time for load-settlement curve prediction is *k* and set the initial value of $w^{s,k}_{,i}; w^{t,k}_{,i}; P^{t,k}_{,i}$ (k=1) for all segments are zeros and Young modulus $E^k_{p,i} = E_p$.

By assume the increasing settlement at pile base is the very small value, $\Delta w^b = 0.001D$, at the first calculation time *k*=1, the settlement at pile tip was calculated by $w^{b,k}_{,n} = k \cdot \Delta w^b$ and tangent stiffness at pile base, the mobilized resistance at pile base are calculated by Equation (2.53) and Equation (2.45)

Starting the calculation from the bottommost segment *i=n*, the initial tangent stiffness at pile shaft was calculated by Equation (2.50), and parameter of $h_{,i}$; $c_{1,i}$; $c_{2,i}$

are determined by Equation (2.52). After that, the accumulated load and settlement at top segment are calculated by

$$\begin{aligned} P_{,i}^{t,k+1} &= P_{,i}^{t,k} + w_{,i}^{b,k} h_{,i} \left(c_{1,i} e^{h_{,i} l_{,i}} - c_{2,i} e^{-h_{,i} l_{,i}} \right) \\ w_{,i}^{t,k+1} &= w_{,i}^{t,k} + \frac{P_{,i}^{t,k+1}}{E_{p,i}^{k} A_p} \frac{c_{1,i} e^{h_{,i} l_{,i}} + c_{2,i} e^{-h_{,i} l_{,i}}}{c_{1,i} e^{h_{,i} l_{,i}} - c_{2,i} e^{-h_{,i} l_{,i}}} \end{aligned} \quad . \tag{2.59}$$

The modified parameter for determination of the tangent stiffness at pile shaft and tangent Young modulus of pile in the next calculation time were determined by

$$\begin{aligned} w_{,i}^{s,k+1} &= w_{,i}^{s,k} + \frac{P_{,i}^{t,k+1}}{K_{s,i}^{k}} \frac{c_{1,i} e^{h_{,i} l_{,i}} + c_{2,i} e^{-h_{,i} l_{,i}}}{c_{1,i} e^{h_{,i} l_{,i}} - c_{2,i} e^{-h_{,i} l_{,i}}} \\ E_{p.i}^{k+1} &= \frac{2 f_c}{\varepsilon_o} \left(\varepsilon_o - \varepsilon_{c,i} = \frac{P_{,i}^{t,k+1} + P_{,i}^{b}}{2 E_{p,i}^{k} A_p} \right) \end{aligned} \quad . \tag{2.60}$$

Next, the load and settlement at the bottommost segment were transferred to the next segment followed continue of force and settlement between two segments, as shown in Equation (2.61). The same procedure was repeated from segment i=n-1 to segment i=1 until obtain the load-settlement at pile head.

$$w_{,i+1}^{b,k+1} = w_{,i}^{t,k+1}; \qquad P_{,i-1}^{b,k+1} = P_{,i}^{t,k+1} \tag{2.61}$$

After storing the recently predicted load-settlement at pile head, the value of $w_{,n}^{b,k}$ was increased following the increase of calculation time, k=k+1 and $w_{,n}^{b,k} = k \cdot \Delta w^{b}$. The whole procedure was repeated until the value of $w_{,n}^{b,k}$ larger than 10% of pile diameter.

Finally, plot the load-settlement curve from storing data.

To extend their single pile analysis to pile group analysis, they adopted the idea of interaction factor at by shaft and pile tip of Randolph and Wroth (1978). In particular, the settlement of one pile in a group could be written as the sum of the settlement due to its own loading plus the settlement due to additional displacement from adjacent piles.

$$w_{j,i} = w^{s}_{j,i} + \sum_{k=1,k\neq j}^{n_p} \left[w^{e}_{j,i}\left(1+\alpha_{sjk}\right) + w^{b}_{j,z=0}\left(1+\alpha_{bjk}\right) \right]$$
$$\alpha_{s\,jk} = \frac{\ln\left(r_m / r_{jk}\right)}{\ln(r_m / r_o)}; \quad \alpha_{b\,jk} = \frac{2}{\pi}\frac{r_o}{r_{jk}} \qquad , \qquad (2.62)$$

the values of $w^{s}_{j,i}; w^{e}_{j,i}; w^{b}_{j,z=0}$ were determined in single pile analysis.

After determination of load-settlement curve of each pile in group considering effects of all pile in group, the performance of pile group was predicted as same as Lee and Xiao (2001), as shown Figure 2.11

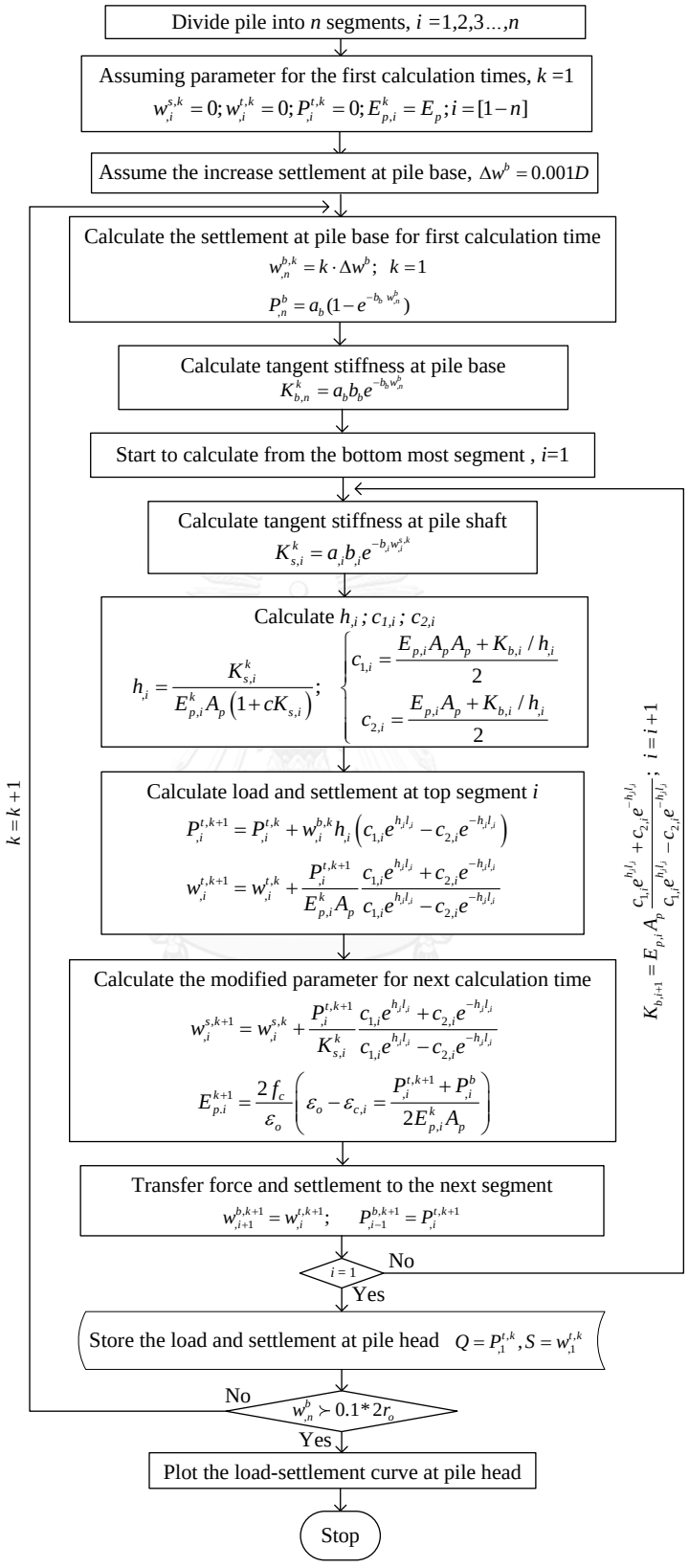

Figure 2.15 Determination for settlement of single pile (Wang et al, 2012))

2.2.7 Modification of load-transfer method considering stiffening effect

Zhang et al. (2014) proposed the new load-transfer method considering the stiffening effect in group pile. In their method pile was divided into *n* segments, as shown in Figure 2.16.

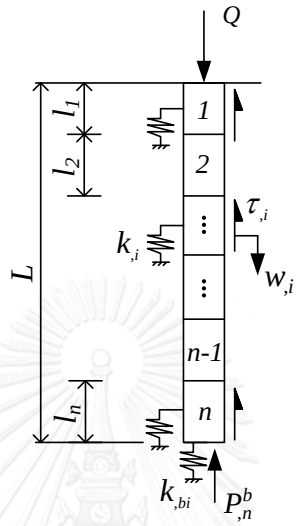

Figure 2.16 Pile model (Zhang et al, 2014)

In single pile analysis, by assuming the settlement of pile and soil at pile-soil interface is compatible, the response of pile segment was described by Equation (2.63) and hyperbolic t-z cure in Figure 2.17.

$$\tau_{,i} = \frac{w_{,i}}{a^h_{,i} + b^h_{,i} w_{,i}} \qquad (2.63)$$

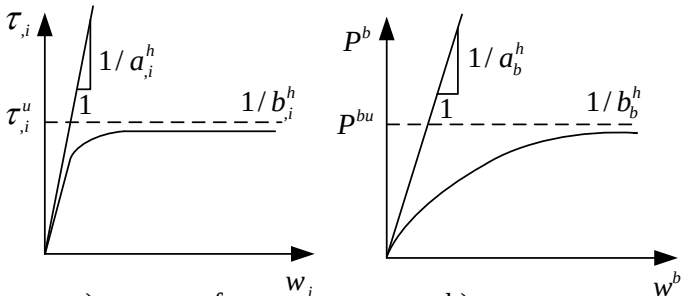

a) t-z curve for pile shaft

b) t-z curve for pile base

Figure 2.17 t-z curves (Zhang et al, 2014)

By adopting the determination of the settlement at pile shaft in elastic stage, Equation (2.64) (Randolph and Wroth, 1978), the parameter, $a_{,i}^{h}$, presented for initial flexibility of Equation (2.63), can be determined by Equation (2.65)

$$w_{,i}^{sh} = \frac{r_o}{G_{s,i}} \ln\left(\frac{r_m}{r_o}\right) \cdot \tau_{,i} = C_{,i} \cdot \tau_{,i} \tag{2.64}$$

$$a_{,i}^{h} = \frac{1}{k_{,i}} = \frac{r_o}{G_{s,i}} \ln\left(\frac{r_m}{r_o}\right) = C_{,i} \tag{2.65}$$

The parameter, $b_{,i}^{h}$, can be determined from the maximum shear stress at pile soil interface, as follows;

$$\frac{1}{b_{,i}^{h}} = \tau_{,i}^{u} = \frac{\tau_{,i}^{f}}{R} \tag{2.66}$$

The settlement at pile base, $w_{,n}^{b}$, related to the mobilized tip resistance, $P_{,n}^{b}$, was described by hyperbolic Equation (2.67) and t-z curve in Figure 2.17

$$P_{,n}^{b} = \frac{w_{,n}^{b}}{a_b^h + b_b^h w_{,n}^{b}} \tag{2.67}$$

The parameter, a_b^h, presented for initial stiffness of Equation (2.67), can be determined by Equation (2.68) (Randolph and Wroth, 1978),

$$a_b^h = \frac{\pi r_o \left(1 - \nu_{sb}\right)}{4G_{sb}} \tag{2.68}$$

The parameter, b_b^h, can be determined from the maximum pile base resistance.

$$\frac{1}{b_b^h} = P^{bu} = \frac{P^{bf}}{R} \tag{2.69}$$

For extension form single pile analysis to pile group analysis, they adopted the works of Randolph and Wroth (1978). In elastic stage, the settlement of soil around the

j was increased by adding settlement induced shear stress from all pile *k* in group which shown in Equation (2.70)

$$\begin{aligned} w_{j,i} &= \frac{r_o}{G_{s,i}} \ln\left(\frac{r_m}{r_o}\right) \cdot \tau_{,i} + \frac{r_o}{G_{s,i}} \sum_{k=1,k\neq j}^{n_p} \ln\left(\frac{r_m}{r_{jk}}\right) \cdot \tau_{k,i} \\ &= w_{jj,i} + \sum_{k=1,k\neq j}^{n_p} w_{jk,i} \end{aligned} \tag{2.70}$$

However, Zhang et al.(2014) proposed that the shaft shear stress of pile $k, \tau_{kj,i}$, induced by the spread of the shaft shear stress of pile $j, \tau_{j,i}$, expressed by Equation (2.71) ,

$$\tau_{kj,i} = \frac{\tau_{j,i} r_o}{r_{kj}}, \tag{2.71}$$

was taken as the negative shear stress and added negative term, $w'_{jk,i}$, in the settlement of soil around pile j

$$w'_{jk,i} = \frac{r_o}{G_{s,i}} \ln\left(\frac{r_m}{r_{jk}}\right) \cdot \tau_{kj,i} = \frac{r_0^2}{G_{s,i} r_{jk}} \ln\left(\frac{r_m}{r_{jk}}\right) \cdot \tau_{kj,i} \tag{2.72}$$

Thus, in elastic stage, the settlement of soil around the *j* was determined by

$$\begin{aligned} w_{j,i} &= \frac{r_o}{G_{s,i}} \ln\left(\frac{r_m}{r_o}\right) \cdot \tau_{,i} + \frac{r_o}{G_{s,i}} \sum_{k=1,k\neq j}^{n_p} \ln\left(\frac{r_m}{r_{jk}}\right) \cdot \tau_{k,i} - \frac{r_0}{G_{s,i}} \sum_{k=1,k\neq j}^{n_p} \frac{r_0}{r_{jk}} \ln\left(\frac{r_m}{r_{jk}}\right) \cdot \tau_{kj,i} \\ &= w_{jj,i} + \sum_{k=1,k\neq j}^{n_p} w_{jk,i} - \sum_{k=1,k\neq j}^{n_p} w'_{jk,i} \end{aligned} \tag{2.73}$$

By assuming the shear stress at pile-soil interface of all pile in group were the same, the Equation changed to Equation (2.74)

$$w_{j,i} = \frac{r_o}{G_{s,i}} \ln\left(\frac{r_m}{r_o}\right) \cdot \left[1 + \sum_{k=1,k\neq j}^{n_p} \frac{\ln(r_m / r_{jk})}{\ln(r_m / r_o)} - \sum_{k=1,k\neq j}^{n_p} \frac{r_0}{r_{jk}} \frac{\ln(r_m / r_{jk})}{\ln(r_m / r_o)}\right] \cdot \tau_{j,i} \tag{2.74}$$

Thus, in the pile group analysis, the determination of parameter, $a_{,i}^{h}$, presented in Equation (2.65) was modified by Equation (2.75)

$$a_{j,i}^{h} = \frac{r_o}{G_{s,i}} \ln\left(\frac{r_m}{r_o}\right) + \frac{r_o}{G_{s,i}} \sum_{k=1,k\neq j}^{n_p} \ln\left(\frac{r_m}{r_{jk}}\right) - \frac{r_0}{G_{s,i}} \sum_{k=1,k\neq j}^{n_p} \frac{r_0}{r_{jk}} \ln\left(\frac{r_m}{r_{jk}}\right)$$
$$= \frac{1}{k_{j,i}} = \frac{1}{k_{jj,i}} + \frac{1}{k_{jk,i}} - \frac{1}{k'_{jk,i}} \qquad (2.75)$$

As the same manner, the determination of parameter a_b^h of pile *j* considering effects of all piles in group, can be determined by Equation (2.76) followed Randolph and Wroth (1979),

$$a_{bj}^{h} = \frac{(1-\nu_{sb})}{4r_o G_{sb}} + \frac{(1-\nu_{sb})}{4r_o G_{sb}} \sum_{k=1,k\neq j}^{n_p} \frac{2}{\pi} \frac{r_o}{r_{jk}} \qquad (2.76)$$

After the preparation of parameters at pile shaft and pile base, the settlement prediction of each pile in group was determined following the standard iterative calculation of load-transfer method (Figure 2.2)

Finally, the same procedure as Lee and Xiao (2001), shown Figure 2.11, was used determine performance of pile group.

2.3 Summary

As mentioning in the introduction (Chapter 1), based on the literate review, it can be seen that;

(1) The currently load-transfer method do not consider the combination of slippage at pile-soil interface and stiffening effect in pile-soil-pile interaction. In particular, Lee & Xiao (2001) and Wang et al. (2012) considered slippage at pile soil interface but no considering the stiffening effect in pile group analysis. Whereas, Mylonakis and Gazetas (1998) and Zhang et al. (2013) considered stiffening effect (Mylonakis & Gazetas, 1998; Zhang et al, 2013) but no considering the slippage at pile-soil interface

(2) The meaning of stiffening effect mentioned in works of Mylonakis and Gazetas (1998) and Zhang et al. (2013) is difference. Mylonakis and Gazetas (1998) focused on response of passive pile to modify the interaction factor of Randolph

and Wroth (1978) whereas Zhang et al. (2013) considered influence of other pile on the response of a pile.

(3) The proposed approach of Wang et al. (2014) used the tangent stiffness for predicting nonlinear settlement of pile group (or in other word, explicit prediction). However, this kind of explicit prediction can be depended on the step-size calculation.

The current issues of load-transfer method is solved as follows

(1) Propose a new nonlinear analytical method for single pile analysis based on the works of Wang et al. (2014), as shown in Chapter 3

(2) Propose a new linear analytical method for pile group considering stiffening effect by the combination the works of Mylonakis and Gazetas (1998) and Zhang et al. (2013), as shown in Chapter 4.

(3) Proposed a new nonlinear analytical method for pile group considering stiffening effect by modification of chapter 3 considering the slippage at pile-soil interface, as shown in Chapter 5.

CHAPTER 3: NONLINEAR ANALYTICAL METHOD FOR SINGLE PILE

3.1 Introduction

In this chapter, the new load-transfer method is proposed by modification and extension from the work of Wang et al. (2014) as follows; (1) the secant modulus is used instead of the tangent stiffness to avoid the calculation step-size dependency, (2) a standard procedure is suggested for determining necessary parameters from site investigation reports. The innovation of proposed approach was validated by compare with previous works. In addition, the proposed approach is also verified by comparing with twenty five static load tests of bored piles in Bangkok.

3.2 Nonlinear analytical method for single piles

3.2.1 Assumptions and mathematical models

Pile is divided into a number of segments as shown in Figure 3.1. The response of a pile segment *i* can be decomposed into inelastic (slippage), $w_{,i}^{s}$, and elastic part (elastic ground deformation), $w_{,i}^{e}$, as shown in Equation (3.1)

$$w_{,i} = w_{,i}^{s} + w_{,i}^{e} \tag{3.1}$$

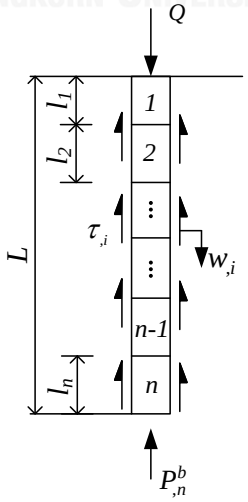

Figure 3.1 The concept of load-transfer approach

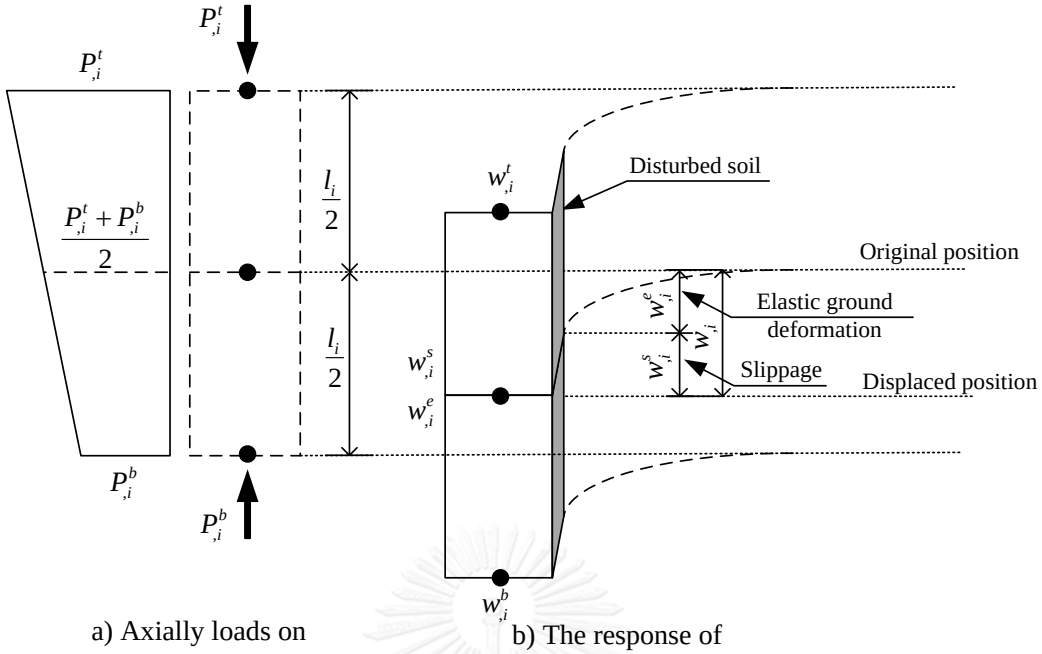

Figure 3.2 The response of pile segment i by applied axial loading

3.2.1.1 Pile shaft model

Following Wang et al. (2012), the relationship between the slippage and mobilized shear stress at pile-soil interface can be described by Equation (3.2) and t-z curve in Figure 3.3.a

$$\tau_{,i} = a_{,i}\left(1 - e^{-b_{,i} w_{,i}^s}\right) \tag{3.2}$$

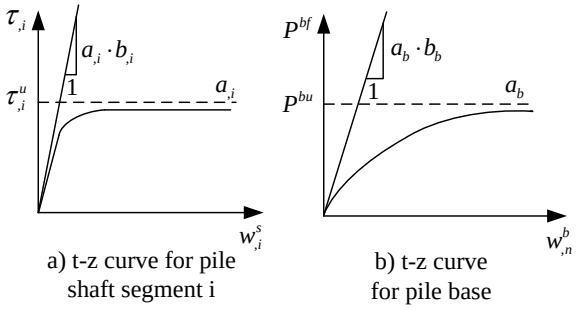

Figure 3.3 t-z curve

Mathematically, the parameter $a_{,i}$ can be considered as the asymptote of Equation (3.2). It was estimated from the maximum unit skin friction, $\tau_{,i}^f$, as follows

$$a_{,i} = \tau_{,i}^{u} = \frac{\tau_{,i}^{f}}{R}, \tag{3.3}$$

where

R is the range [0.80-0.95] (Clough & Duncan, 1973) and

$$\tau_{,i}^{f} = \begin{cases} \alpha_{,i} Su_{,i} & ; \quad \text{for clay} \\ \beta_{,i} \sigma_{v,i}^{'} & ; \quad \text{for sand} \end{cases} \tag{3.4}$$

Except the value of $\sigma_{v,i}^{'}$ is determined from unit weight, the parameters $\alpha_{,i}, \beta_{,i}, Su_{,i}$ in Equation (3.4) can be determined by SPT value (Boonyatee et al, 2015). In particular, for clay

$$\begin{aligned} Su_{,i} &= 0.685 \cdot N_{SPT,i} \quad (\text{t/m}^2) \\ \alpha_{,i} &= 0.41854 + 0.78067 \cdot e^{\left(-Su_{,i}/5.99492\right)}, \end{aligned} \tag{3.5}$$

and for sand

$$\begin{aligned} \beta_{,i} &= 0.018 + 0.000911 \cdot e^{\phi_{,i}^{'}/6.457} \\ \phi_{,i}^{'} &= 27.1 + 0.3 \cdot N_{SPT,i}^{'} - 0.00054 \cdot \left(N_{SPT,i}^{'}\right)^2 \end{aligned} \tag{3.6}$$

$$N_{SPT,i}^{'} = 0.77 \cdot \log_{10}\left(200 / \sigma_{v,i}^{'}\right) \cdot N_{SPT,i} \quad \text{(Meyerhof, 1976)} \tag{3.7}$$

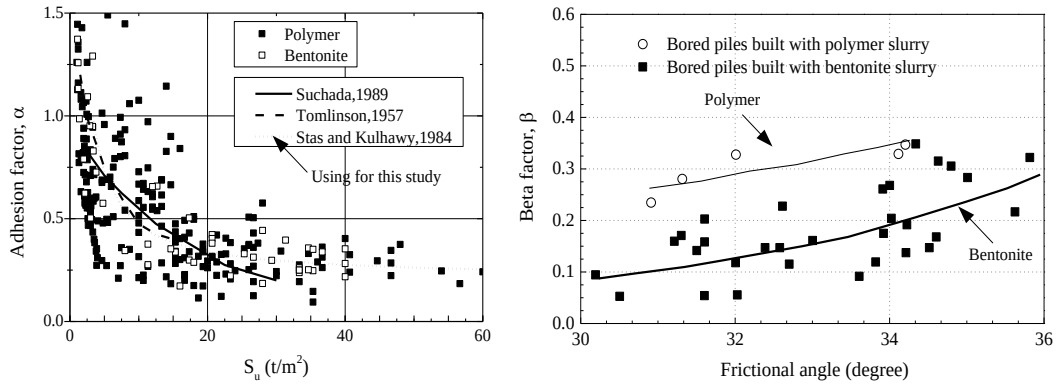

a) α and Su b) β and ϕ'

Figure 3.4 The reduction factor for pile shaft in clay and sand

The parameter $b_{,i}$ in Equation (3.2) can be determined by Equation (3.8) where the r_m is assumed to be $r_m \approx 2.5 \cdot L \cdot (1-\nu_s)$ (Randolph & Wroth, 1978)

$$b_{,i} = \frac{1}{\frac{r_0}{G_{s,i}} \ln\left(\frac{r_m}{r_0}\right) \cdot a_{,i}} = \frac{1}{C_{,i} \cdot a_{,i}}$$

$$C_{,i} = \frac{r_0}{G_{s,i}} \ln\left(\frac{r_m}{r_0}\right)$$

(3.8)

The elastic ground deformation is determined following Randolph and Wroth (1978)

$$w^e_{,i} = \frac{r_o}{G_{s,i}} \ln\left(\frac{r_m}{r_o}\right) \cdot \tau_{,i} = C_{,i} \cdot \tau_{,i} \qquad (3.9)$$

The shear modulus of the ground, $G_{s,i}$, is determined by Equation (3.10) (Imai & Tonouchi, 1982)

$$G_{s,i} = 1412 \cdot (N_{SPT})^{0.68} \quad (\text{t/m}^2) \qquad (3.10)$$

3.2.1.2 Pile base model

The settlement at pile tip, w^b, related to the mobilized tip resistance, P^b, is described by Equation (3.11) and t-z curve in Figure 3.3b.

$$P^b_{,n} = a_b(1 - e^{-b_b w^b_{,n}}) \qquad (3.11)$$

The parameter a_b in Equation (3.11) can be determined by

$$a_b = P^{bu} = \frac{P^{bf}}{R}, \qquad (3.12)$$

where

$$P^{bf} = \begin{cases} A_p \sigma'_{vb} N^*_q & ; \text{ for sand} \\ A_p \left(9 \cdot Su + \sigma_{vb}\right) & ; \text{ for clay} \end{cases} \qquad (3.13)$$

$$N^*_q = 0.539 + 0.64 \cdot e^{\phi'/30.662}$$

The parameter b_b in Equation (3.11) can be determined from the initial stiffness proposed by Randolph and Wroth (1978)

$$b_b = \frac{4G_{sb}r_0}{a_b\left(1-\nu_b\right)} \tag{3.14}$$

3.2.2 Algorithm

The flow chart of the proposed algorithm is shown in Figure 3.6. At the beginning, the loading is divided into ten steps from zeros to the ultimate capacity of the pile which determined by Equation (3.15)

$$Q_{ult} = 2\pi r_o \sum_{i=1}^{n} \tau_{,i}^{f} l_i + P^{bf} \tag{3.15}$$

For each load step, the settlement, S_j, of a pile j is determined by the Subroutine SA. By storing the settlements and corresponding loads Q_j=Q from ten steps load-settlement curve of a pile in the group can be constructed

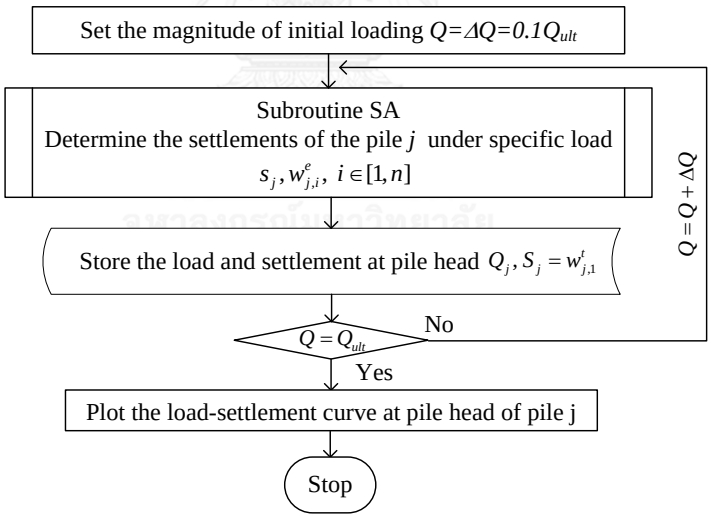

Figure 3.5 The flow chart to determine load - settlement curve of single pile

In the Subroutine SA, a pile j is divided into several segments. Then the settlement at pile base is assumed to be $w_{j,n}^{b}$ for determining the mobilized base resistance from Eq.(3.11). By Eq.(3.16), the settlement at the bottom can be related to settlements $\left(w_{j,n}^{s}; w_{j,n}^{s}\right)$ at the middle of the segment and the elastic compression ($w_{j,n}^{c}$) of the lower half of the segment as follows;

$$w_{j,n}^{b} = w_{j,n}^{s} + w_{j,n}^{e} - w_{j,n}^{c} \tag{3.16}$$

$$\begin{aligned} w_{j,n}^{c} &= \frac{1}{2}\cdot\left[P_{j,n}^{b} + \frac{P_{j,n}^{t} + P_{j,n}^{b}}{2}\right]\cdot\frac{l_n}{2E_pA_p} = \left[\frac{2P_{j,n}^{b}}{2} + \frac{P_{j,n}^{s} + P_{j,n}^{b} + P_{j,n}^{b}}{2}\right]\cdot\frac{l_n}{4E_pA_p} \\ &= \left[4P_{j,n}^{b} + \tau_{j,n}\cdot 2\pi r_0\cdot l_n\right]\cdot\frac{l_n}{8E_pA_p} \end{aligned} \tag{3.17}$$

Substitute Eq.(3.2), Eq.(3.9) and Eq.(3.17) into Eq.(3.16), the relationship between $w_{j,n}^{b}$ and $w_{j,n}^{s}$ can be rewritten as

$$\begin{aligned} w_{j,n}^{b} &= C_{j,n}\cdot\tau_{j,b} + w_{j,n}^{s} - \left[4P_{j,n}^{b} + \tau_{j,b}\cdot 2\pi r_0 l_{,n}\right]l_{,n} \\ &= C_{j,n}\left[a_{,n}\left(1-e^{-b_{j,n}w_{j,n}^{s}}\right)\right] + w_{j,n}^{s} - \left[4P_{j,n}^{s} + a_{j,n}\left(1-e^{-b_{j,n}w_{j,n}^{s}}\right)\cdot 2\pi r_0\cdot l_{,n}\right]\frac{l_{,n}}{8E_pA_p} \end{aligned} \tag{3.18}$$

Here the value of $w_{j,n}^{s}$ is implicitly determined from Eq.(3.18) by the Newton-Raphson algorithm instead of an explicit algorithm used in Wang et al. (2012) to avoid the dependency on calculation step-size.

After the value of $w_{j,n}^{s}$ has been calculated, and substituted into Eq.(3.9) for determining the elastic ground deformation, ($w_{j,n}^{e}$) by

$$w_{j,i}^{e} = C_{j,i}a_{j,i}\left(1-e^{-b_{j,i}w_{j,i}^{s}}\right) \tag{3.19}$$

As the same manner, the mobilized pile resistance can be obtained from Eq.(3.2), the applying load ($P_{j,n}^{t}$) and the settlement ($w_{j,n}^{s}$) at the top of the segment can be determined by

$$\begin{aligned} P_{j,n}^{s} &= 2\pi r_0\cdot l_{j,n}\cdot a_{,i}\left(1-e^{-b_{,i}w_{,i}^{s}}\right) \\ P_{j,n}^{t} &= P_{j,n}^{b} + P_{j,n}^{s} \\ w_{j,n}^{t} &= w_{j,n}^{b} + \left(\frac{P_{j,n}^{t} + P_{j,n}^{b}}{2}\right)\frac{l_{j,n}}{E_pA_p} \end{aligned} \tag{3.20}$$

Since the values at the top of the pile tip segment are similar to those at the bottom of the segment above, $w_{j,i-1}^{b} = w_{j,i}^{t}; P_{j,i-1}^{b} = P_{j,i}^{t}$, the same procedure can be repeated on the

adjacent segment in sequence until the settlement and the applying load at the pile head are obtained..

The whole process is repeated by increasing the value of $w_{,n}^{b}$ in a step of $\Delta w_{,n}^{b}$ if $P_{,1}^{t} \prec Q_j$.

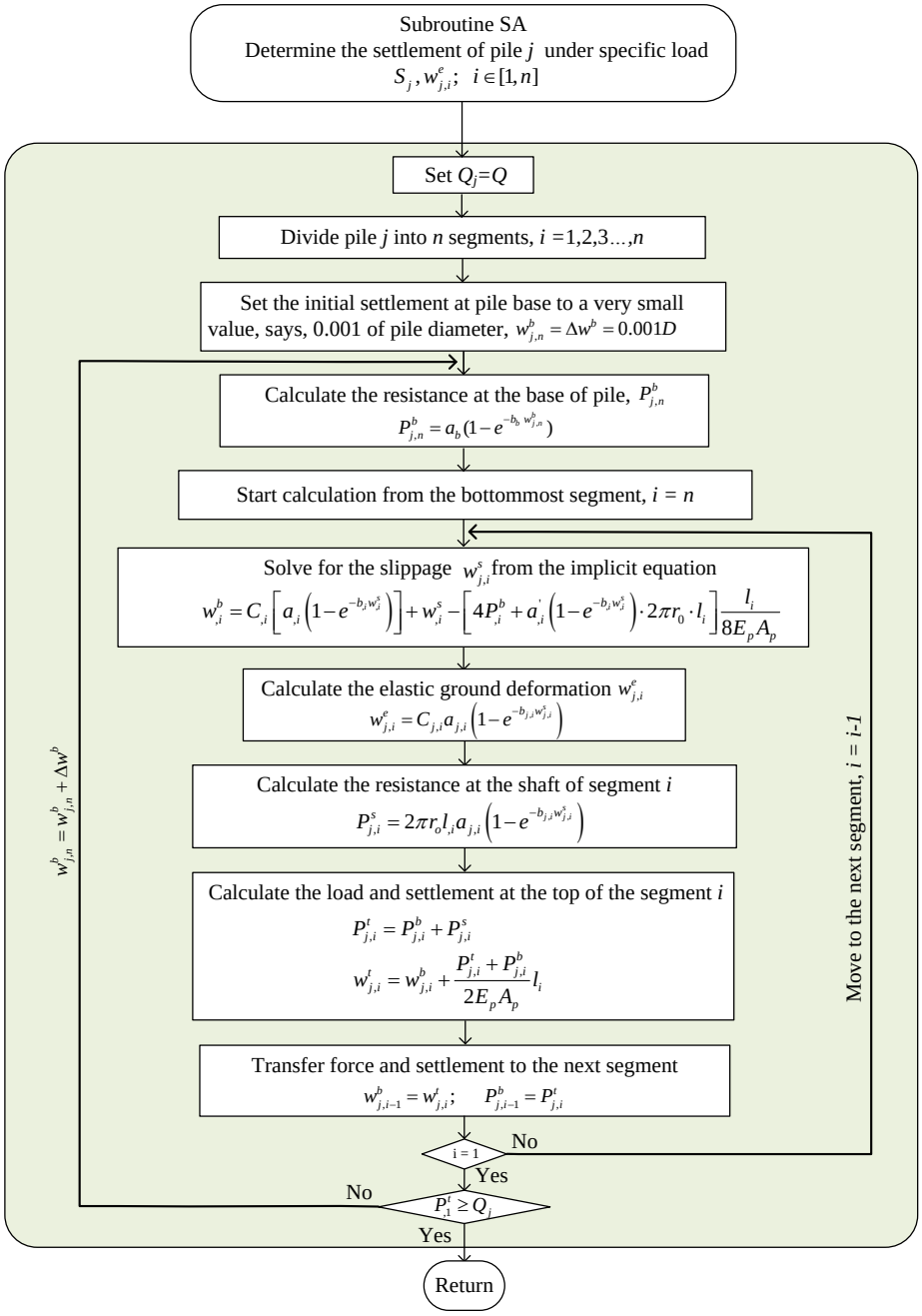

Figure 3.6 The flow chart for Subroutine SA

3.3 Comparison with prior work

3.3.1 Calculation step-size dependency

To demonstrate capabilities of the proposed algorithm, a simulation of a field test (He, 2002) is carried out and compared with the prediction by Wang et al. (2012). The field test was performed on a concrete pile with the diameter of 0.8 m and the length of 47.6 m. The Young's modulus of the concrete as reported was 30 GPa. Relevant soil properties which were used by Wang et al. (2012) are summarized in Table 3.1

Table 3.1 Soil profile and parameters used in the analysis by Wang et al. (2012)

Strata	Depth (m)	τ_f (kPa)	a (kPa)	b (1/m)
1. Silty clay	0 - 9.15	35.1	39	197.2
2. Silty clay	9.15 - 12.45	53.1	59	208.8
3. Silt	12.45 - 17.25	45.0	50	166.9
4. Fine sand	17.25 - 27.46	57.6	64	353.8
5. Silt	27.46 - 35.50	57.6	64	347.1
6. Silt	35.5 - 47.60	62.1	69	608.7
		–	1344*	150.0**

Remarks: * is a_b for pile tip, ** is b_b for pile tip

Firstly, the dependency of the algorithm proposed by Wang et al. (2012) on the calculation step-size is investigated. As shown in Figure 3.7 the predictions obtained from their algorithm varied with the values of $\Delta w_{,n}^{b}$. A good agreement with the measurement is obtained by assuming $\Delta w_{,n}^{b}$ to be 1 mm. When the similar parametric study is carried out with the proposed algorithm, it can be seen from Figure 3.8 that the predictions from all cases overlap with others and are not affected by the value of $\Delta w_{,n}^{b}$

.

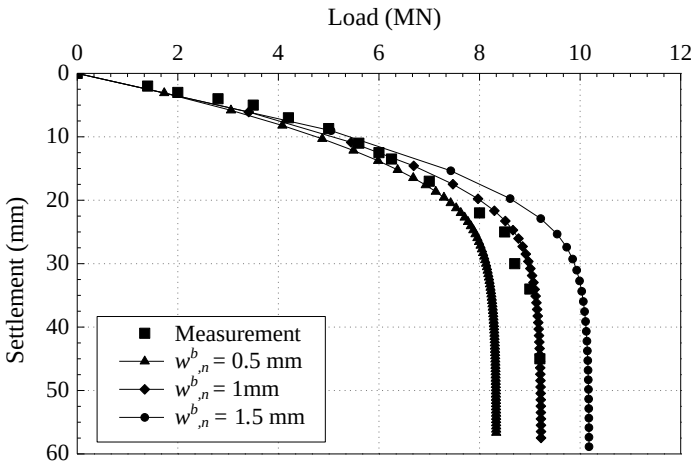

Figure 3.7 Load-settlement curves obtained from the algorithm of Wang et al. (2012)

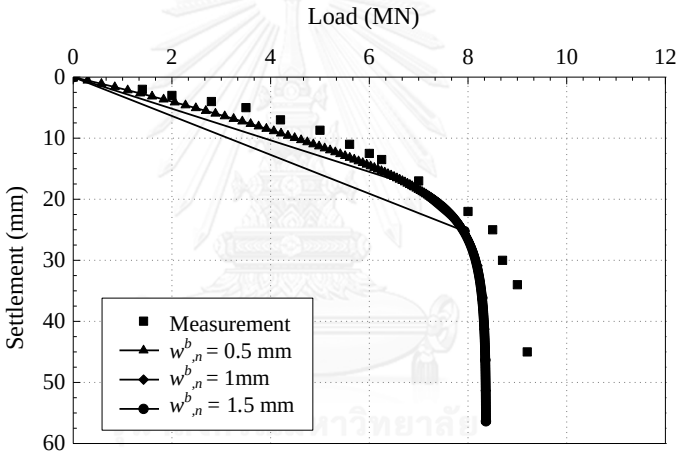

Figure 3.8 Load-settlement curves obtained from the proposed algorithm

3.3.2. Settlement profile of the outer zone

Mylonakis and Gazetas (1998), Zhang et al. (2014) proposed load transfer methods which consider the response of ground in far field and the interaction among piles in a group. However, the influence of the shaft friction extended over large because the slippage was not considered in their works. As the results, the settlement profile was overestimated in these methods.

By allowing the slippage at the pile-soil interface, the influence of shaft friction will be limited in a narrow zone once the plastic deformation had been occurred. The

deformation of ground in the outer area will be controlled mainly by its elastic behavior and will be smaller than those predicted by the non-slip models.

As an example, simulations of a field test by O'Neil at al. (1982) using slip and non-slip models are shown in Figure 3.9. The ground settlement profiles are determined when the pile head displacement is 1.0 mm, which is in the zone that all models successfully simulated the measured load-settlement curve. It can be seen from the figure that the ground settlement profile of the slip model is much smaller than those obtained from the non-slip models.

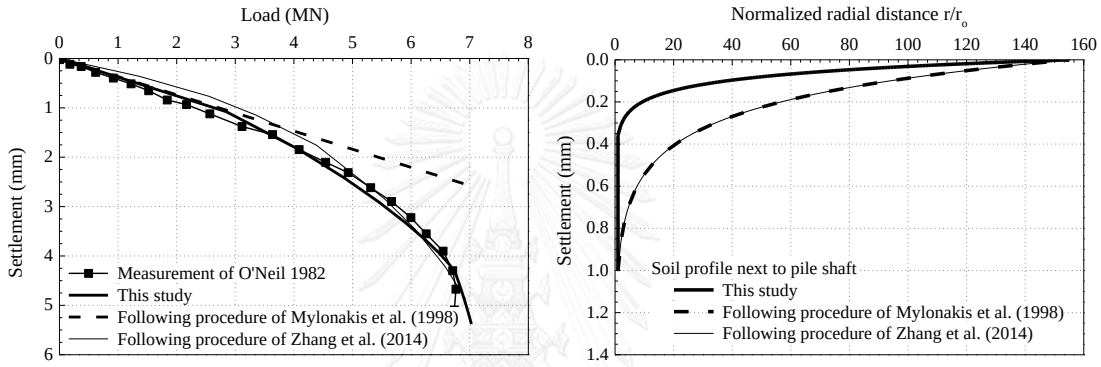

a) Load – displacement at pile head

b) Ground surface settlement profile

Figure 3.9 Simulations of a field test by slip and non-slip models.

3.4 Verification

3.4.1 Field tests in Bangkok

In this study, the performances of twenty five bored piles in Bangkok are estimated by the proposed method and compared with static pile load test results (ASTM 1143). The Bangkok ground formation can be divided into two parts. The upper part consists of 12~18 m of soft clay layers with the undrained shear strength of 5~25 kPa. It is underlain by layers of stiff to hard clay and dense sand as shown in Table 3.2. The diameters and lengths of piles are 1~2 m and 47~66 m, respectively. Most of pile tip are embedded in dense sand layers. Almost piles are built with polymer slurry during their constructions. Young modulus of concrete as estimated from the strength of concrete is 28 GPa.

Table 3.2. Subsoils relevant to pile foundations in Bangkok (Boonyatee et al, 2015; Likitlersuang et al, 2013)

Strata	Depth (m)	Description	SPT	Su (t/m2)
Crust	0 – 2	Weathered crust or backfills		
Upper layers	1 – 16	Very soft to medium stiff clays		0.5 - 2.5
The 1st clay	10 – 25	Stiff to very stiff clays	8 - 40	4.0 - 14.0
The 1st sand	14 – 38	Medium to very dense sand	18 – 50++	
The 2nd clay	24 – 43	Very stiff to hard clays	50++	> 15
The 2nd sand	30 – 58	Very dense sand	50++	

The test piles were equipped with 4~10 strain gauges along their length. The elastic shortenings were also monitored by rod extensometers installed at pile tips. The maximum test loads ranged between 10.0~45.5 MN, corresponding to 2.0~2.5 times of the design loads of the piles. The ratio between the end bearing resistance and the pile head load at the maximum loading condition can be determined, as shown Figure 3.10, basing the embedded strain gauges. It can be seen that, around 0.4~30% of the applying loads were sustained by the end bearing resistance while the remaining was sustained by the shaft resistance.

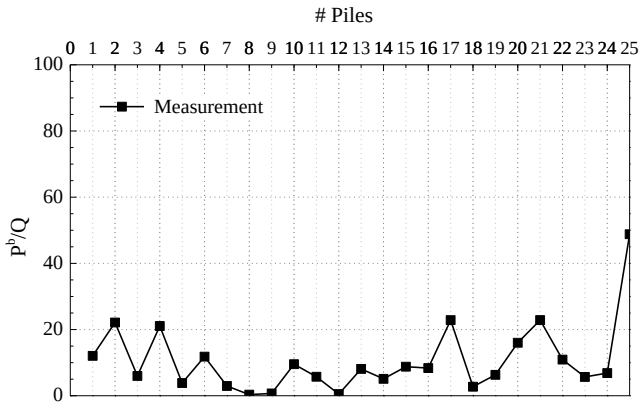

Figure 3.10 The ratio between base resistance and applied load at pile head at maximum loading condition

3.4.2 Compare with measured results.

For the interest of discussion, the load-settlement curve of pile #1, representing successfully predicted cases, is shown in Figure 3.11. To justify the accuracy of the proposed method, the mean ($\bar{x}$) and standard error (*SE*) of the mismatch between predicted and measured settlements at the same load are determined by

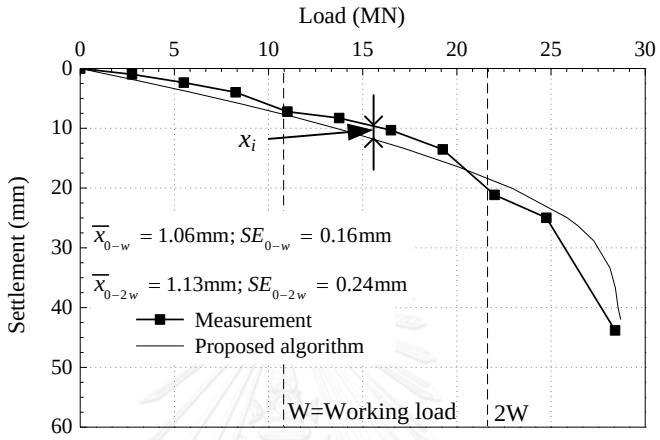

Figure 3.11 Load – settlement curve of pile #1

$$\bar{x} = \frac{\sum_{i=1}^{n} x_i}{n} \tag{3.21}$$

$$SD = \sqrt{\frac{\sum_{i=1}^{n} (x_i - \bar{x})^2}{n-1}} \tag{3.22}$$

$$SE = \frac{SD}{\sqrt{n}}, \tag{3.23}$$

where x_i is the difference between predicted and measured settlements at the same load, *SD* is the standard deviation, *n* is the number of comparison points. In this study, the range between zero and working load level is divided into 10 intervals. Therefore, the comparison are made at eleven points (n=11). For the range between zero and 2 times of working load, the comparison point is 21.

The standard error is adopted in this study instead of the coefficient of determination (R^2) because the latter is only suitable for linear regression analyses (Cameron & Windmeijer, 1997; Rangaswamy, 1995). Statistically speaking, the average of the

difference between predicted and measured values will lay inside the range of $\pm 1.96SE$ at 95% degree of confidence. The smaller standard error, the better is the agreement between the predicted and measured values. In the case of pile #1 (Figure 3.11) the $\bar{x}$ and *SE* values calculate over the range from zero to working load level are 1.06 mm and 0.16 mm, respectively. In other words, predicted values tend to be larger than measured values by 1.06 mm on average, with the error band of ± 0.32 mm at 95% degree of confidence. Compare to the typical allowance of 10 mm (Eurocodes 7), it can be concluded that the prediction will be on the conservative side with an acceptable degree of error for practical use. A similar interpretation is also made over the range from zero to two of working loads in order to evaluate the performance of the proposed approach under high degree of pile utilization. The $\bar{x}$ and *SE* values over this range are 1.13 mm and 0.24 mm, respectively. The larger values imply that the accuracy of prediction is inferior to the former case.

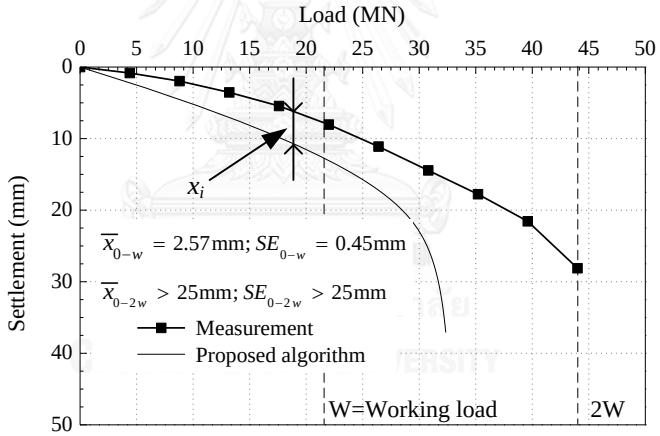

Figure 3.12 Load – settlement curve of pile #22

Similarly, the interpretation is made for pile #22 (Figure 3.12) which represents poor prediction cases. The values of $\bar{x}$ and *SE* over the working load level are 2.57 mm and 0.45 mm, respectively. The same parameters over the range of two of working loads become larger than 25 mm. This poor performance is the result of the underestimation of the ultimate capacity of the pile which might be associated with the uncertainties in construction and ground parameters. Since these factors are not uncommon and practically unavoidable, they are considered them in terms of statistic anomaly and are not be investigated further.

The values of $\bar{x}$ and *SE* of all cases are calculated and summarized in Figure 3.13. With the applied load in working load level, the $\bar{x}$ and *SE* range between 0.6 ~ 2.7 mm and 0.1~0.4 mm, respectively. The predictions are always larger than the measurements. When the interpretation is made over the range of two of working loads, the values of $\bar{x}$ and *SE* become larger as shown in Figure 3.14. In particular, there are five cases that $\bar{x}$ and *SE* are larger than 25 mm due to the reason mentioned earlier. When the five outlier cases are excluded, the $\bar{x}$ and *SE* values are in the range of 0.2~ 3.4 mm and 0.15-0.4 mm, respectively.

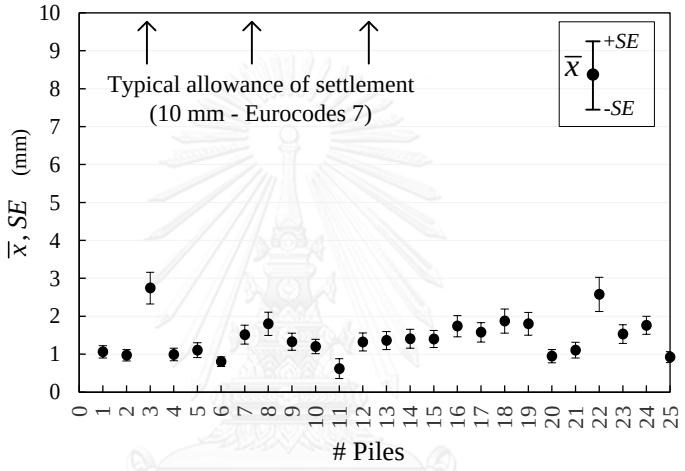

Figure 3.13 Summary of $\bar{x}$ and SE of load-settlement curves

(0 ~ working load level)

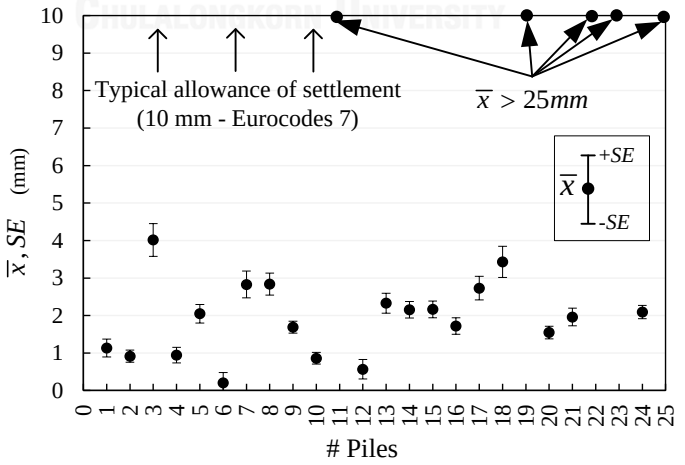

Figure 3.14 Summary of $\bar{x}$ and SE of load-settlement curves

(0 ~ 2 times of working load level)

The axial load distribution along depth of pile #1 is shown in Figure 3.15. The values of $\bar{x}$ and *SE* are also calculated for the mismatch (x_i) defined by the difference between predicted and measured loads at the same depth normalized by the working load of the pile. As shown in the same figure, the $\bar{x}$ and *SE* of the axial load distribution at the working load are 0.56% and 0.95%, respectively. In other words, the calculated axial load tend to be larger than the measured value by 0.56% on average with the error band of $\pm$1.86% at 95% degree of confidence.

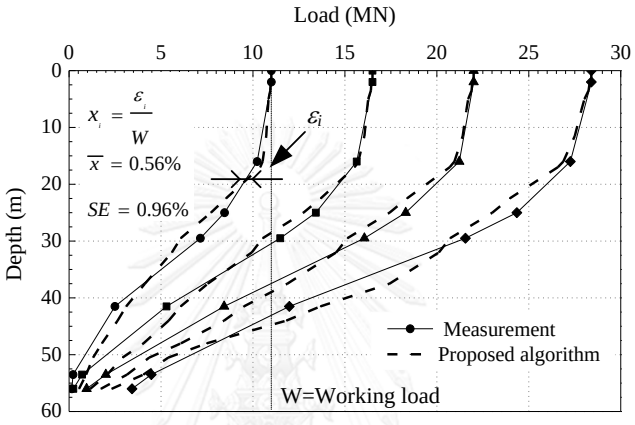

Figure 3.15 Axial load distribution of pile #1

For a comparison purpose, the axial load distribution along depth of pile #22 is shown in Figure 3.16. As expected, the prediction performance is inferior to the case of pile #1. The $\bar{x}$ and *SE* for the axial load distribution at working load are 9.15% and 1.03%, respectively.

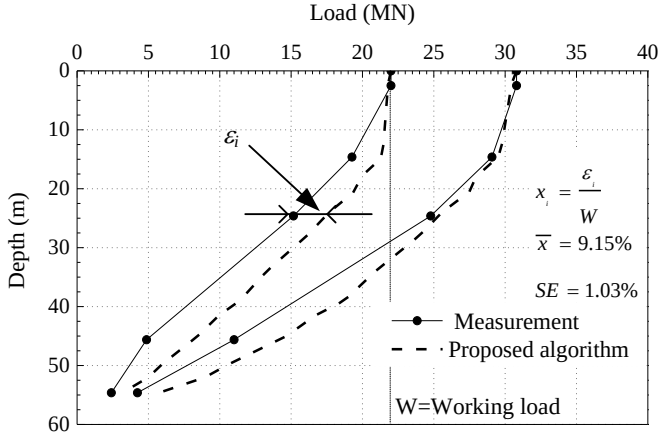

Figure 3.16 Axial load distribution of pile #22

Since it is exhaustive to show $\bar{x}$ and *SE* of all loading steps, only the values at working load level of the studied cases are presented in Figure 3.17. The $\bar{x}$ and *SE* are found to be in the range of -5% ~ 15% and 0.4~2.1%, respectively.

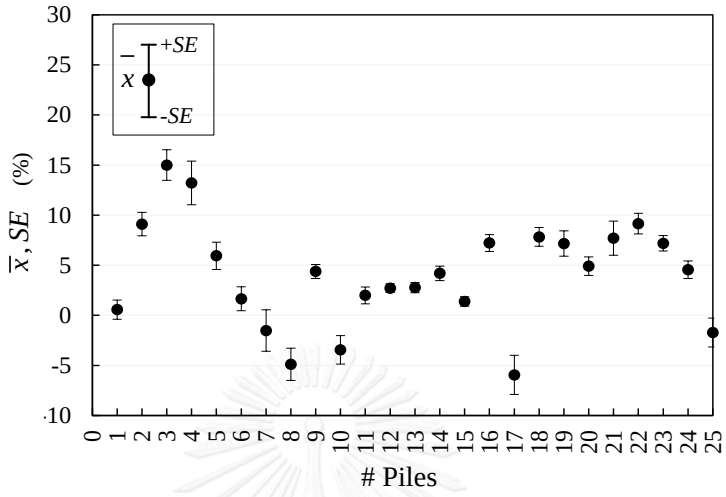

Figure 3.17 Summary of $\bar{x}$ and SE of axial load distribution (at working load level)

3.5 Conclusion

A load-transfer procedure for determining the settlement of single piles under vertical loading was presented. The proposed method is driven by an implicit algorithm which is not affected by the calculation step-size. Its performance was validated by twenty five static load test results of instrumented bored piles in Bangkok. Using parameters interpreted from site investigation reports, the proposed method overestimated measured settlements under working load levels by 0.6-2.7 mm on average. The differences between predicted and measured axial load distributions were in the range of -5% ~ 15% of the working load of the piles. Based on these statistics, the accuracy of the proposed method is found to be sufficient for practical purposes when a safety margin of two is applied.

CHAPTER 4: LINEAR ANALYTICAL METHOD FOR PILE GROUP CONSIDERING STIFFENING EFFECT

4.1 Introduction

Poulos (1968) firstly used linear boundary element method (BEM) to propose the interaction factor and simple equation for predicting the settlement of group piles. As the same level, Randolph & Wroth (1979) also proposed the linear elastic close-from solution by using the interaction factor concept. However, these approaches do not consider the stiffening effect due to other piles in the nearby areas (Chen et al, 2011)

Many later studies tried to modify the interaction factor method by considering the stiffening effect. It can be seen that, the modifications based on complex approaches including BEM (Sharnouby & Novak, 1985; 1990), Finite layer methods (Chow, 1986; Southcott & Small, 1996), Fictitious pile theory (Cao et al, 2007; Chen et al, 2011), hybrid approaches (Basile, 1999; Chow, 1986) are the best tool for considering the stiffening effect. However, they was required a lot of calculation effort.

The modifications based on closed-form solution of Randolph & Wroth (1979) (Mylonakis & Gazetas, 1998; Zhang et al, 2014) are deemed more suitable for engineering calculation. However, there have the differences on the applications of the stiffening effect between the former (Mylonakis and Gazetas, 1998) and the later authors (Zhang et al, 2014). In particular, the former authors modified the interaction factor of Randolph and Wroth (1978) by considering the response of passive pile on the modification of its settlement. Whereas, the later authors considered the presence of passive pile to modify the settlement active pile.

Thus, in this chapter, a new approach is proposed by an extension from the works of Mylonakis & Gazetas (1998) and Zhang et al (2014). The proposed approach is compared with the previous works, Finite element analysis (FEA) and experiment in elastic homogenous ground.

In shortly, this chapters is divided by into four parts: (1) Review and discussion the Interaction factor and stiffening effect; (2) Development of a linear analytical method

for settlement prediction of pile group considering the stiffening effect; (3) Verification of proposed approach (4) Conclusion.

4.2 Revisit to the interaction factor and stiffening effect

Poulos (1968) was firstly determined the interaction factor by using two-piles models in Figure 4.1. In this models, with the same applied load Q on two piles, the settlement of pile #1 would be larger than its value in single pile having the same condition because of the induced settlement due to the settlement of neighbor pile. Based on the induced settlement and settlement under own load of pile #1, the interaction factor can be determined by Equation (4.1). This factor depends on the stiffness ratio of piles and soil, the length of piles, the distance between two piles

$$\alpha_{21} = {}^{s_{21}}\!/_{s_1} \tag{4.1}$$

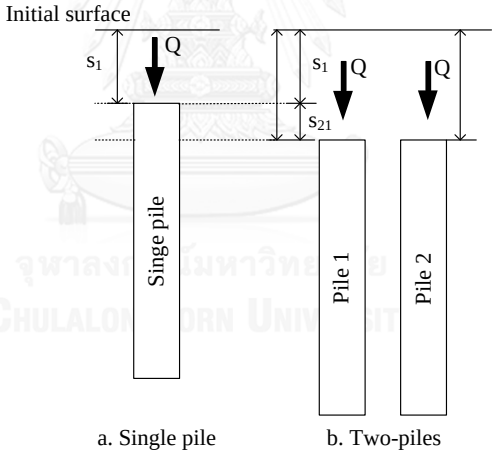

Figure 4.1 Determination of the interaction factor (Poulos, 1968).

By using the interaction factor, settlement of a pile in group can be easily determined by Equation (4.2) (Poulos, 1968). The settlement of a pile consists of its own settlement and the ones induced by other piles in the group.

$$S_i = \bar{s}\left(P_1 + P_2\alpha_{21} + .. + P_n\alpha_{n1}\right), \tag{4.2}$$

It is pointed out by Basile (1999), Cao et al (2007) and Chen et al. (2011) that overestimated results were obtained from Equation 4.2 due to two factors (1) the

settlement of a pile becomes smaller when other piles exist in the vicinity, (2) the interaction factor is affected by the number of piles in group.

To modify the interaction factor method of Poulos based on the linear elastic closed-form solution, the basic works of Randolph and Wroth (1979), Mylonakis and Gazetas (1998) and Zhang et al. (2014) were revisited in next paragraphs.

Randolph and Wroth (1979) proposed a close-from solution for settlement prediction of group piles based on interaction factor concept. In their work, the settlement at the shaft and base pile can be calculated by Equation (4.3) and (4.4), respectively. In addition, the settlement at pile head in can be determined by Equation (4.5).

$$w^{sh} = \frac{\tau_o r_o}{G_s}\ln\left(\frac{r_m}{r_o}\right) = C\cdot\tau_o \qquad (4.3)$$

$$C = \frac{r_o}{G_s}\ln\left(\frac{r_m}{r_o}\right)$$

$$w^{b} = \frac{P_b(1-\nu)}{4r_o G_s} \qquad (4.4)$$

$$w^{t} = \frac{P^t / r_o G_s}{\left(\frac{4}{(1-\upsilon)} + \frac{2\pi}{\ln(r_m/r_o)}\frac{L}{r_o}\frac{\tanh(\mu L)}{\mu L}\right)} \qquad (4.5)$$

$$\mu L = 2(L/ro)^2 \Big/ \left[ln(r_m/r_o)(E_p/G_s)\right]$$

The settlement of neighbor piles was assumed to be same as the ground deformation, which can be determined from Equations (4.6) and (4.7). Therefore, the interaction at pile shaft can be determined from Equations (4.1), (4.3) and (4.6), as followed Equation (4.8). In the same manner, the interaction factors at the pile base and pile head can be derived as shown in Equation (4.9) and (4.10).

$$U(r) = \frac{\tau_o r_o}{G_s}\ln\left(\frac{r_m}{r}\right) \qquad (4.6)$$

$$U_b(r) = \frac{P^b(1-\nu_b)}{4r_o G_{sb}}\frac{2r_o}{\pi r} \qquad (4.7)$$

$$\alpha_{sjk} = \frac{\ln\left(r_m / r_{jk}\right)}{\ln(r_m / r_o)} \tag{4.8}$$

$$\alpha_{b\,jk} = \frac{2}{\pi}\frac{r_o}{r_{jk}} \tag{4.9}$$

$$\alpha_{jk} = \frac{\left(\frac{4}{1-\nu_{sb}} + \frac{2\pi\rho}{\ln\left(r_m / r_o\right)}\frac{L}{r_o}\right)}{\left(\frac{4}{1-\nu_{sb}}\frac{r_{jk}}{2r_o/\pi + r_{jk}} + \frac{2\pi\rho}{\ln\left(r_m / r_o\right) + \ln\left(r_m / r_{jk}\right)}\frac{L}{r_o}\right)} - 1 \tag{4.10}$$

In addition, based on the Equation (4.2), (4.8) and (4.9) and assumed the same shear stress at pile shaft, the settlement of the shaft and base of each pile in group can be accounted the effects on another pile group by using Eq.(4.11) and (4.12), respectively.

$$\begin{aligned} w_j^{sh} &= w_{jj}^{sh} + \sum_{k=1,k\neq j}^{n_p} w_{jk}^{sh} \\ &= \frac{\tau_j r_o}{G_s}\ln\left(\frac{r_m}{r_o}\right)\cdot\left[1+\sum_{k=1,k\neq j}^{n_p}\frac{\ln(r_m / r_{jk})}{\ln(r_m / r_o)}\right] = \frac{\tau_j r_o}{G_s}\ln\left(\frac{r_m}{r_o}\right)\left[1+\sum_{k=1,k\neq j}^{n_p}\alpha_{sjk}\right] \end{aligned} \tag{4.11}$$

$$w_j^b = w_{jj}^b + \sum_{k=1,j\neq k}^{n_p} w_{jk}^b = \frac{P^b\left(1-\nu_b\right)}{4r_o G_{sb}}\left[1+\sum_{k=1,j\neq k}^{n_p}\alpha_{bjk}\right] \tag{4.12}$$

However, Mylonakis and Gazetas (1998) protested that neighbor piles was settle at the same rate with the ground deformation. They proposed the model including three steps to modify the interaction factor of Randolph and Wroth (1979), as shown in Figure 4.2.

As the loaded pile (active pile) settles (step 1), the surrounding ground will also settle (step 2) and induce the settlement on the unloaded pile (or in another words, the passive pile). However, the settlement of passive pile should be less than the surrounding ground because of the incompatibility of their stiffness (step 3). Therefore, the interaction factor will be smaller than the one determined by Equation (4.8). They defined this phenomenon as the stiffening effect. Based on an assumption that the interaction between pile shafts is stronger than those between pile bases, they proposed a new formula for determining the interaction factor as follows;

$$\alpha_{jk} = \xi \frac{\ln\left(r_m / r_{jk}\right)}{\ln(r_m / r_o)}, \tag{4.13}$$

where ξ is the diffraction factor which is smaller than 1.

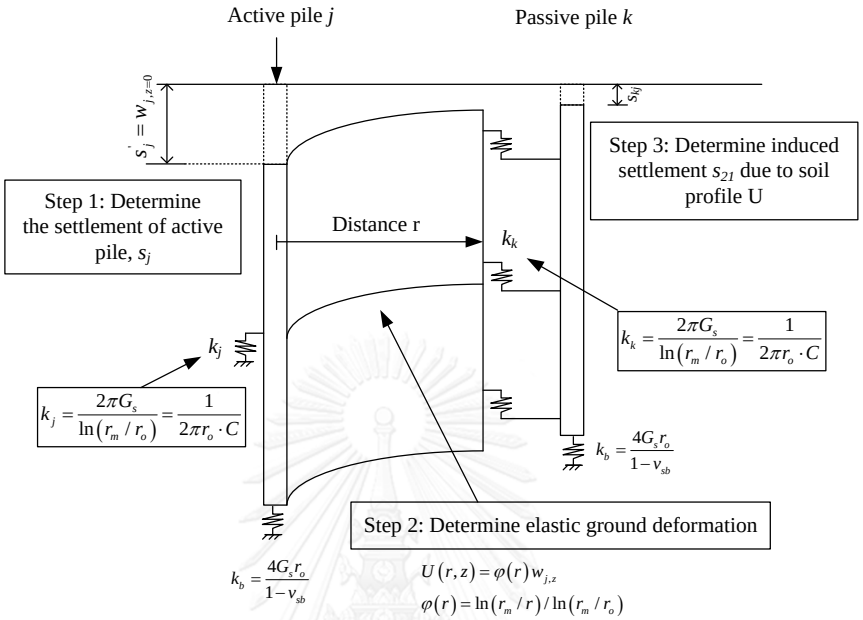

Figure 4.2 Determination of interaction factor (Mylonakis and Gazetas, 1998)

Zhang et al. (2014) also mentioned the stiffening effect, but the meaning was different from Mylonakis and Gazetas (1998). In their model, Figure 4.3, the passive pile settled at the same rate with the surrounding ground.

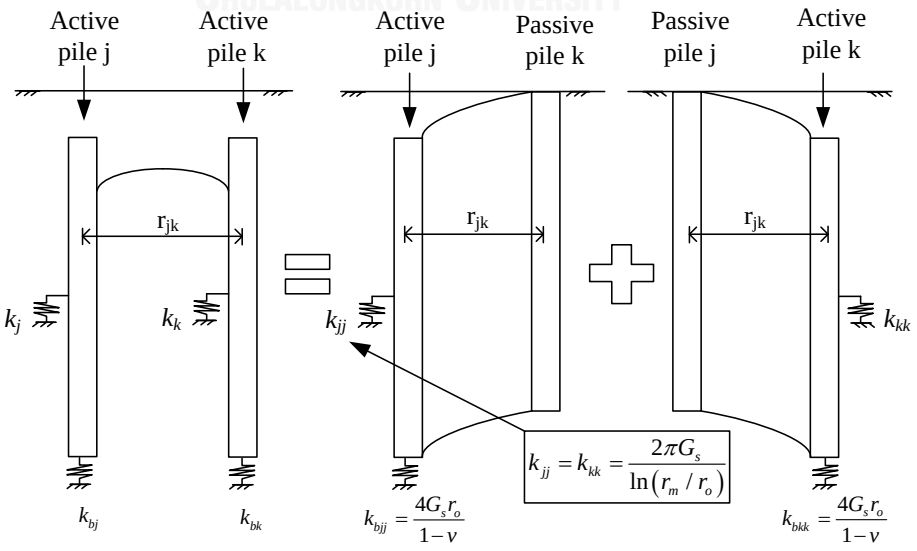

Figure 4.3 Interaction between 2 piles (Zhang et al. 2013)

However, Zhang et al. (2014) proposed that the shaft shear stress of pile k, τ_{kj}, induced by the spread of the shaft shear stress of pile j, τ_j, expressed by

$$\tau_{kj} = \frac{\tau_j r_o}{r_{kj}}, \tag{4.14}$$

was taken as the negative shear stress and added negative term, $w'_{jk,i}$, in the settlement of soil around pile j

$$w_{jk}^{sh'} = \frac{r_o}{G_s} \ln\left(\frac{r_m}{r_{jk}}\right) \cdot \tau_{kj} = \frac{r_0^2}{G_{s,i} r_{jk}} \ln\left(\frac{r_m}{r_{jk}}\right) \cdot \tau_{kj} \tag{4.15}$$

In the final, the Equation (4.11) proposed by Randolph and Wroth (1979), can be modified for considering stiffening effect of neighbor piles by

$$w_j^{sh} = \frac{\tau_j r_o}{G_s} \ln\left(\frac{r_m}{r_o}\right) \cdot \left[1 + \sum_{k=1,k\neq j}^{n_p} \frac{\ln(r_m / r_{jk})}{\ln(r_m / r_o)} - \sum_{k=1,k\neq j}^{n_p} \frac{r_0}{r_{jk}} \frac{\ln(r_m / r_{jk})}{\ln(r_m / r_o)}\right] \tag{4.16}$$

By change the Equation (4.16) to the form of stiffness, the stiffness at the shaft of the active pile j, k_j in Figure 4.3, can be expressed by

$$\frac{1}{k_j} = \frac{1}{k_{jj}} + \frac{1}{k_{jk}} - \frac{1}{k'_{jk}} \tag{4.17}$$

where k_j is the combined stiffness at the shaft of pile j

$k_{jj} = \dfrac{2\pi G_s}{\ln\left(r_m / r_o\right)}$ is the original stiffness at the shaft of pile j

$k_{jk} = \dfrac{2\pi G_s}{\ln\left(r_m / r_{jk}\right)}$ is the contribution of the settlement at the shaft of pile k on pile j

$k'_{jk} = \dfrac{2\pi G_s}{\frac{r_o}{r_{jk}} \ln\left(r_m / r_{jk}\right)}$ is the stiffening effect due to pile k on pile j

4.3 Linear analytical method for pile group considering stiffening effect.

4.3.1 Assumptions and mathematic models

In this part, a new proposed model is extension from the model of Mylonakis and Gazetas (1998) by adopted the work of Zhang et al. (2014). In particular, the stiffness at the shaft of active pile *j* in Figure 4.2 is calculated based on Equation (4.17) (Zhang et al, 2014) for considering stiffening effect due to other nearby piles in group, as follows;

$$\frac{1}{k_j} = \frac{1}{k_{jj}} - \frac{1}{k'_{jk}} = \frac{\ln\left(r_m / r_o\right)}{2\pi G_s} - \frac{\ln\left(r_m / r_{kj}\right)}{2\pi G_s} \tag{4.18}$$

Compare calculated stiffness in Equation (4.18) to the stiffness at pile shaft in Figure 4.2, the term of k'_{jk} presented for considering the stiffening effect, is added. Compare Equation (4.18) to the Equation (4.17), the term of k_{jk} is removed because passive pile *k* has no load at pile head.

In case of one active pile and multi-passive pile, which presents for considering stiffening effect of all piles in group on an active pile, Equation (4.18) can be changed to

$$\begin{aligned}\frac{1}{k_j} &= \frac{1}{k_j} - \frac{1}{k'_{jk}} = \frac{\ln\left(r_m / r_o\right)}{2\pi G_s} - \frac{\sum_{k=1, j\neq i}^{n} \frac{r_o}{r_{jk}} \ln\left(r_m / r_{jk}\right)}{2\pi G_s} \\ &= \frac{\ln\left(r_m / r_o\right)}{2\pi G_s} \cdot \left(1 - \left[\sum_{k=1,k\neq j}^{n} \frac{r_o}{r_{kj}} \ln\left(\frac{r_m}{r_o}\right)\right] / \ln\left(\frac{r_m}{r_o}\right)\right) \\ &= 2\pi r_o \cdot C \cdot \left(1 - \left[\sum_{k=1,k\neq j}^{n} \frac{r_o}{r_{kj}} \ln\left(\frac{r_m}{r_o}\right)\right] / \ln\left(\frac{r_m}{r_o}\right)\right)\end{aligned} \tag{4.19}$$

where $C = \frac{r_o \cdot \ln(r_m / r_o)}{G_s}$ was already mentioned in Equation (4.3).

It is seen that, in Equation (4.19) the stiffening effect of all pile in group can be simplified by a new parameter, as follows

$$\zeta_j = 1 - \left[\sum_{k=1,k\neq j}^{n} \frac{r_o}{r_{kj}} \ln\left(\frac{r_m}{r_o}\right) \right] / \ln\left(\frac{r_m}{r_o}\right) \tag{4.20}$$

However, this parameter can be negative in cases of group piles having the number of passive pile *k* larger than 16. Example, the 5x5-piles pile group case having pile length, L = 50 m, r_o = 1 m, ν_s = 0.5, s/D=3. Thus, in this study, the proposed stiffening parameter in (4.20) is modified by

$$\zeta_j = 1 - \left[\sum_{k=1,k\neq j}^{n} \frac{r_o}{r_{kj}} \ln\left(\frac{r_{ms}}{r_o}\right) \right] / \ln\left(\frac{r_m}{r_o}\right), \tag{4.21}$$

r_{ms} is the corrected r_m considering the stiffening effect due to other nearby pile.

To proposed the determination of r_{ms} , there have some studied cases including one active pile and multi-passive pile were analyzed by 3D Finite Element Analysis (Plaxis 3D). The outline of the studied cases are shown in Figure 4.4. The active piles in all cases were loaded with a constant magnitude load and the properties of soil, piles and load were the same for all cases.

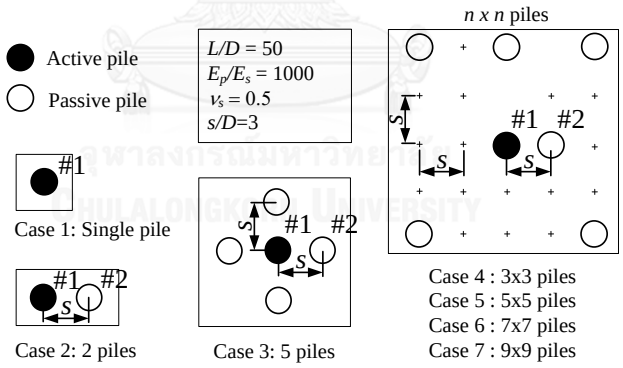

Figure 4.4 The outline of studied cases for proposing the determination of r_{ms}

The settlements of active pile #1 were predicted and normalized with the settlement of single pile, as shown in Figure 4.5. Following the 3D FEA results, it can be seen that, the settlements of active pile #1 became less as the number of pile in the group increased and slowly decrease when number of piles was larger than 81. For 81-piles group piles, the settlement of the loaded pile reduced by 12.42% compared to the single pile case. Besides, the predictions from proposed Equation (4.17) of Zhang et al. (2014)

underestimate the settlement of active piles #1. Based on the curve fitting with 3D FEA results, the proposed r_{ms} can be determined following

$$r_{ms} = 0.02r_m + 10r_o \tag{4.22}$$

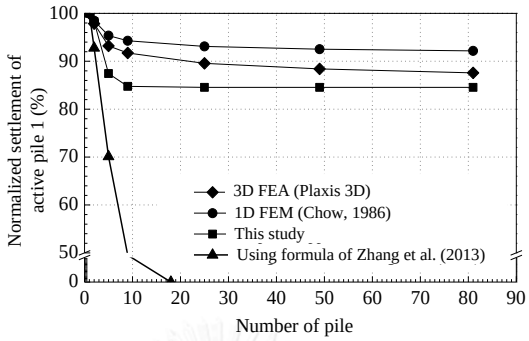

Figure 4.5 Settlement of active pile 1 when number of passive pile increase

In finally, the new proposed model based on the modification of the model in Figure 4.2 can be showed Figure 4.6.

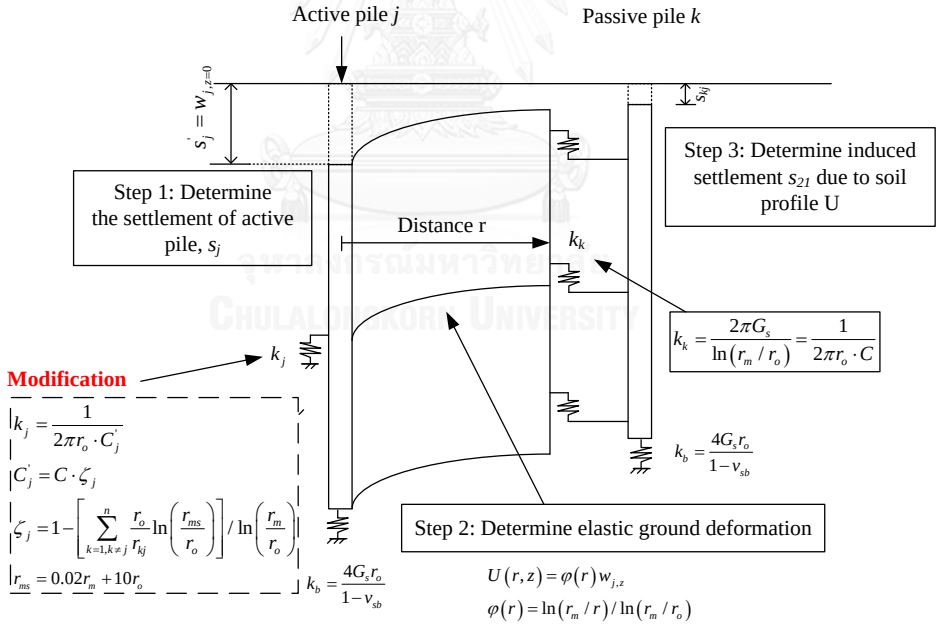

Figure 4.6 Determination of interaction factor considering the stiffening effect

4.3.2 Algorithm

The model in Figure 4.6 is used for determining the interaction factor between two pile considering the stiffening effect due to other pile in the nearby areas. Following

Figure 4.6, firstly, the determination of settlement along depth of an active pile in homogenous ground can be calculated by the root of following Equation (4.23).

$$E_p A_p \frac{d^2 w_{j,z}}{dz^2} - k_j w_{j,z} = 0, \tag{4.23}$$

where $k_{j,z}$ is determined by Equation (4.19)

The general solution of Equation (4.23) can be written by

$$w_{j,z} = c_1 e^{\lambda_j z} + c_2 e^{-\lambda_j z} \tag{4.24}$$

To solve Equation (4.24), the boundary condition at pile head and pile base are considered as follows;

$$\begin{cases} E_p A_p \dfrac{dw_{j,z}}{dz}\Big|_{z=0} = -1 \text{ (unit load)} \\ E_p A_p \dfrac{dw_{j,z}}{dz}\Big|_{z=L} = -k_b w_{1,L} \end{cases}, \tag{4.25}$$

Base on Equation (4.24) and (4.25), the solutions of Equation (4.24) can be obtain as follows;

$$\begin{aligned} c_1 &= \frac{-e^{-\lambda_j L}\left(k_b - a_1\right)}{a_j\left[e^{\lambda_j l}\left(k_b + a_j\right) + e^{-\lambda_j l}\left(k_b - a_j\right)\right]} \\ c_2 &= \frac{e^{\lambda_j L}\left(k_b + a_1\right)}{a_j\left[e^{\lambda_1 l}\left(k_b + a_j\right) + e^{-\lambda_1 l}\left(k_b - a_j\right)\right]}, \\ \lambda_j &= \sqrt{k_j / E_p A_p}\,; a_j = \sqrt{k_{1z} E_p A_p} \end{aligned} \tag{4.26}$$

Secondly, the ground deformation made by settlement of active pile can be determined by Equation;

$$\begin{aligned} U(r_{kj}, z) &= \varphi(r_{kj})\left(c_1 e^{\lambda_j z} + c_2 e^{-\lambda_j z}\right) \\ \varphi(r_{kj}) &= \frac{\ln\left(r_m / r_{kj}\right)}{\ln\left(r_m / r_o\right)} \end{aligned} \tag{4.27}$$

Thirdly, the settlement of passive pile induced by ground deformation can be determined following the root of Equation (4.28) (Mylonakis & Gazetas, 1998)

$$E_p A_p \frac{d^2 w_{kj,z}}{dz^2} - k_k \left[w_{kj,z} - U(r_{kj}, z) \right] = 0 \tag{4.28}$$

The solution of Equation (4.28) can be written by;

$$\begin{aligned} w_{kj,z} &= c_{21} \mathrm{e}^{\lambda_k z} + c_{22} \mathrm{e}^{-\lambda_k z} - \frac{\lambda_k^2}{\lambda_j^2 - \lambda_k^2} \varphi(r_{kj}) \left(\mathrm{c}_1 \mathrm{e}^{\lambda_j z} + \mathrm{c}_2 \mathrm{e}^{-\lambda_j z} \right) \\ \lambda_k &= \sqrt{k_k / E_p A_p} \; ; a_k = \sqrt{k_k E_p A_p} \end{aligned} \tag{4.29}$$

To solve the Equation (4.29), the boundary condition at head and base of passive pile are considered as follows;

$$\begin{cases} E_p A_p \dfrac{dw_{kj,z}}{dz} |_{z=0} = 0 \\ E_p A_p \dfrac{dw_{kj,z}}{dz} |_{z=l} = -k_b w_{kj}(l) \end{cases} \tag{4.30}$$

Base on Equation (4.29) and (4.30), the solution of Equation (4.28) can be obtained as follows;

$$\begin{cases} c_{21} = \dfrac{-\frac{\lambda_k \lambda_j}{\lambda_j^2 - \lambda_k^2} \varphi(r_{kj}) (c_1 - c_2) \mathrm{e}^{-\lambda_k l} \left(1 - \frac{k_b}{a_k} \right) + \frac{\lambda_k}{\lambda_j^2 - \lambda_k^2} \varphi(s) \left[c_1 \mathrm{e}^{\lambda_j l} \left(\lambda_j + \frac{k_b \lambda_k}{a_k} \right) - c_2 \mathrm{e}^{-\lambda_j l} \left(\lambda_j - \frac{k_b \lambda_k}{a_k} \right) \right]}{\left[\mathrm{e}^{\lambda_k l} \left(1 + \frac{k_b}{a_k} \right) - \mathrm{e}^{-\lambda_k l} \left(1 - \frac{k_b}{a_k} \right) \right]} \\ c_{22} = \dfrac{-\frac{\lambda_k \lambda_j}{\lambda_j^2 - \lambda_k^2} \varphi(r_{kj}) (c_1 - c_2) \mathrm{e}^{\lambda_k l} \left(1 - \frac{k_b}{a_k} \right) + \frac{\lambda_k}{\lambda_j^2 - \lambda_k^2} \varphi(s) \left[c_1 \mathrm{e}^{\lambda_j l} \left(\lambda_j + \frac{k_b \lambda_k}{a_k} \right) - c_2 \mathrm{e}^{-\lambda_j l} \left(\lambda_j - \frac{k_b \lambda_k}{a_k} \right) \right]}{\left[\mathrm{e}^{\lambda_k l} \left(1 + \frac{k_b}{a_k} \right) - \mathrm{e}^{-\lambda_k l} \left(1 - \frac{k_b}{a_k} \right) \right]} \end{cases}$$

The interaction factor between 2 piles is determined by ratio unit settlement at the top of passive pile and active pile, as shown in Eq. (4.31)

$$\alpha_{21} = \frac{w_{kj,z=0} = s_{21u}}{w_{j,z=0} = s_{1u}^{'}} = \frac{c_{21} + c_{22}}{c_1 + c_2} - \frac{\lambda_k^2}{\lambda_j^2 - \lambda_k^2} \varphi(r_{kj}) \tag{4.31}$$

By using the new interaction factor, the settlement of each pile in group considering stiffening effect, can be determined by

$$S_i = \left(Q_1 s_{1u}^{'} \alpha_{i1} + Q_2 s_{2u}^{'} \alpha_{i2} + \ldots Q_i s_{iu}^{'} \cdot 1 + \ldots + Q_n s_{nu}^{'} \alpha_{in} \right) \tag{4.32}$$

The performance of pile group is determined based on the condition of the pile cap. For flexible raft condition which all piles was under same applied load, the settlement each pile determined by Equation (4.32). Basing on the settlement of each pile, the settlement distribution of pile group is obtain.

For rigid cap condition which all piles displace at the same rate, the reaction of each pile can be determined by,

$$\begin{cases} S_1 = \left(Q_1 s'_{1u} \cdot 1 + Q_2 s'_{2u} \alpha_{12} + \ldots Q_i s'_{iu} \alpha_{1i} + \ldots + Q_n s'_{nu} \alpha_{in}\right) \\ \quad \ldots\ldots \\ S_i = \left(Q_1 s'_{1u} \alpha_{i1} + Q_2 s'_{2u} \alpha_{i2} + \ldots Q_i s'_{iu} \cdot 1 + \ldots + Q_n s'_{nu} \alpha_{in}\right) \\ S_1 = \ldots = S_i = \ldots = S_n \end{cases} . \quad (4.33)$$

By the summation of resistance of each pile, the resistance of pile group is determined.

4.4 Verification

4.4.1 Verification with 3D FEA

To validate the proposed approach, performances of pile groups under flexible and rigid cap conditions were analyzed by the proposed method and compared to 3D FEA (Plaxis 3D) and the predictions from other previous approaches (Poulos, 1968; Mylonakis & Gazetas, 1998; Zhang et al, 2014).

Firstly, for the flexible cap condition which all piles have same applied load and the settlement of center pile is the maximum values. Thus, the settlements of center piles in 5, 9, 25, 49 and 81-piles group with flexible pile cap (Figure 4.7), were determined and showed in Figure 4.8. For the comparison purpose, the obtain values were normalized by solutions of 3D FEA. The values from Poulos's approach are the largest whereas those from the proposed method are closest to the 3D FEA results. The well agreement between predicted settlements from the proposed approach and 3D FEA are obtained because the more number pile of the group is, the more stiffening effect occur.

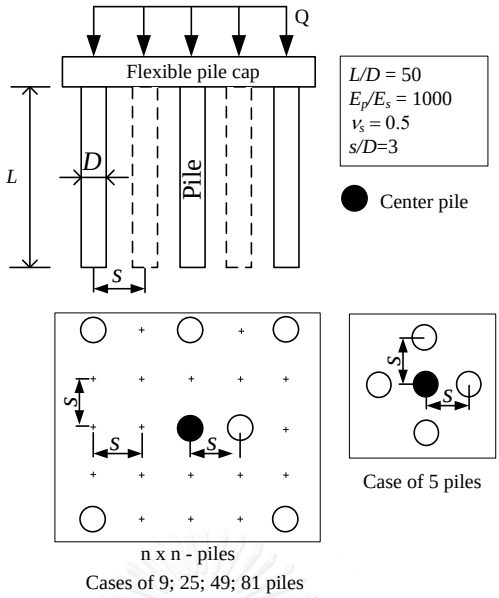

Figure 4.7 5, 9, 25, 49 and 81-piles pile groups with flexible cap

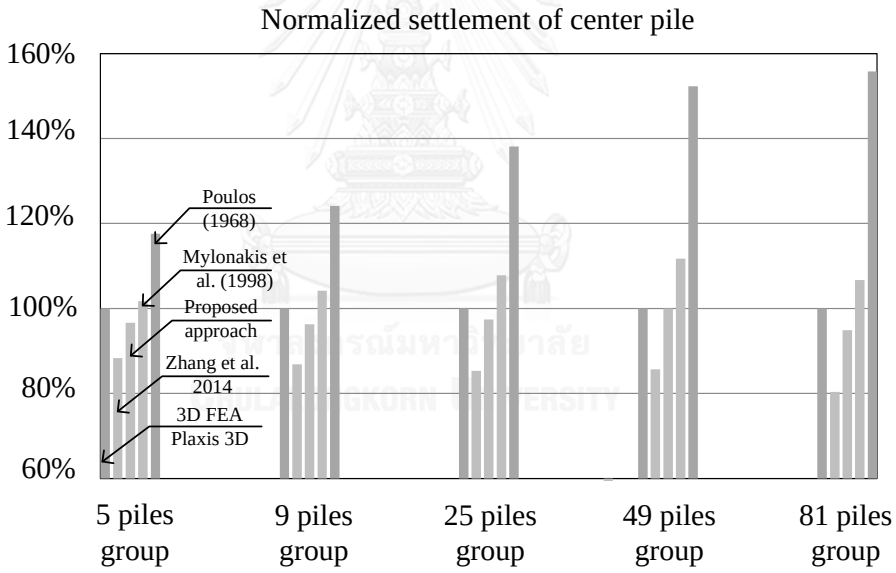

Figure 4.8 Normalized settlements of center piles in group piles with flexible cap condition

For rigid cap condition which all piles displace at the same rate, the reaction of each pile in a group was determined and normalized by the reaction of the center pile in the corresponding case. From the results in Figure 4.9 for 9-piles pile group and Figure 4.10 for 25-piles pile group, it can been seen that the distribution of load obtain from the proposed approach method are the closet results to the 3D FEA. The well agreement

between predicted load distribution from proposed approach and 3D FEA are obtained because the larger the settlement of the center pile is, the larger the reaction at corner pile.

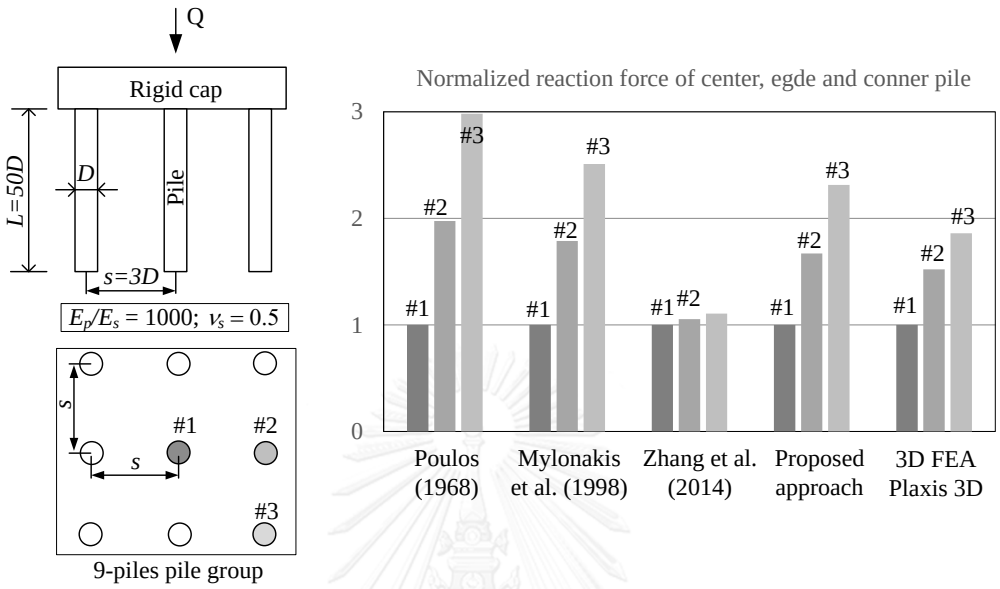

Figure 4.9 Load distributions among piles in 9-piles pile group under rigid cap

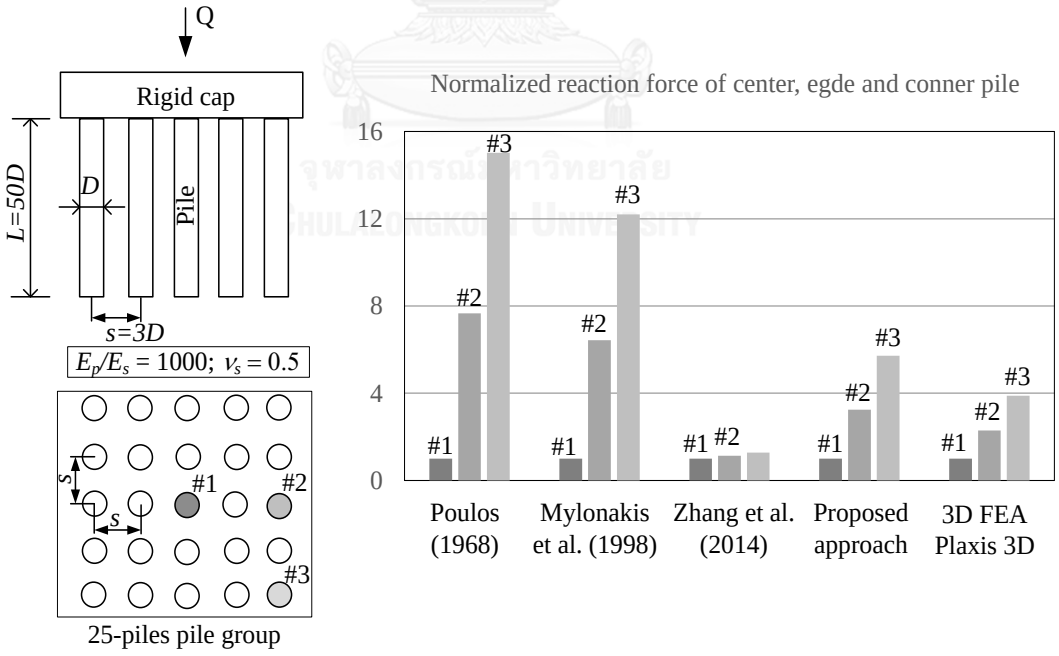

Figure 4.10 Load distributions among piles in 25-piles pile group under rigid cap

4.4.2 Verification with experiment

In addition to 3D FEA, experiments on reduced scale models were also carried out for verification purpose.

4.4.2.1 Experiment setup

A reduced scale model is implemented in 1g to investigate the stiffening effect in pile groups. An artificial homogenous elastic ground made of Jelly is prepared in a container with the size of 30x40x60 cm^3 (width x length x height).

The Young modulus of the ground is determined from the unconfined compression test (Figure 4.11.a) and confined compression test (Figure 4.11.b). The specimens having diameter of 10 cm and the height of 3 to 4 cm.

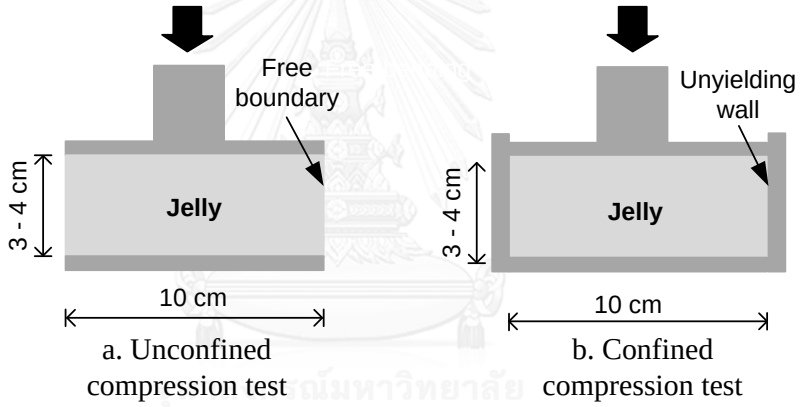

Figure 4.11 Determination of the Young modulus of the ground

The unconfined compression test results are shown in Figure 4.12. It can be seen that, the slope, or in other words, the Young modulus varies with the stress level in the range of 7~74 kPa. The confined compression test results are shown in Figure 4.13. The constraint Young modulus determined from the graph is around 2000 kPa. Using the relationship between constraint and unconstraint Young modulus as shown in Equation (4.34) and assuming the Poisson's ratio in the range of 0.495~0.499, the unconstraint Young modulus from the latter test was found to be in the range of 12~60 kPa.

$$E_{constrain} = \frac{E(1-\nu)}{(1-2\nu)(1+\nu)} \tag{4.34}$$

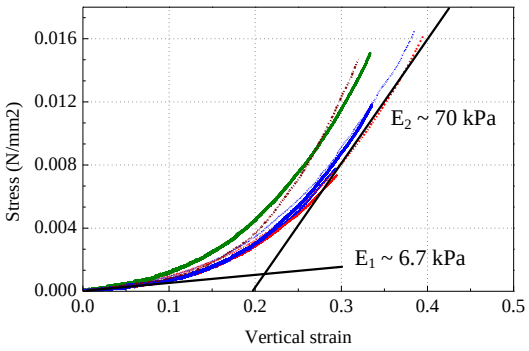

Figure 4.12 Unconfined compression test results

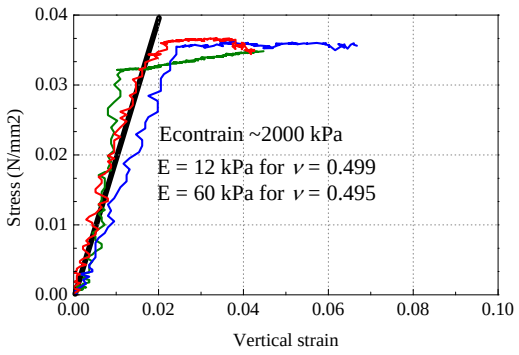

Figure 4.13 Confined compression test results

To check the homogeneity of ground, couple samples were taken randomly from twelve locations for determined the water content. The homogeneity study of the ground that can be expressed by the relationship between F (F-static) and F_{crit}. The F is a ratio of two variances (MS) of water contents including variance between group and variance within group. The F_{crit} is a function of the degrees of freedom of the numerator (df – between group), the denominator (df – within group) and the significance level (α). This kind of evaluations are typically described by using one-way analysis of variance (ANOVA) Figure 4.14

Anova analysis

The moisture of couple samples from in 12 random locations

No-Location	F1 (sample 1)	F2 (sample 2)
1	94.577	94.591
2	94.524	94.568
3	94.582	94.658
4	94.660	94.606
5	94.620	94.563
6	94.575	94.559
7	94.637	94.593
8	94.709	94.623
9	94.632	94.607
10	94.618	94.570
11	94.618	94.612
12	94.674	94.588

Anova: Single factor

Description

	Count	Sum	Mean	Variance	SS
F1	12	1135.425	94.619	0.002	0.027
F2	12	1135.137	94.595	0.001	0.009

Anova α 0.050

Source	SS	df	MS	F	P value	Fcrit
Between group	0.003	1	0.003	2.081	0.163	4.301
Within group	0.036	22	0.002	**If F < Fcrit**		
Total	0.040	23	0.002		**Homogenous**	

Figure 4.14 Anova analysis for checking the homogenous of ground

The model pile are made of Cypress wood. Following the JIS Z2101 Standard, the Young modulus of wood was found to be 33.1 MPa at the water content of 12% (Ross, 2010) . Since the pile absorb some water from the made ground. It was suspected that the Young modulus might vary with the water content. Therefore, the Young modulus

at various water content were also determined as shown in Figure 4.15. The Young modulus decrease as the water content increases.

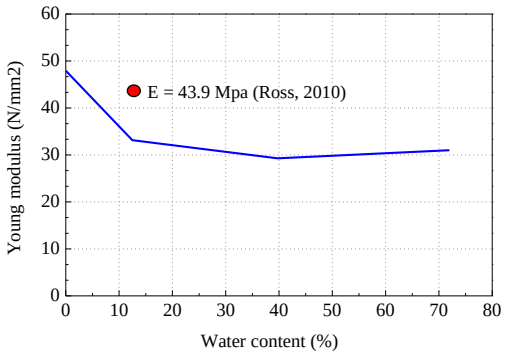

Figure 4.15 Young modulus of Cypress wood with water content

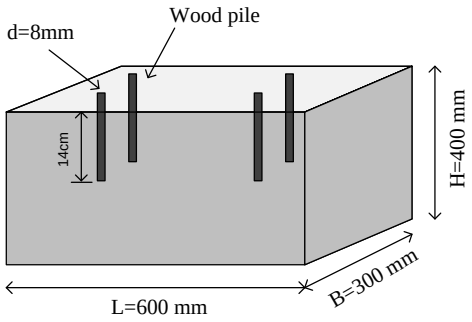

Figure 4.16 Outline of model piles and container.

To avoid the boundary effect, the thickness of soil below pile tip should be larger than two of pile length (Randolph &Wroth, 1978). In addition, the distance from a pile to the container wall should be larger than ten times of pile diameter (Poulos, 1980). According to these guidelines, the diameter and the length of piles were set to 8 mm and 140 mm, respectively. The outline of model is shown in Figure 4.16.

To investigate the stiffening effect, comparisons were made on the settlements of piles which have the difference number of piles in the vicinity. The tests were carried out in the seven batches on the ground and the pile arrangements as shown in Figure 4.17. The parameter of the tests were summarized in Table 4.1

Table 4.1 The parameter of pile group

Pile cap condition	n_p	r/d	$h_{container}/L$	Ep (kPa)	Es (kPa)	E_p/E_s
Free	1 2 5 9 25	3	~ 4	~30000	~10	~ 3000

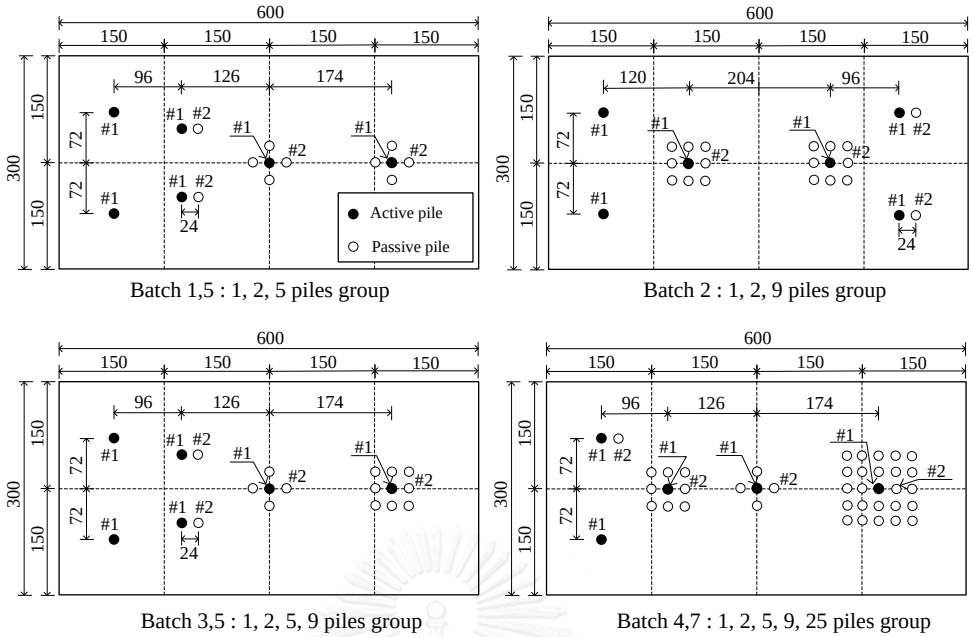

Figure 4.17 The intended experiment models in container

The test preparation including 6 steps is shown in Figure 4.18. Firstly, the 80^0C hot water was prepared. The gelatin powder in the 6% by weight of water was mixed with hot water. After that, the mixing was poured into the container. The wood piles, hanged pile fix frame and clip (Figure 4.19), were inserted in container. This system was cured for 30 hour in 20^0C cold environment. Finally, the fix frame would be removed as the Jelly was made. Finally, the loading system on the frame load was setup. The photos for experiment batches were showed in Figure 4.20.

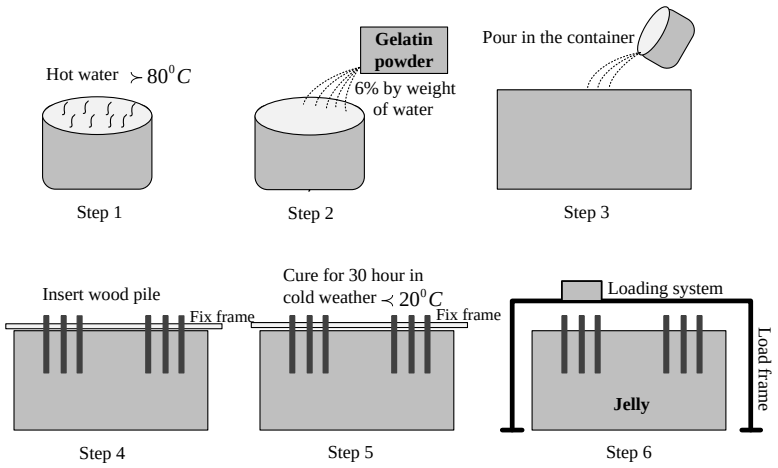

Figure 4.18 The test preparation

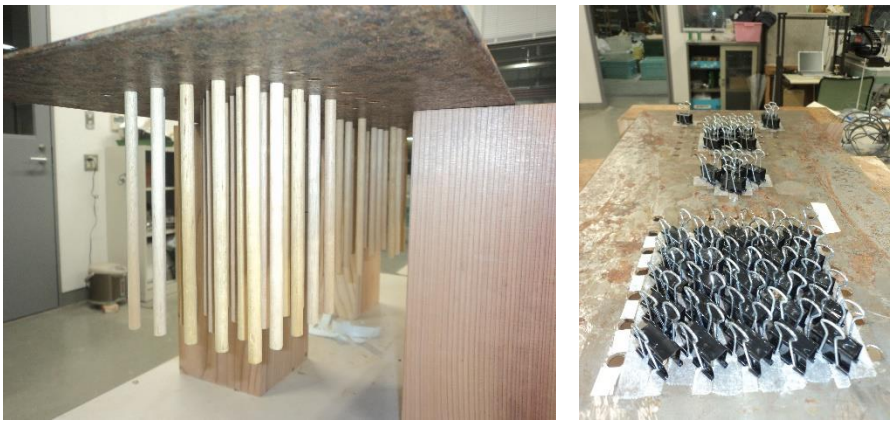

Figure 4.19 Step up the pile into the ground

Bach 1 Batch 2

Batch 3 Batch 4

Figure 4.20 Complete experiment sample

In each batch, tests were carried out on each pile group in sequence. For each pile group, the active pile was loaded by a geared motor while the displacement of itself and

a passive pile (pile #2) were measured by laser displacement gauges at the resolution 0.02 mm. The applying load on the active pile was also measured by a load cell with the capacity of 50 N.

4.4.2.2 Experiment results

Figure 4.21 shows the load-settlement curves of active piles (pile #1) and passive pile (pile #2) from all test. It can be seen that under the same load, the settlement of pile and passive piles decrease as the number of piles in group increases.

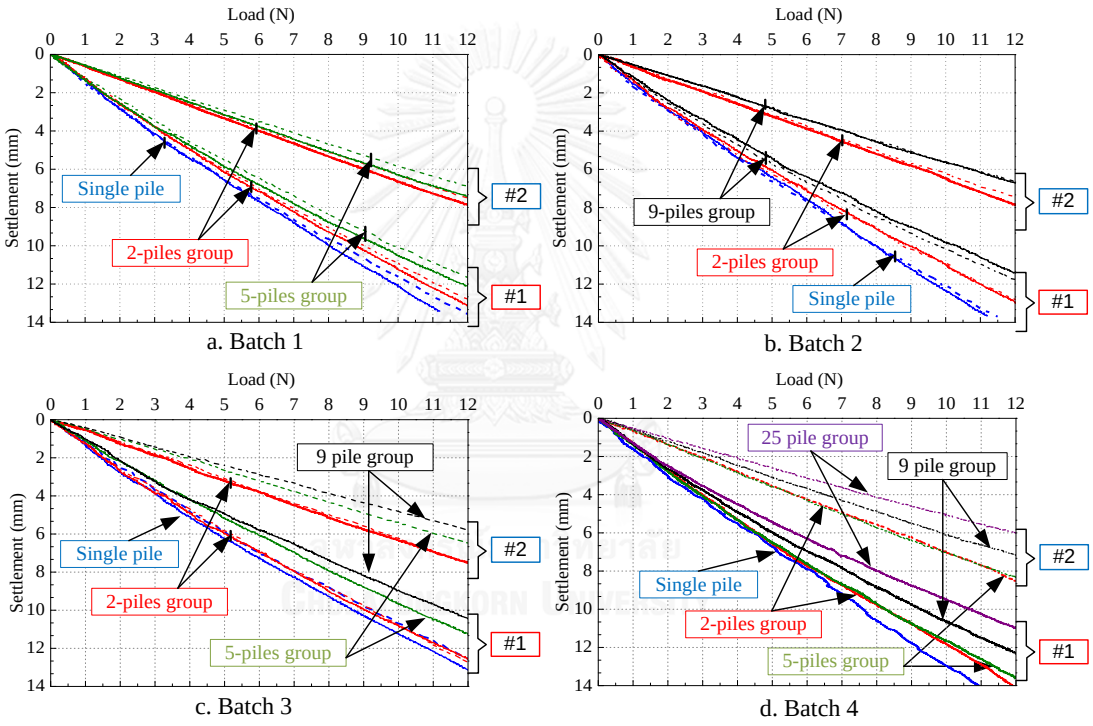

Figure 4.21 The influence of pile number on the load-settlement curves of active and passive piles

4.3.2.3 Comparison with experiment results.

Following Figure 4.17, the pile group models from experiment batches are summarized in Figure 4.22. In specifically, there have 5 kinds of pile arrangement including 1, 2, 5, 9, 25-piles pile groups.

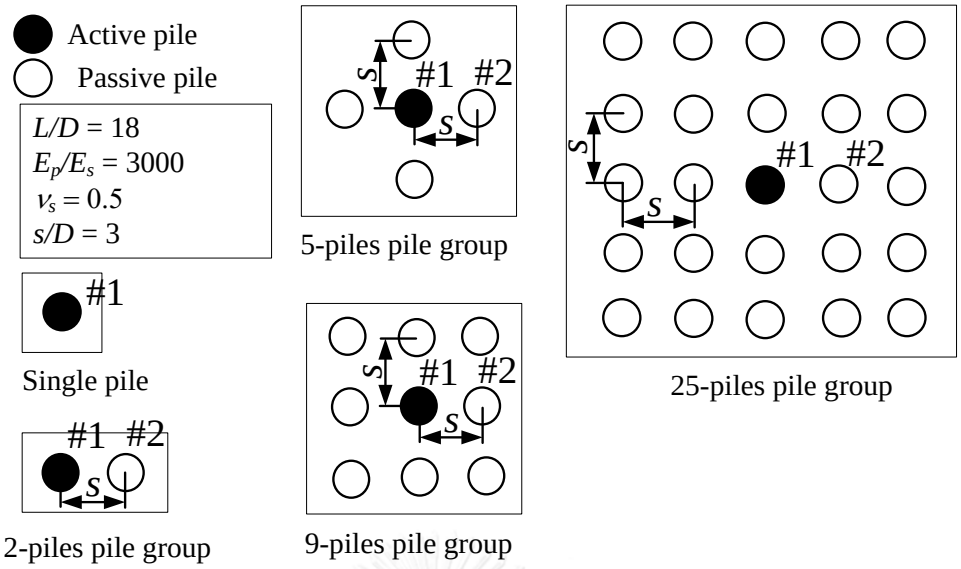

Figure 4.22 Outline of experiment models

With the same input parameter from the experiment condition showed in Figure 4.22, the settlements of pile #1, #2 in all groups were predicted by proposed method and other methods (3D FEA; Chow, 1986; Zhang et al, 2013). It is noted that, the methods of Poulos, (1968) and Mylonakis and Gazetas (1998) cannot simulate for these cases.

For the comparison purpose, the measured settlements of active pile #1 and passive pile #2 of each group piles was normalized with settlements of single pile in the corresponding batches. Whereas, the predicted settlements of pile #1 and #2 of each group piles were normalized with predicted settlements of single pile in the corresponding methods. Besides that, the measured and predicted interaction factors between pile #2 and pile #1 in each group piles were also determined.

Firstly, the normalized predicted settlements of pile #1 are compared with the normalized measured values, as shown in Figure 4.23. From the experiment results, it can be seen that, the settlement of active pile #1 was decrease around 20% when number of piles becomes 25 piles. The proposed approach got results which experiment and 3D FEA whereas, the work of Zhang et al. (2013) is not compatible.

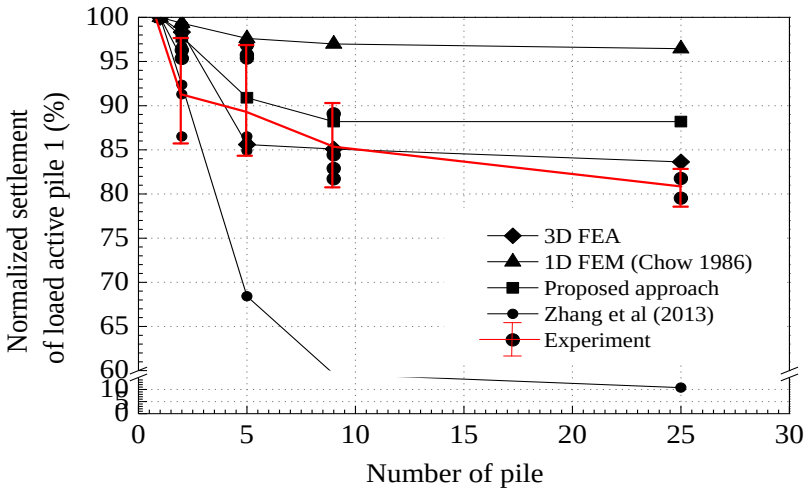

Figure 4.23 Settlement of active pile surrounding by various arrangement of passive pile

Besides, the normalized predicted settlements of passive pile (pile #2) were also compared with normalized measured values, as shown in Figure 4.24. From the experiment results, it can be seen that, the settlement of pile #2 reduced around 12% when number of piles becomes 25 piles. Besides, the proposed approach also get a good agreement which experiment results.

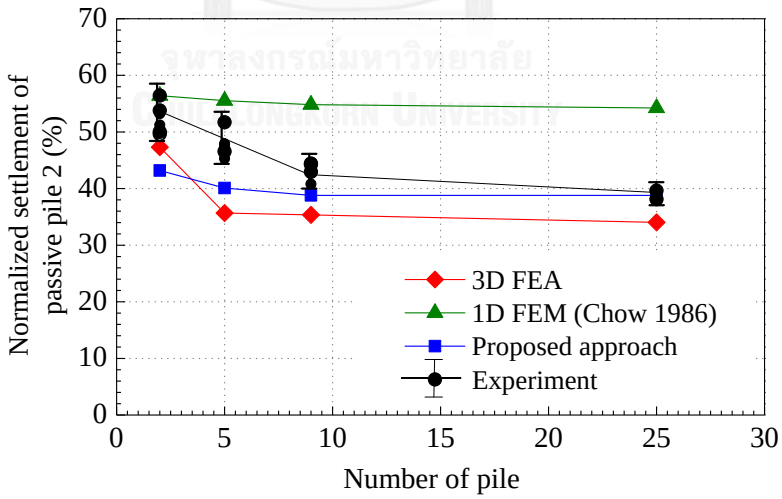

Figure 4.24 Settlement of passive pile induced by settlement of active pile

Finally, the predicted interaction factors determined by the predicted settlements of piles #1 and #2 were also compared with those from measurements, as shown in Figure 4.25. From the experiment result, the interaction factors decrease is around 12% when number of piles becomes 25 piles. Although, the results of proposed approach are not well fit with experiment results but the results are fit with complex prediction of 3D FEA.

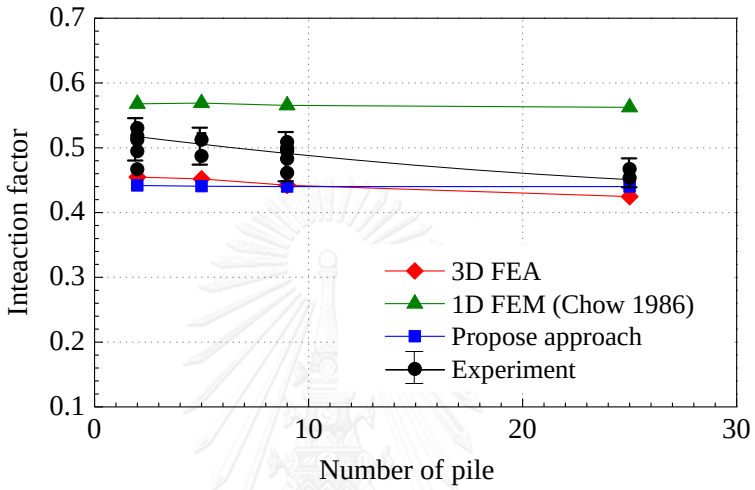

Figure 4.25 Interaction factor of 2 piles considering the influence of another pile in group

4.5 Conclusion

1. A new method for linear analysis of group piles response was developed. By considering the stiffening effect from shrouding piles, the proposed method is more accurate and more economic compared to other method in literature. Prediction by the proposed method agreed well with the results from FEA (Plaxis 3D) and experiment data.

2. The reduction in settlement of a pile when there are other piles in the vicinity, or the stiffening effect, was experimentally investigated. From the experiment results in an artificial elastic ground, it was observed that comparing to the settlement of a single pile under same loading, the settlement of an active pile decreases to 7%, 9%, 15% and 20% when it is surrounding by 1,4,8, 24 passive piles, respectively.

The induced settlement on a passive pile also decrease when number of piles in group increases. Based on the experiments, the settlement of a passive pile decrease by 4%, 9% and 15% for 5-piles, 9-piles, 25-piles group piles, when compared to 2-piles cases.

3. Based on the experiments, the ratio between the settlements of passive pile and active pile, or interaction factor, becomes smaller when the number of pile in group increases. The interaction factors for 2, 5, 9, 25-piles group are 0.52, 0.51, 0.48, 0.46 , respectively

CHAPTER 5: NONLINEAR ANALYSIS FOR GROUP PILE RESPONSE CONSIDERING STIFFENING EFFECT

5.1 Introduction

In this chapter, a new method for predicting the nonlinear response of group piles is proposed. The settlement of a pile is divided into the elastic and inelastic. The elastic component is determined by the method in the previous chapter while the inelastic component, or the slippage, is determined based on an exponential response model. The analysis result of a pile is used together with the interaction factor that considers the stiffening effect for the analysis of pile group. The proposed method is verified by field test results under rigid and flexible cap conditions.

5.2 Nonlinear analytical for group piles incorporating the stiffening effect

5.2.1 Assumptions and mathematic models

The proposed model is extended from the linear model in the chapter 4 by modifying at three places as shown in Figure 5.1. Firstly, the response of the active pile *j* is analyzed by the nonlinear analysis of single pile which was explained in chapter 3 instead of the linear method. However, the parameter $C_j^{'}$ is used instead of *C* for considering the stiffening effect. The modification is done by multiplying *C*, showed in Equation (3.3), with a reduction factor ζ_j, as follows;

$$C_j^{'} = C \cdot \zeta_j$$
$$\zeta_j = 1 - \left[\sum_{k=1,k\neq j}^{n} \frac{r_o}{r_{kj}} \ln\left(\frac{r_{ms}}{r_o}\right) \right] / \ln\left(\frac{r_m}{r_o}\right) \quad (5.1)$$

By the modification of *C* parameter, the b_j parameter in Equation (3.3) and elastic ground deformation, w_j^e,in (3.9) become

$$b_j^{'} = \frac{1}{C_j^{'} \cdot a} \quad (5.2)$$

$$w_j^e = C_j^{'} \cdot \tau \quad (5.3)$$

Secondly, the ground settlement around the active pile is only influenced by the elastic part instead of the total settlement. Thirdly, the response at pile base is modelled by a nonlinear function nonlinear of the linear elastic one.

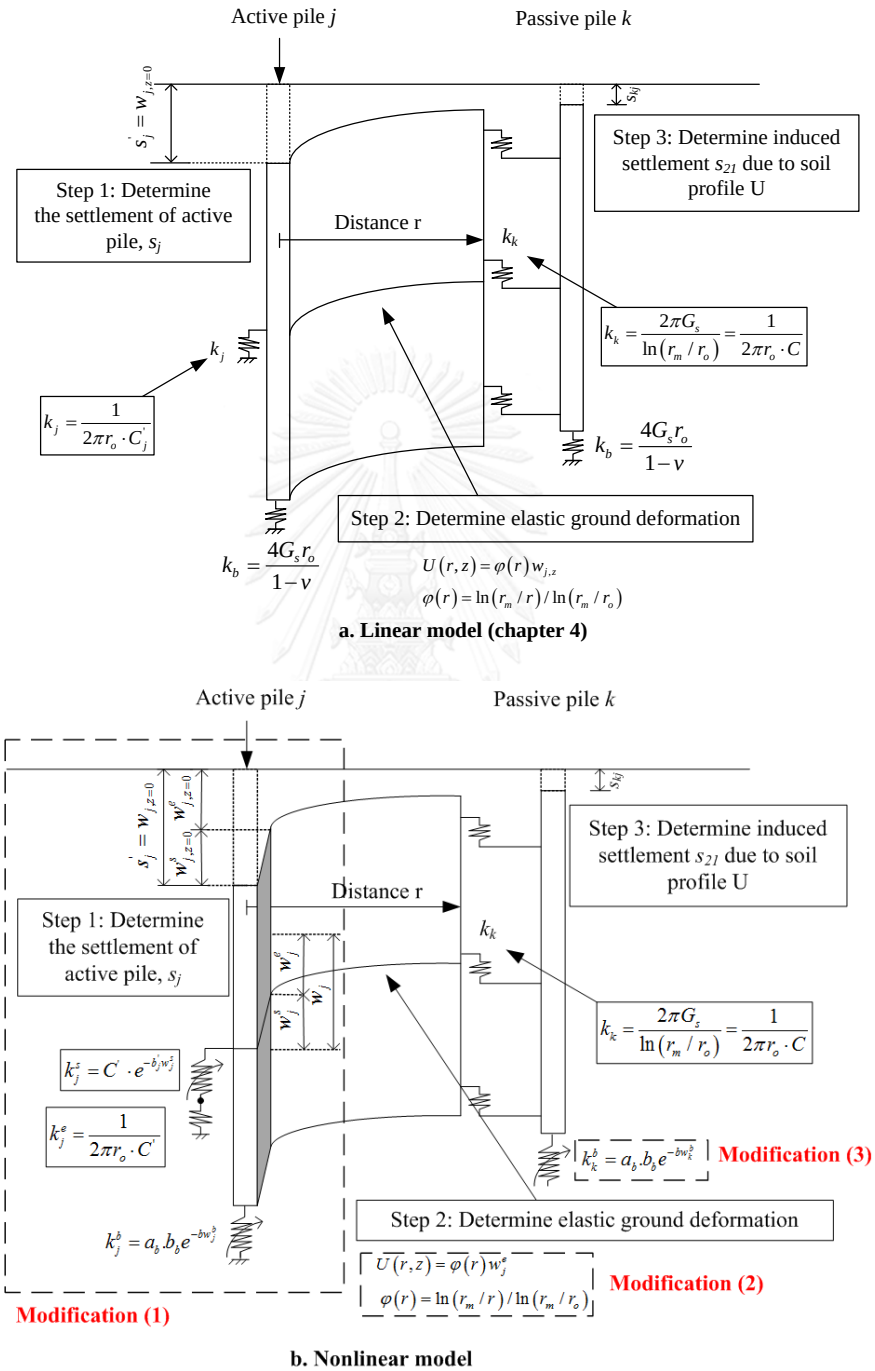

Figure 5.1 Comparison between the linear and nonlinear models

5.2.2 Algorithm

The model in Figure 5.1.b is used for determining the settlement of a pile considering the effects from all piles in the group. The calculation procedure is presented by flow chart in Figure 5.2. The step 1 in Figure 5.1.b is implemented in Subroutine GA. The step 2 and 3 in Figure 5.1.b are implemented in Subroutine GB.

Following Figure 5.2, at the beginning, the loading is divided into ten steps from zeros to the ultimate capacity of the pile which determined by Equation (3.15)

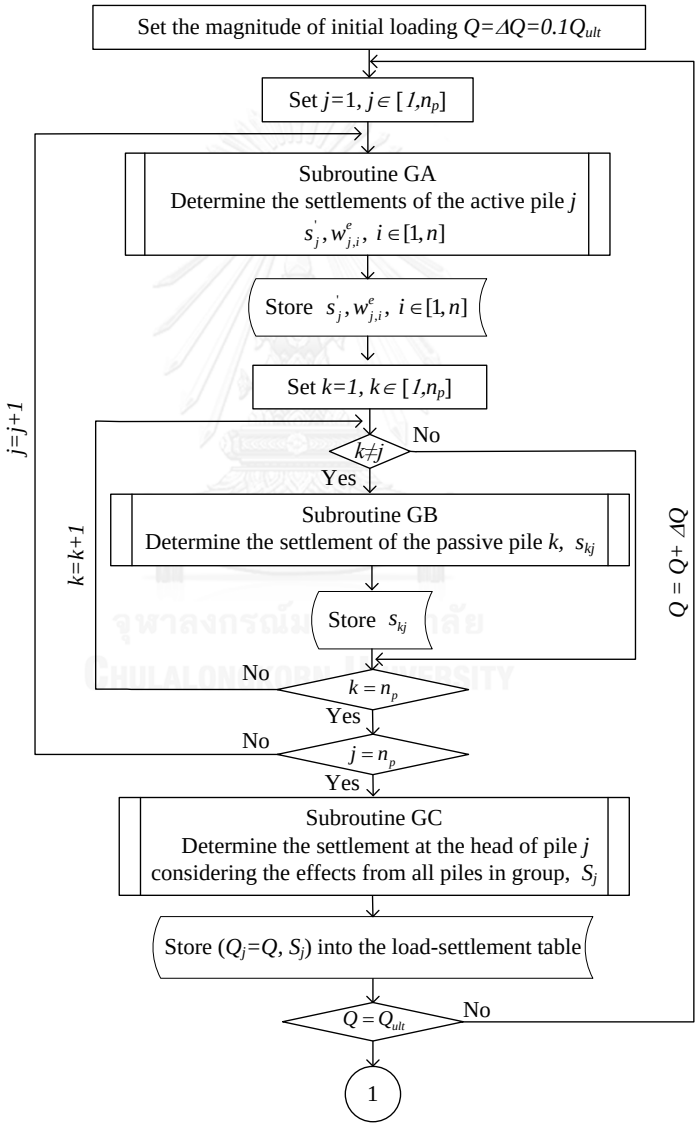

Figure 5.2 Determination of the load-settlement curve of each pile in a group

For each load step, the settlement of each active pile is determined by the Subroutine GA (Figure 5.3). The calculated value $s_j^{'}$, and the elastic settlement $w_{j,i}^{e}$, $i \in [1,n]$ are store together with the applying load level (Q). Subroutine GA is almost the same as the subroutine SA (Figure 3.6) expect the parameter *C*, b_j are modified as mention earlier.

Then the induced settlement of each passive pile s_{kj} is determined by the Subroutine GB and stored for later calculations.

After the settlements of active and passive piles are determined, the total settlement of a pile is calculated in Subroutine GC by combining its own settlement with the induced settlements from other piles.

By storing the total settlements and corresponding loads from ten steps, load-settlement curve of a pile in the group can be constructed and will be used further in determining the response of group piles.

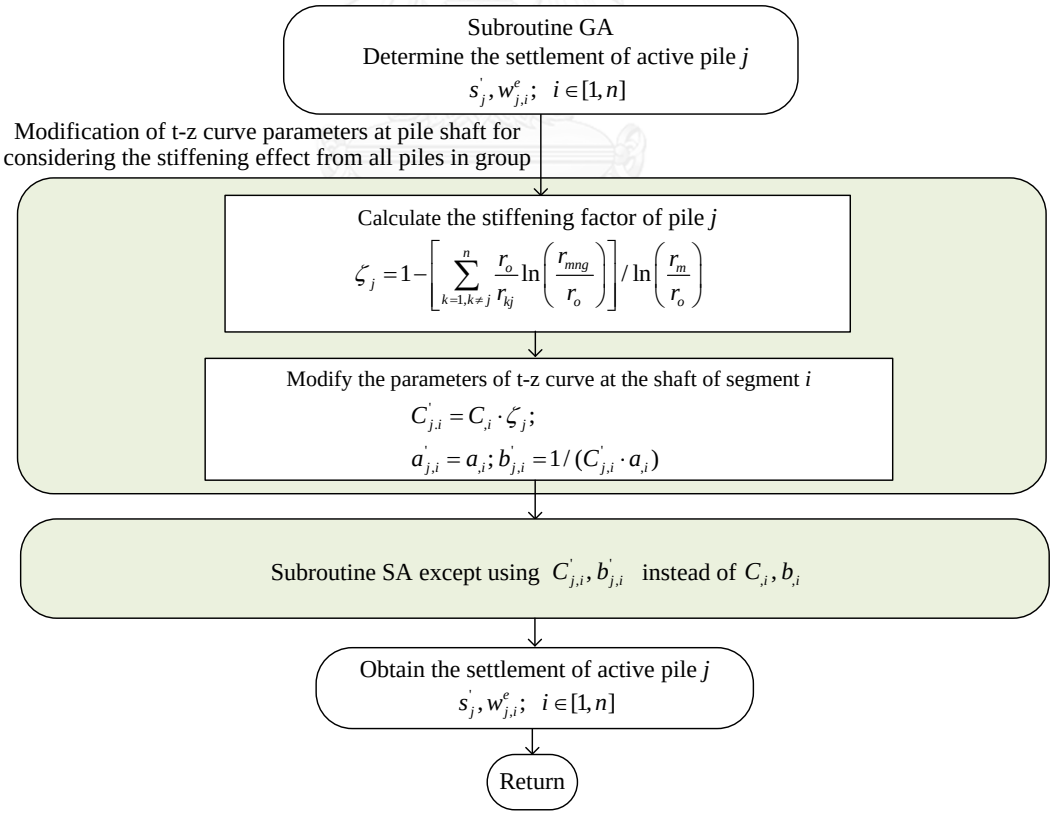

Figure 5.3 Flowchart of Subroutine GA

The subroutine GB, Figure 5.4, is used to calculate the settlement of a passive pile due to an active pile. The calculation can be divided into two steps. Firstly, the settlement field induced by the active pile (pile *j*) is calculated. Then, the settlement of the passive pile is determined based on the equilibrium of force along of the pile which are mobilized by the relative settlement between the pile and the ground. (Equation (5.4))

$$\begin{aligned} P_{,i}^{s} &= \frac{2\pi G_{s,i} l_i}{\ln\left(\frac{r_m}{r_o}\right)} \tau_z = \frac{2\pi G_{s,i} l_i}{\ln\left(\frac{r_m}{r_o}\right)} \left(w_{,i} - U_{kj,i} \right) \\ &= \frac{2\pi G_{s,i} l_i}{\ln\left(\frac{r_m}{r_o}\right)} \left(w_{,i}^{b} + \frac{P_{,i}^{t} + 3P_{,i}^{b}}{8E_p A_p} l_p - U_{kj,i} \right) \end{aligned} \tag{5.4}$$

Firstly, a very small value is assumed for settlement at pile base, says, 0.0001 of pile diameter. Then the reaction force at pile base is determined by Equation (3.11). The load settlement at the top of the base segment are calculated by Equation (5.5) and (5.6)

$$P_{,i}^{t} = P_{,i}^{b} + P_{,i}^{s} = \frac{1}{1 - \frac{2\pi G_{s,i} l_i^2}{8E_p A_p \ln\left(r_m / r_o\right)}} \cdot \left[P_{,i}^{b} + \frac{2\pi G_{s,i} l_i}{\ln\left(r_m / r_o\right)} \left(w_{,i}^{b} + \frac{3P_{,i}^{b}}{8E_p A_p} l_i - U_{kj,i} \right) \right] \tag{5.5}$$

$$w_{,i}^{t} = \frac{P_{,i}^{t} + P_{,i}^{b}}{2E_p A_p} l_i + w_{,i}^{b} \tag{5.6}$$

Since the values at the top of the pile base segment are similar to those at the bottom of the segment above, $w_{,i-1}^{b} = w_{,i}^{t}; P_{,i-1}^{b} = P_{,i}^{t}$, the same procedure can be repeated on the adjacent segment in sequence until the settlement and the applying load at the pile head are obtained.

If the load at pile head is smaller than zeros, the whole process will be repeated by increasing $w_{,n}^{b}$, $w_{,n}^{b} = w_{,n}^{b} + \Delta w^{b}$.

The iterative calculation for predicting the settlement of active pile in Subroutine GA and passive pile in Subroutine GB are easy done in excel by the goal seek function.

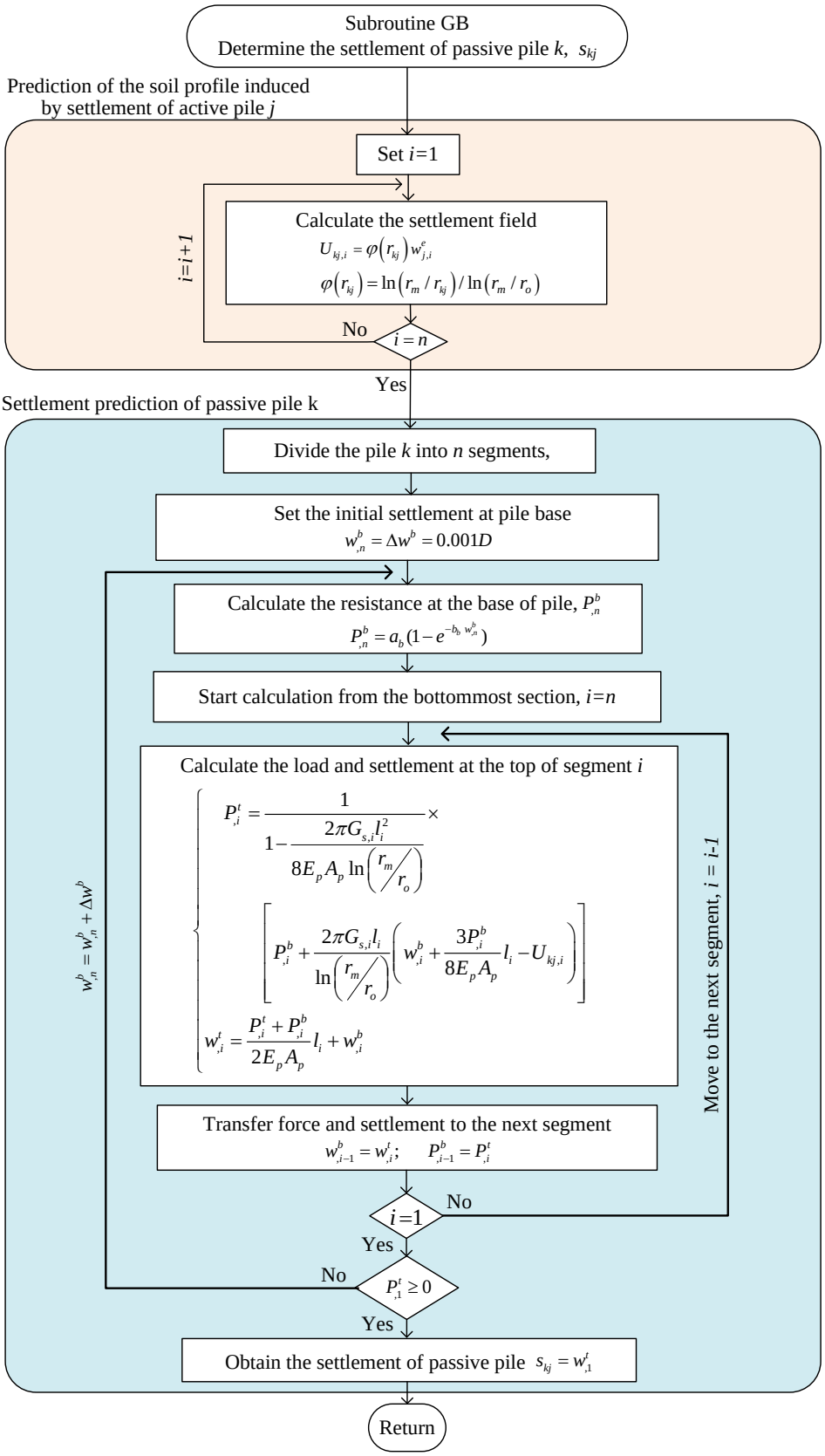

Figure 5.4 Flowchart of Subroutine GB

In the Subroutine GC, Figure 5.5, the settlement S_j of the pile j, is determined by combining its own settlement with induced settlement from remaining pile as follows;

$$S_j = s_j^{'} + \sum_{k=1,k\neq j}^{n_p} s_{jk} \,. \qquad (5.7)$$

The calculation is repeated for next piles

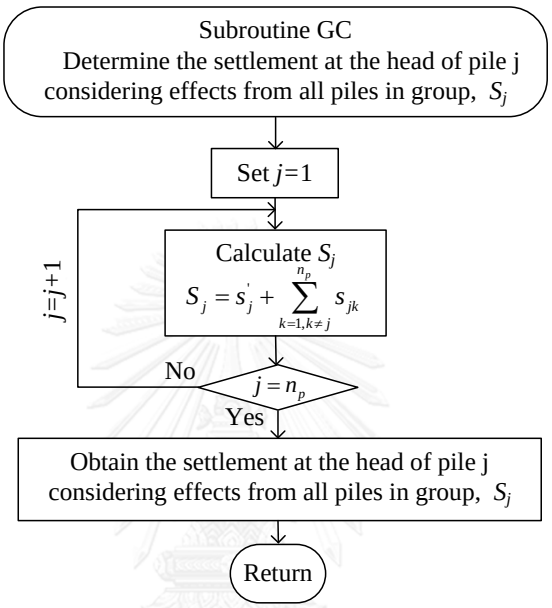

Figure 5.5 Flow chart for Subroutine GC

Based on the pile cap condition, the performance of pile group is determined as shown in Figure 5.6.

For rigid cap condition which all piles displace at the same rate, the resistance of each pile at an arbitrary settlement is interpolated from the load-settlement curve stored in the Subroutine GC. The resistance of the group is obtained from the summation of all piles resistance. The develop program determines the resistance at ten equal displacement steps between zeros and the settlement at ultimate capacity of the corner piles, and uses them for generating the load-settlement curve of pile group.

For flexible cap condition which all piles are loaded under the same magnitude, the settlement distribution in pile group is determined based on the load-settlement curve stored in the Subroutine GC.

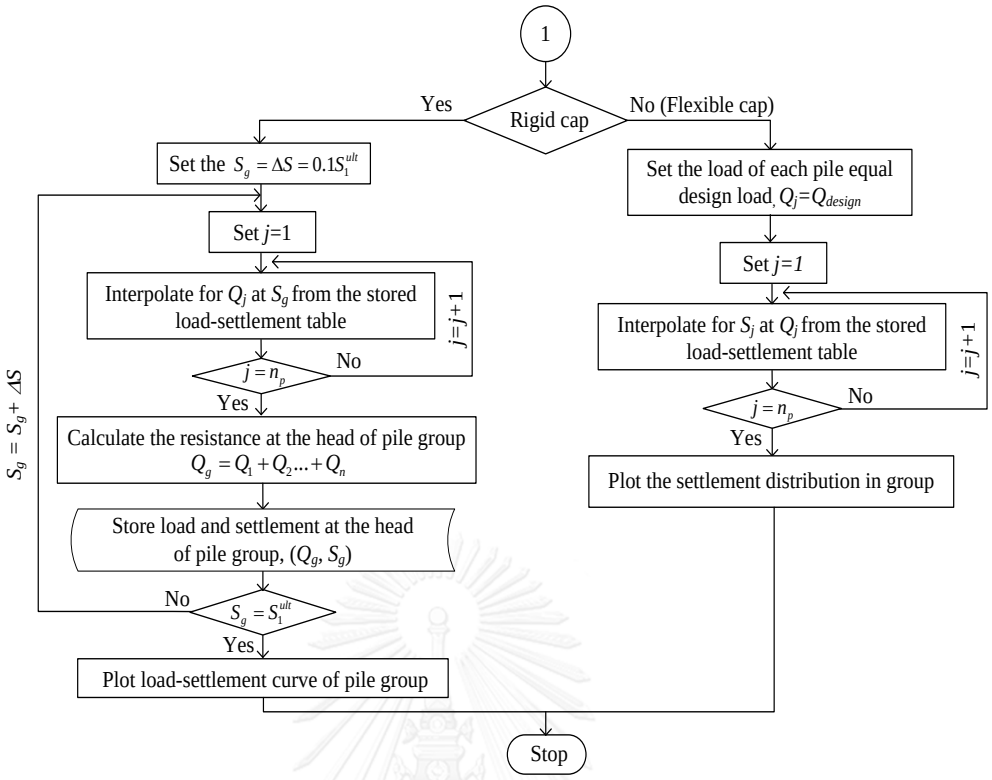

Figure 5.6 Flow chart to determine the responses of group piles under rigid cap and flexible cap conditions

5.3 Verification

The proposed approach is verified with three field tests of group piles consisting of 5-piles and 9-piles group under rigid cap condition and a 112-piles group pile under flexible cap condition.

5.3.1 Case 1: Five-piles group under rigid cap condition

Load tests, sponsored by The United States Federal Highway Administration, were implemented until failure on a 5-piles group pile at a site in San Francisco (Briaud et al, 1989). The subsoil founds on the bedrock and consists of three parts. First part, from the surface to 1.37 m, is the sandy gravel fill. Second part, from 1.37 to 12.2 m, is the layer made by a hydraulic fill of clean sand. Final part, From 12.2 to 14.3 m, is the interbedded layers of stiff clay and sand. The properties of sand clean sand and the layout of pile and subsoils are shown in Figure 5.7

Since the piles were installed through predrilled holes of 300 mm diameter and 1.37 m depth, the resistance of pile shaft and elastic shorting over the predrilled length are not considered in this study.

The piles are divided into 19 segments consisted of 1 segment for sand gravel layer, 7 segments from 1.37 to 1.52 m, 4 segments from 1,52 to 2.44 m and 7 segments from 2.44 to 9.1 m. By using the back-calculated coefficient of lateral earth pressure, K_s, was 1.72 (Lee & Xiao, 2001) and $R=0.8$, the parameter for t-z curves at pile shaft are determined by

$$a_{,i} = \frac{K_s \tan\left(\varphi^{'}\right)\sigma^{'}_{v,i}}{R}$$
$$b_{,i} = \frac{G_{s,i}}{a_{,i} \cdot r_o \cdot \ln(r_m / r_o)} \qquad (5.8)$$

In addition the parameters of a_b and b_b for t-z curve at pile base can be followed Equation (3.12) and (3.14)

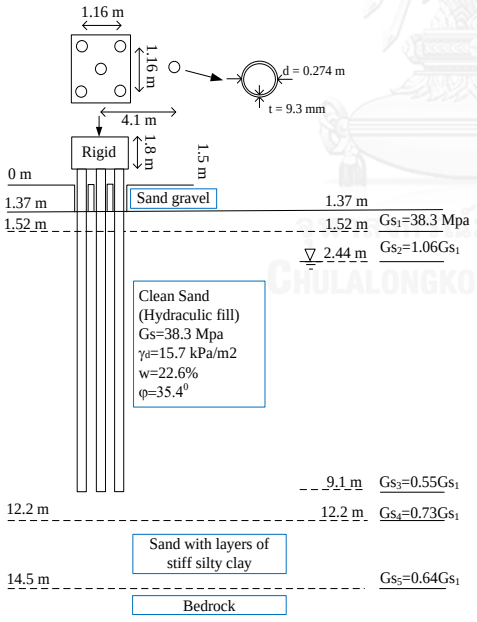

Figure 5.7 Properties of piles and soils (Mandolini & Viggiani, 1997)

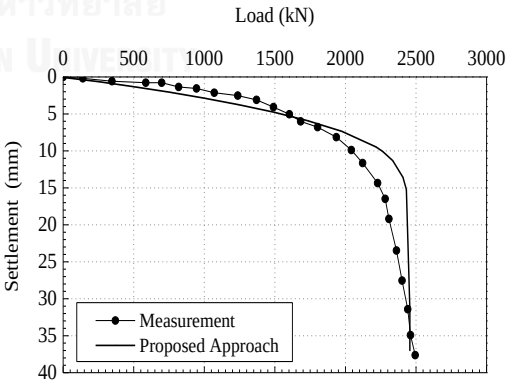

Figure 5.8 Predicted and measured of load–settlement curves

The settlement of pile group was calculated by proposed algorithm. The comparison between predicted and measured load-settlement curves of the group pile is shown in Figure 5.8. It can be seen that the good agreement was obtained.

5.3.2 Case 2: Nine-piles group under rigid cap condition

O'Neill (1982) implemented a number of full scales test on single piles and 3x3 piles group at University of Houston. The properties of the ground are shown in Figure 5.9. Piles were closed-ended steel-pipe piles with diameter of 273 mm and a wall thickness of 9.3 mm. Piles were installed up to depth of 13.1 m into stiff overconsolidated clay. The spacing in 3x3 piles group was three times of pile diameter.

The piles are also divided into 19 segments from surface to depth of 13.1 m. By assuming the back-calculated reduction factor of pile shaft resistance $\alpha = 0.34$ and *R=0.95*, the parameter for each segments was determined by

$$a_{,i} = \frac{\alpha \cdot Su_{,i}}{R}$$
$$b_{,i} = \frac{G_{s,i}}{a_{,i} \cdot r_o \cdot \ln(r_m / r_o)} \qquad (5.9)$$

The parameters of a_b and b_b for t-z curve at pile base can be determined by Equation (3.12) and (3.14). It was founded that a_b =123 kN by Lee and Xiao (2001)

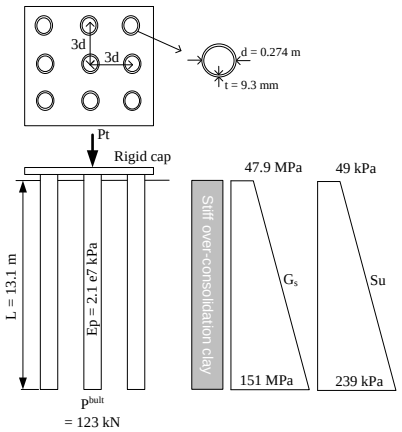

Figure 5.9 Test layout and soil profile for piles and pile group test by O'Neill et al. (1982) (as reported by Chow, 1986)

The predicted load-settlement curves of single piles and 3x3 piles groups were compared with the measurements, as shown in Figure 5.10 and Figure 5.11. The good agreements between predicted and measured load-settlement curves were obtained. Compare to method of Lee and Xiao (2001), the propose approach are almost the same.

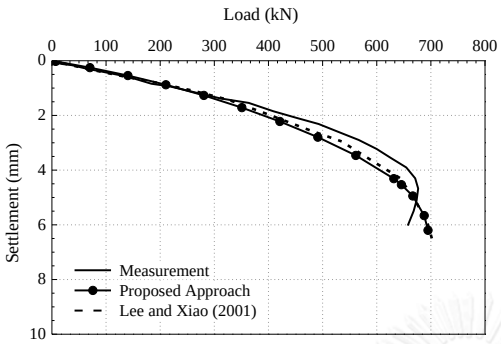

Figure 5.10 Load-settlement curves of single pile

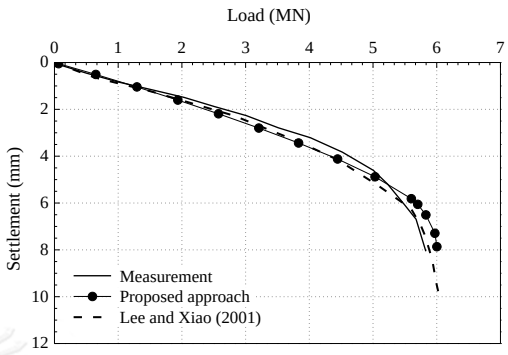

Figure 5.11 Load-settlement curves of nine pile group

5.3.3 Case 3: 112-bored piles foundation under flexible cap condition

A liquid storage tank was found on a 800 mm thick flexible circular concrete raft supported by 112 bored piles throughout. The soil profile and parameters are summarized in Figure 5.12 . The elastic modulus, E_u, of the clays are assumed to be 750 times of their undrained shear strengths, i.e., $E_u = 750Su$. The pile arrangement is assumed according to Lee and Xiao (2001). A static-load test was implemented by filling the tank with 160 MN of water in 10 days period.

For the analysis procedure, the piles are also divided into 19 segments. By assuming the back-calculated reduction factor of pile shaft resistance $\alpha = 0.5$ and $R=0.9$, the parameter for t-z curves at shaft segments was determined by Equation (5.9). The parameter for base model can be determined by Equation (3.12) and (3.14).

The settlements of six piles were determined under uniform load-distribution and compared with their filed measurements, as shown in Figure 5.13. It can see that the predictions agree well with the measurements and in the same degree of accuracy with the method of Lee and Xiao (2001).

When compared to the use of conventional t-z curve method and the interaction factor of Poulos (1968) (Reese, 1996; Viiayvergiya, 1997), the proposed method gave better estimate due to the consideration of slippage and stiffening effect. Prediction error by the proposed method and a conventional method (Viiayvergiya, 1997) are 0.5% and 10%, respectively.

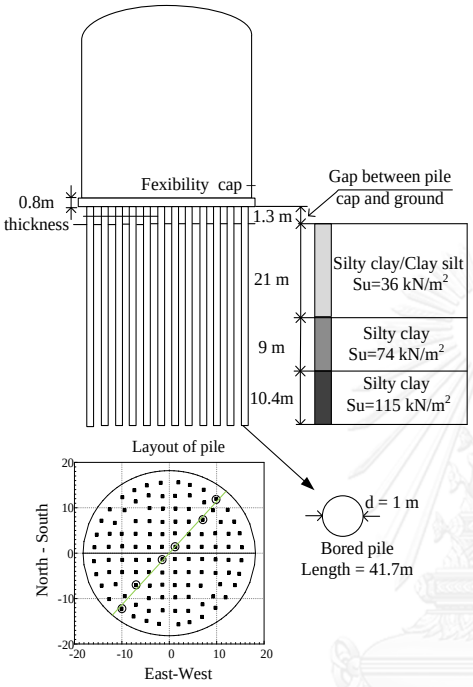

Figure 5.12 Properties of soil and pile in liquid storage tank case study (Georgiadis et al, 1989)

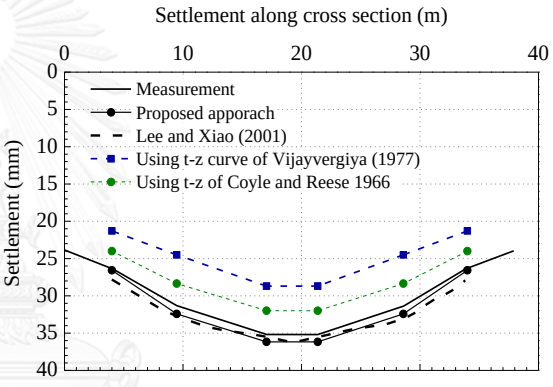

Figure 5.13 Predicted and observed settlement distributions under Liquid storage tank

5.4 Conclusion

The linear analysis was extended for analyzing the nonlinear responses of group piles. In the newly developed approach, the settlement of a pile is decomposed into elastic and inelastic parts (slippage). Firstly, the settlements of active piles considering the slippages and stiffening effect are determined. Then the induced settlements of passive pile are determined from the elastic settlement of active piles. By comparing with field test results, the proposed method gave better estimates than those obtained from conventional load-transfer methods and the interaction factor of Poulos (1968). Prediction error by the former and the latter are 0.5% and 10%, respectively.

CHAPTER 6: CONCLUSION AND RECOMMENDATIONS

6.1 Finding of research

In this study, new methods for the settlement analyses of single piles and group piles, are proposed. Key findings can be summarized as follows;

1. A new nonlinear load-transfer method for the settlement analysis of axially loaded piles considering slippage at pile-soil interface was proposed. It was verified by comparing with twenty five static load tests of bored piles in Bangkok. With input parameters deduced from conventional site investigation reports, the proposed method overestimated measured settlements under working load levels by 0.6 ~ 2.7 mm on average. The differences between predicted and measured axial load distributions were in the range of -5% ~ 15% of the working load of the piles. Based on these statistics, the accuracy of the proposed method was found to be sufficient for practical use

2. The reduction in settlement of a pile when there are other piles in the vicinity, or the stiffening effect, was experimentally investigated. From the experiment results in an artificial elastic ground, it was observed that comparing to the settlement of a single pile under same loading, the settlement of an active pile decreases to 7%, 9%, 15% and 20% when it is surrounding by 1,4,8, 24 passive piles, respectively.

   The induced settlement on a passive pile also decrease when number of piles in group increases. Based on the experiments, the settlement of a passive pile decrease by 4%, 9% and 15% for 5-piles, 9-piles, 25-piles group piles, when compared to 2-piles cases.

3. Based on the experiments, the ratio between the settlements of passive pile and active pile, or interaction factor, becomes smaller when the number of pile in

group increases. The interaction factors for 2, 5, 9, 25-piles group are 0.52, 0.51, 0.48, 0.46 , respectively

4. A new method for linear analysis of group piles response was developed. By considering the stiffening effect from shrouding piles, the proposed method is more accurate and more economic compared to other method in literature. Prediction by the proposed method agreed well with the results from FEA (Plaxis 3D) and experiment data.

5. The linear analysis was extend for analyzing the nonlinear responses of group piles. In the newly developed approach, the settlement of a pile is decomposed into elastic and inelastic parts (slippage). Firstly, the settlements of active piles considering the slippages and stiffening effect are determine. Then the induced settlements of passive pile are determined from the elastic settlement of active piles. By comparing with field test results, the proposed method gave the better estimates than those obtained from conventional load-transfer methods and the interaction factor of Poulos (1968). Prediction error by the former and the latter are 0.5% and 10%, respectively.

6.2 Recommendation for further researches.

Although a number of works have been done in this thesis, there are still have some issues which required further investigation and can be listed as follows;

1. The installation effect is not considered in this study
2. The long-term settlement of piles is not considered in this study
3. The experiment were carried out in an artificial elastic material. It is better if these experiments will be conducted under more realistic ground condition

REFERENCES

Armaleh S and Desai C (1987) Load-deformation response of axially loaded piles. Journal of geotechnical engineering, 113(12): 1483-1500.

Basile F (1999) Non-linear analysis of pile groups. Proceedings of the Institution of Civil Engineers-Geotechnical Engineering, 137(2): 105-115.

Boonyatee T, Tongjarukae J, Uaworakunchai T and Ukritchon B (2015) A Review on Design of Pile Foundations in Bangkok. Geotechnical Engineering, SEAGS & AGSSEA,, 46(1): 76-85.

Bowles J E (1988) Foundation analysis and design.

Briaud J, Tucker L and Ng E (1989) Axially loaded 5 pile group and single pile in sand, *Proceedings of the 12th International Conference on Soil Mechanics and Foundation Engineering*.

Butterfield R and Banerjee P (1971) The elastic analysis of compressible piles and pile groups. Geotechnique, 21(1): 43-60.

Cameron A C and Windmeijer F A (1997) An R-squared measure of goodness of fit for some common nonlinear regression models. Journal of Econometrics, 77(2): 329-342.

Cao M, Chen L and Chen S (2007) An innovative approach to evaluate the behaviour of vertically loaded pile groups based on elastic theory. Journal of Lowland Technology International, 9(1): 1-10.

Chen S, Song C and Chen L (2011) Two-pile interaction factor revisited. Canadian Geotechnical Journal, 48(5): 754-766.

Chow Y (1986) Analysis of vertically loaded pile groups. International Journal for Numerical and Analytical Methods in Geomechanics, 10(1): 59-72.

Clough G W and Duncan J M (1973) Finite element analysis of retaining wall behavior. Journal of Soil Mechanics & Foundations Div, 99(sm 4).

Coyle H M and Reese L C (1966) Load transfer for axially loaded piles in clay. Journal of Soil Mechanics & Foundations Div, 92(SM2, Proc Paper 4702).

Fleming K, Weltman A, Randolph M and Elson K (2008) Piling engineeringCRC press.

Georgiadis M, Pitilakis K, Tsotsos S and Valalas D (1989) Settlement of a liquid storage tank founded on piles, *Proceedings of the 12th International Conference on Soil Mechanics and Foundation Engineering, Rio de Janeiro*.

He J (2002) Experimental research on vertical bearing properties of base-grouting bored cast-in-place pile. CHINESE JOURNAL OF GEOTECHNICAL ENGINEERING-CHINESE EDITION-, 24(6): 743-746.

HIRAYAMA H (1990) Load-settlement analysis for bored piles using hyperbolic transfer functions. Soils and Foundations, 30(1): 55-64.

Hognestad E (1951) *Study of combined bending and axial load in reinforced concrete members*.

Imai T and Tonouchi K (1982) Correlation of N-value with S-wave velocity and shear modulus. In: Proceedings of the 2nd European symposium on penetration testing: 57–72.

Kezdi A (1975) Pile foundations. Foundation engineering handbook: 556-600.

Lee C (1993) Settlement of pile groups—practical approach. Journal of Geotechnical Engineering, 119(9): 1449-1461.

Lee K and Xiao Z (2001) A simplified nonlinear approach for pile group settlement analysis in multilayered soils. Canadian Geotechnical Journal, 38(5): 1063-1080.

Likitlersuang S, Teachavorasinskun S, Surarak C, Oh E and Balasubramaniam A (2013) Small strain stiffness and stiffness degradation curve of Bangkok clays. Soils and Foundations, 53(4): 498-509.

Mandolini A and Viggiani C (1997) Settlement of piled foundations. Géotechnique, 47(4): 791-816.

Meyerhof G (1976) BEARING CAPACITY AND SETTLEMTN OF PILE FOUNDATIONS. Journal of Geotechnical and Geoenvironmental Engineering, 102(ASCE# 11962).

Mindlin R D (1936) Force at a point in the interior of a semi-infinite solid. Physics, 7(5): 195-202.

Mylonakis G and Gazetas G (1998) Settlement and additional internal forces of grouped piles in layered soil. Geotechnique, 48(1): 55-72.

O'Neill M W, Hawkins R A and Mahar L J (1982) Load transfer mechanisms in piles and pile groups. Journal of the Geotechnical Engineering Division, 108(12): 1605-1623.

Poulos H (1968) Analysis of the settlement of pile groups. Geotechnique, 18(4): 449-471.

Poulos H G and Davis E H (1980) Pile foundation analysis and design.

Randolph M F and Wroth C (1979) An analysis of the vertical deformation of pile groups. Geotechnique, 29(4): 423-439.

Randolph M F and Wroth C P (1978) Analysis of deformation of vertically loaded piles. Journal of Geotechnical and Geoenvironmental Engineering, 104(ASCE 14262).

Rangaswamy R (1995) A text book of agricultural statisticsNew Age International.

Reese L, Hudson W and Vijayvergiya V (1900) An investigation of the interaction between bored piles and soil, *Soil Mech & Fdn Eng Conf Proc/Mexico/*.

Ross R J (2010) Wood handbook: Wood as an engineering material.

Seed H and Reese L (1957) The Action of Clay Along Friction Piles. J Geoteh Engng, 504: 92.

Sharnouby B E and Novak M (1985) Static and low-frequency response of pile groups. Canadian Geotechnical Journal, 22(1): 79-94.

Sharnouby B E and Novak M (1990) Stiffness constants and interaction factors for vertical response of pile groups. Canadian geotechnical journal, 27(6): 813-822.

Southcott P and Small J (1996) Finite layer analysis of vertically loaded piles and pile groups. Computers and Geotechnics, 18(1): 47-63.

Vijayvergiya V (1977) Load-movement characteristics of piles, *Ports'77. 4 th annual symposium of the American Society of Civil Engineers, Waterway, Port, Coastal and Ocean Division, Long Beach, California, v. 2.*

Wang Z, Xie X and Wang J (2012) A new nonlinear method for vertical settlement prediction of a single pile and pile groups in layered soils. Computers and geotechnics, 45: 118-126.

Zhang Q-q, Zhang S-m, Liang F-y, Zhang Q and Xu F (2015) Some observations of the influence factors on the response of pile groups. KSCE Journal of Civil Engineering, 19(6): 1667-1674.

Zhang Q Q, Li S C, Liang F, Yang M and Zhang Q (2014) Simplified method for settlement prediction of single pile and pile group using a hyperbolic model. Int. J. Civ. Eng, 12(2): 179-192.

APPENDIX

This appendix is included some flowcharts for my proposed method, as follows

1. The flowchart for parameter determination
2. The flowchart of performance prediction for axially loaded pies
3. The flowchart of performance prediction for axially loaded pie groups

Flow chart 1: Parameter determination procedure

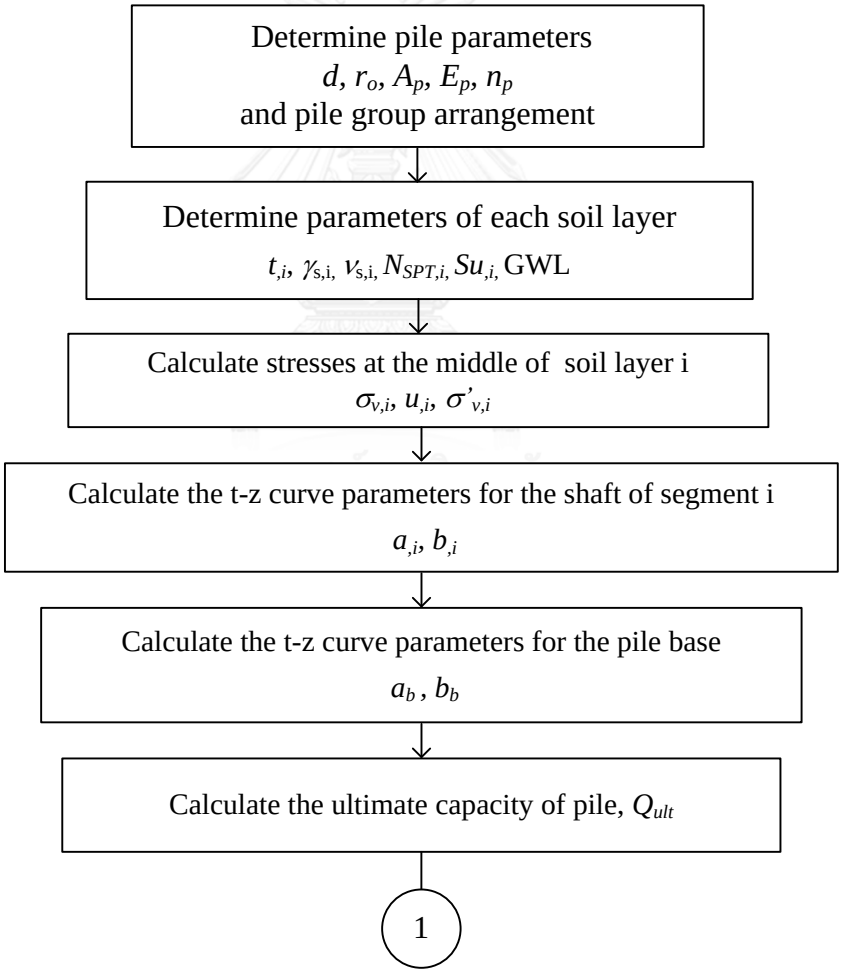

Explanation for parameter estimation procedure

1. **To calculate the total stress, water pressure, effective stress at the middle of soil layer i**

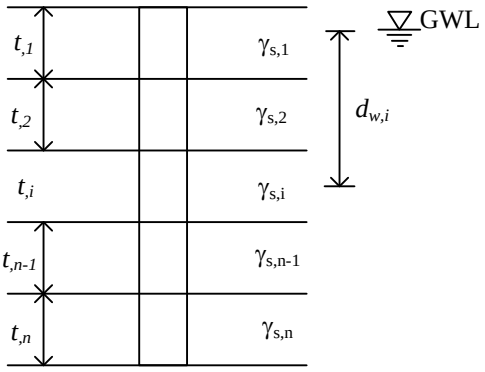

$$\sigma_{v,i} = \gamma_{s,1} t_1 + \gamma_{s,1} t_2 + ... + \gamma_{s,i} \frac{t_i}{2}$$

$$u_{,i} = \gamma_w d_{w,i}$$

$$\sigma'_{v,i} = \sigma_{v,i} - u_i$$

2. To calculate the t-z curve parameters for the shaft of segment i

a. Determination of $a_{,i}$

$$a_{,i} = \frac{\tau_{f,i}}{R}$$

where

$$R \in [0.80\text{-}0.95]$$

$$\tau^f_{,i} = \begin{cases} \alpha_{,i} Su_{,i} & ; \text{ for clay} \\ \beta_{,i} \sigma'_{v,i} & ; \text{ for sand} \end{cases}$$

For clay

$$Su_{,i} = 0.685 \cdot N_{SPT,i} \quad (\text{t/m}^2) \qquad \text{(Boonyatee et al, 2015)}$$

$$\alpha_{,i} = 0.41854 + 0.78067 \cdot e^{\left(-Su_{,i}/5.99492\right)} \qquad \text{(Boonyatee et al, 2015)}$$

For sand

$$\beta_{,i} = 0.018 + 0.000911 \cdot e^{\phi'_{,i}/6.457} \qquad \text{(Boonyatee et al, 2015)}$$

$$\phi'_{,i} = 27.1 + 0.3 \cdot N_{SPT,i} - 0.00054 \cdot \left(N'_{SPT,i}\right)^2 \qquad \text{(Boonyatee et al, 2015)}$$

$$N'_{SPT,i} = 0.77 \cdot \log_{10}\left(200 / \sigma'_{v,i}\right) \cdot N_{SPT,i}$$ (Meyerhof, 1976)

$\sigma'_{v,i}$ was calculated in step 3

b. Determination of $b_{,i}$

$$b_{,i} = \frac{1}{C_{,i} \cdot a_{,i}}$$

$$C_{,i} = \frac{r_0}{G_{s,i}} \ln\left(\frac{r_m}{r_0}\right)$$

$$G_{s,i} = 1412 \cdot \left(N_{SPT}\right)^{0.68} \ (\text{t/m}^2)$$ (Imai & Tonouchi, 1982)

$$G_{s,i} = \frac{500 \cdot Su_{,i}}{2(1+\upsilon_{s,i})} \ (\text{t/m}^2)$$ for clay without N_{SPT} (Bowles, 1988)

$$r_m \approx 2.5 \cdot L \cdot (1-\nu_s)$$ (Randolph and Wroth, 1978)

3. To calculate the t-z curve parameters for the pile base

a. Determination of a_b

$$a_b = \frac{P^{bf}}{R_b}$$

where

$R_b \in [0.80\text{-}0.95]$ (Clough and Duncan, 1967)

$$P^{bf} = \begin{cases} A_p \sigma'_{vb} N_q^* & ; \text{ for sand} \\ A_p \left(9 \cdot Su + \sigma_{vb}\right) & ; \text{ for clay} \end{cases}$$ (Boonyatee et al, 2015)

$$N_q^* = 0.539 + 0.64 \cdot e^{\phi' / 30.662}$$ (Boonyatee et al, 2015)

$\sigma'_{vb}, \sigma_{vb}$ were calculated in step 3

b. Determination of b_b

$$b_b = \frac{4G_{sb}r_0}{(1-\nu_b)a_b}$$ (Randolph and Wroth, 1978)

4. To calculate the ultimate capacity of pile

$$Q_{ult} = 2\pi r_o \sum_{i=1}^{n} \tau_{,i}^{f} l_i + P^{bf}$$

Flowchart 2: Performance prediction for axially loaded piles

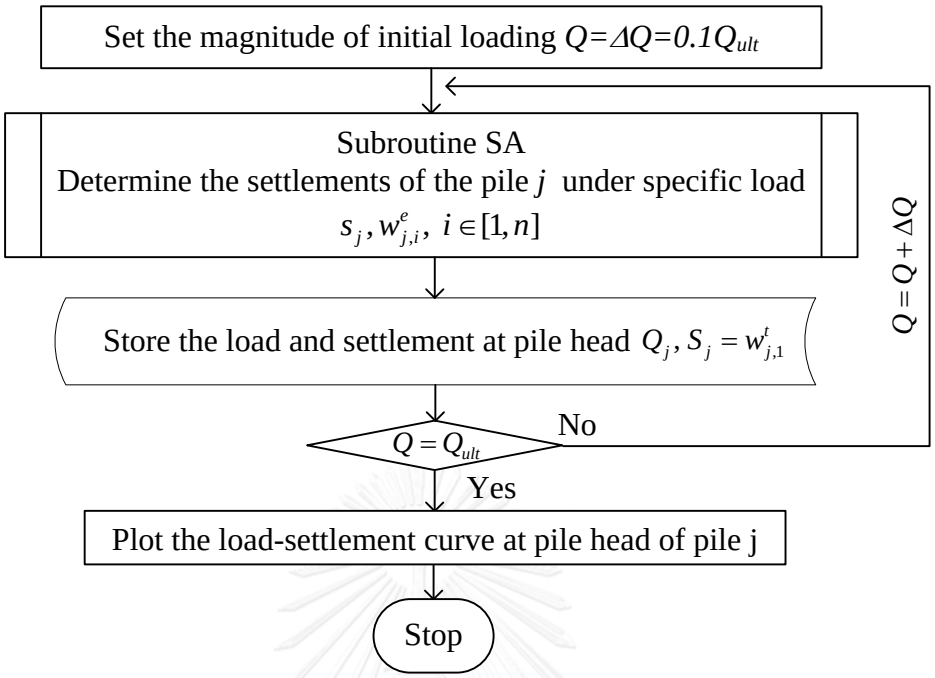

Flowchart 3: Performance prediction for axially loaded pie groups

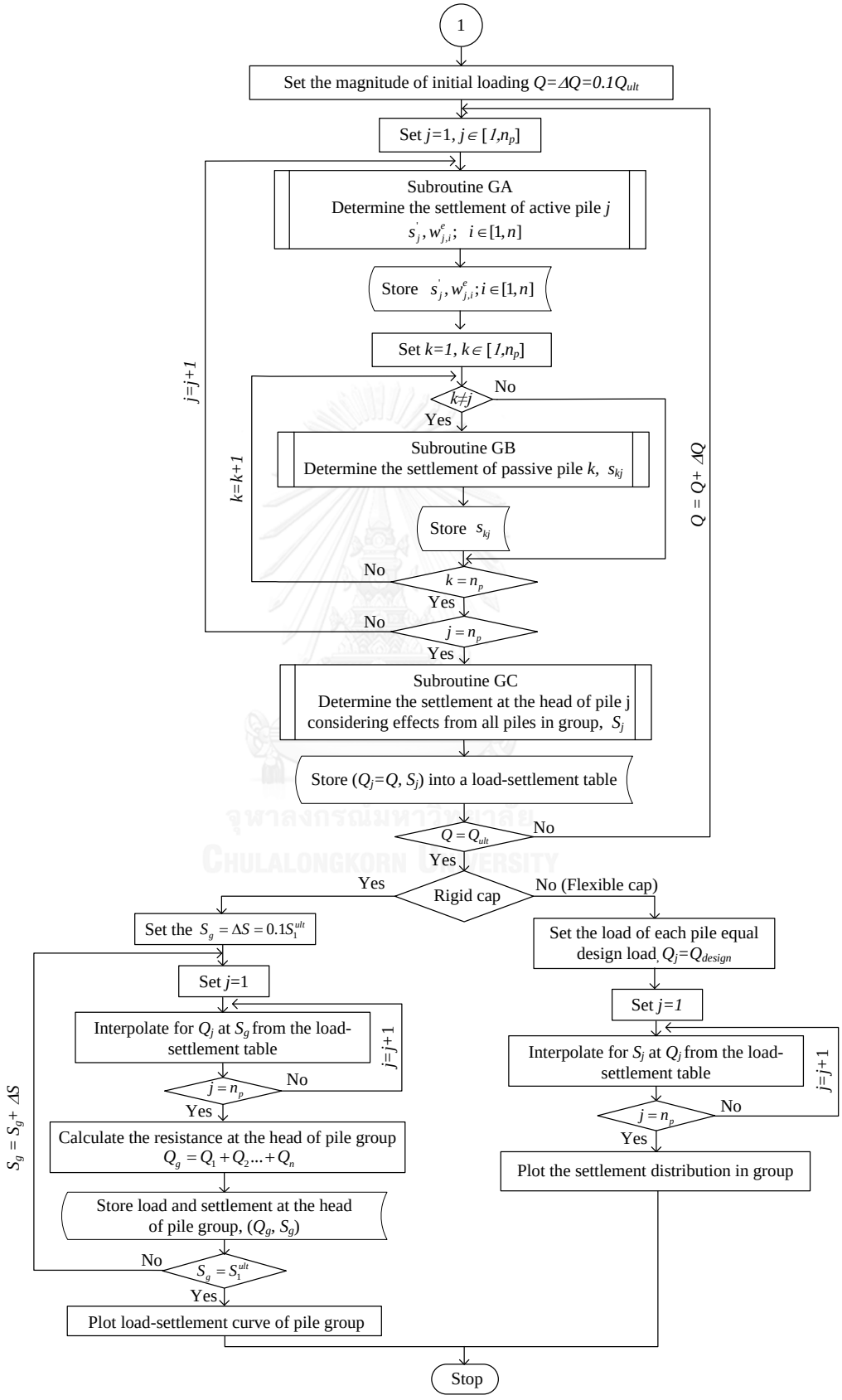

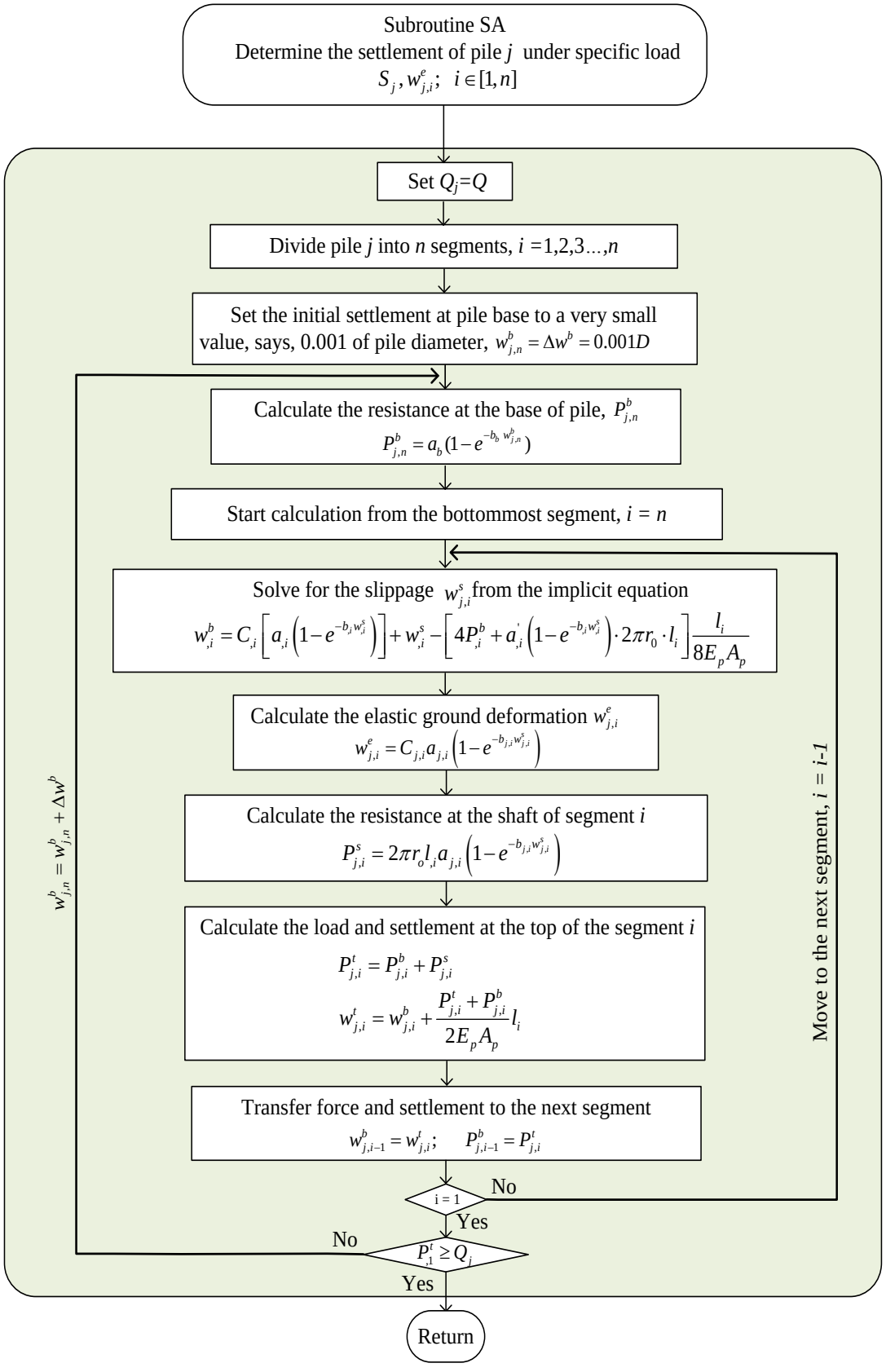
Subroutine SA
Determine the settlement of pile j under specific load
$S_j, w^e_{j,i};\ i \in [1,n]$
Set Q_j=Q
Divide pile j into n segments, i =1,2,3...,n
Set the initial settlement at pile base to a very small value, says, 0.001 of pile diameter, $w^b_{j,n} = \Delta w^b = 0.001D$
Calculate the resistance at the base of pile, $P^b_{j,n}$
$P^b_{j,n} = a_b(1-e^{-b_b w^b_{j,n}})$
Start calculation from the bottommost segment, i = n
Solve for the slippage $w^s_{j,i}$ from the implicit equation
$w^b_{,i} = C_{,i}\left[a_{,i}\left(1-e^{-b_j w^s_j}\right)\right] + w^s_{,i} - \left[4P^b_{,i} + a'_{,i}\left(1-e^{-b_j w^s_j}\right)\cdot 2\pi r_0 \cdot l_i\right]\frac{l_i}{8E_pA_p}$
Calculate the elastic ground deformation $w^e_{j,i}$
$w^e_{j,i} = C_{j,i}a_{j,i}\left(1-e^{-b_{j,i}w^s_{j,i}}\right)$
Calculate the resistance at the shaft of segment i
$P^s_{j,i} = 2\pi r_o l_{,i} a_{j,i}\left(1-e^{-b_{j,i}w^s_{j,i}}\right)$
Calculate the load and settlement at the top of the segment i
$P^t_{j,i} = P^b_{j,i} + P^s_{j,i}$
$w^t_{j,i} = w^b_{j,i} + \frac{P^t_{j,i} + P^b_{j,i}}{2E_pA_p}l_i$
Transfer force and settlement to the next segment
$w^b_{j,i-1} = w^t_{j,i};\quad P^b_{j,i-1} = P^t_{j,i}$
i = 1
No
Yes
Move to the next segment, i = i-1
$P^t_{,1} \geq Q_j$
No
Yes
$w^b_{j,n} = w^b_{j,n} + \Delta w^b$
Return

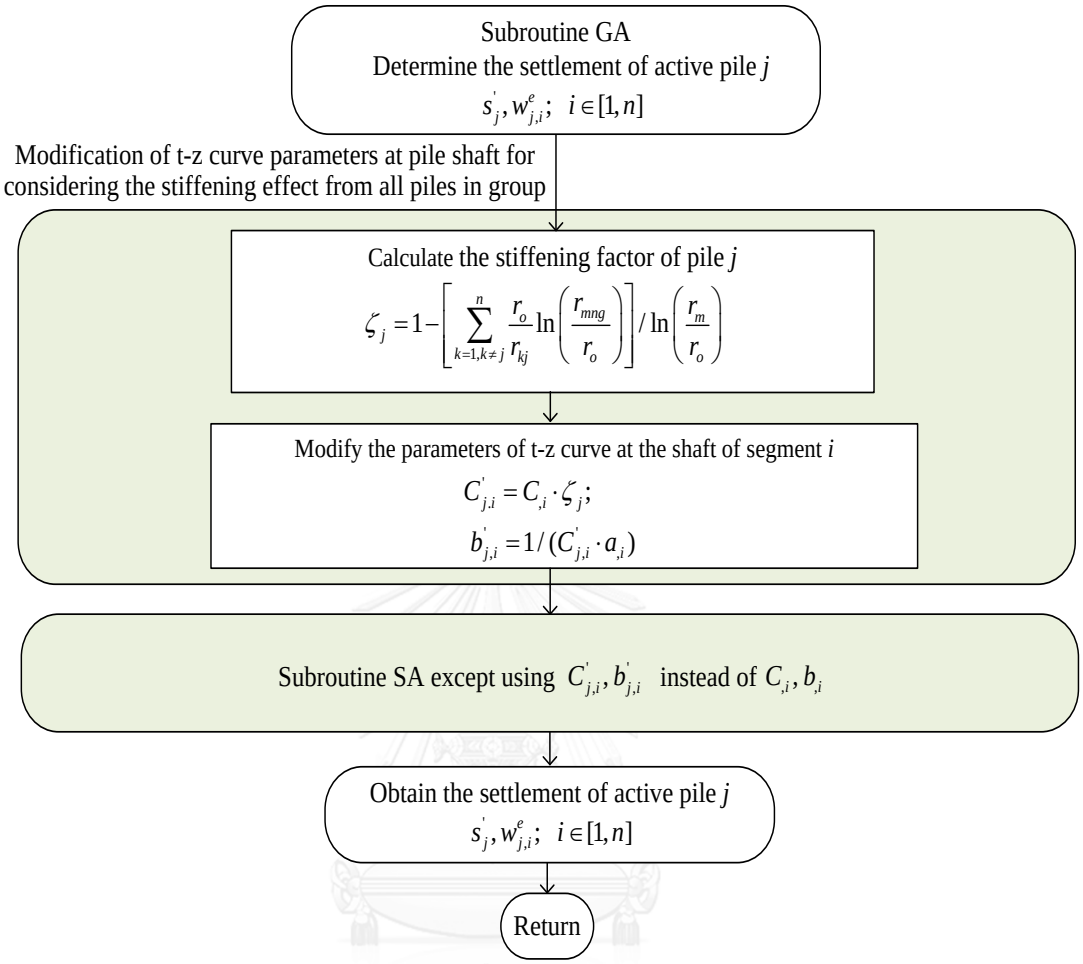

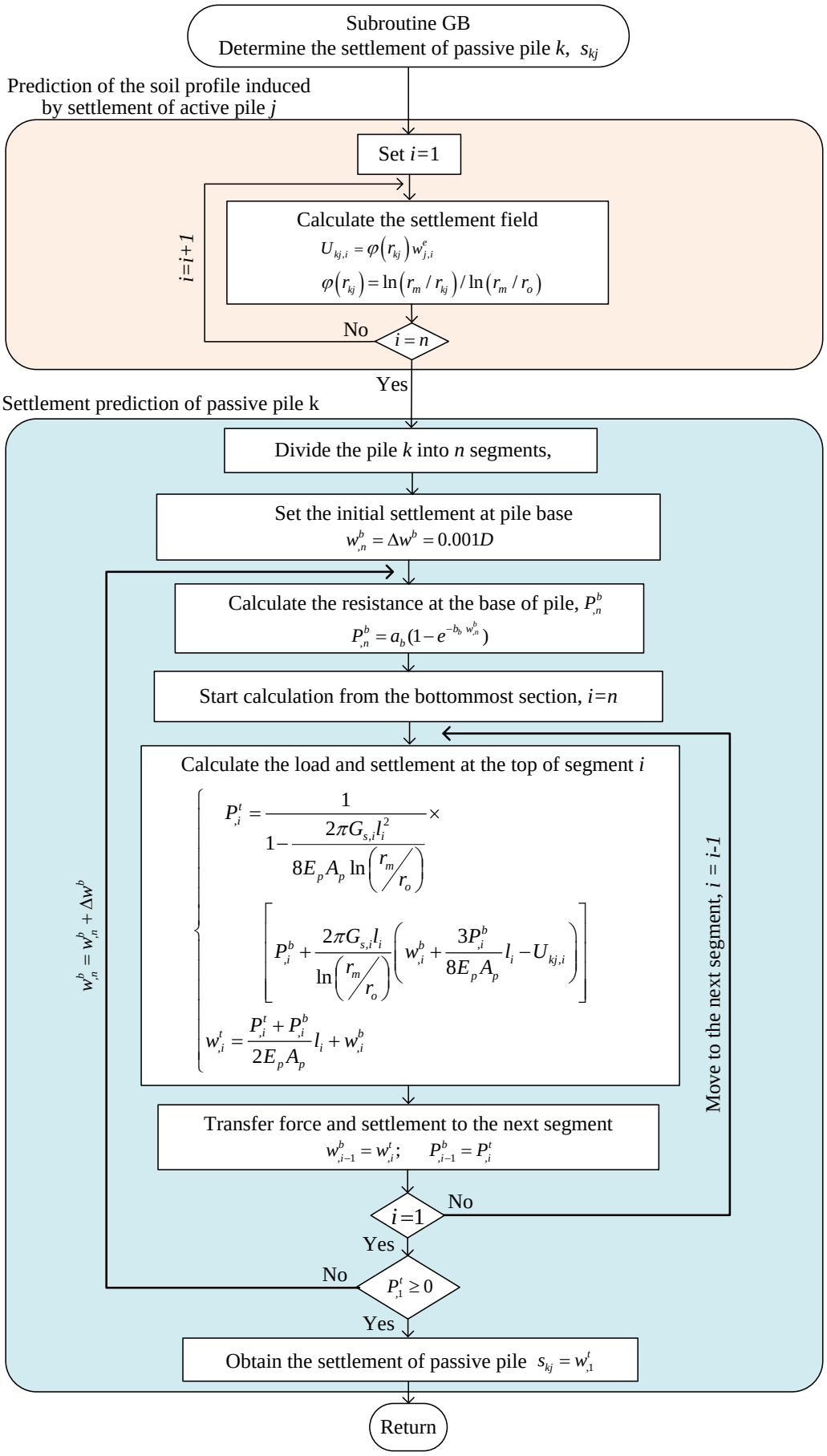
Subroutine GB
Determine the settlement of passive pile k, s_{kj}
Prediction of the soil profile induced by settlement of active pile j
Set i=1
Calculate the settlement field
$U_{kj,i} = \varphi(r_{kj}) w^e_{j,i}$
$\varphi(r_{kj}) = \ln(r_m / r_{kj}) / \ln(r_m / r_o)$
i=i+1
No
$i = n$
Yes
Settlement prediction of passive pile k
Divide the pile k into n segments,
Set the initial settlement at pile base
$w^b_{,n} = \Delta w^b = 0.001D$
Calculate the resistance at the base of pile, $P^b_{,n}$
$P^b_{,n} = a_b(1 - e^{-b_b w^b_{,n}})$
Start calculation from the bottommost section, i=n
Calculate the load and settlement at the top of segment i
$P^t_{,i} = \frac{1}{1 - \frac{2\pi G_{s,i} l_i^2}{8 E_p A_p \ln(r_m / r_o)}} \times \left[P^b_{,i} + \frac{2\pi G_{s,i} l_i}{\ln(r_m / r_o)} \left(w^b_{,i} + \frac{3P^b_{,i}}{8E_p A_p} l_i - U_{kj,i} \right) \right]$
$w^t_{,i} = \frac{P^t_{,i} + P^b_{,i}}{2E_p A_p} l_i + w^b_{,i}$
$w^b_{,n} = w^b_{,n} + \Delta w^b$
Transfer force and settlement to the next segment
$w^b_{,i-1} = w^t_{,i}$; $P^b_{,i-1} = P^t_{,i}$
Move to the next segment, i = i-1
i=1
No
Yes
$P^t_{,1} \geq 0$
No
Yes
Obtain the settlement of passive pile $s_{kj} = w^t_{,1}$
Return

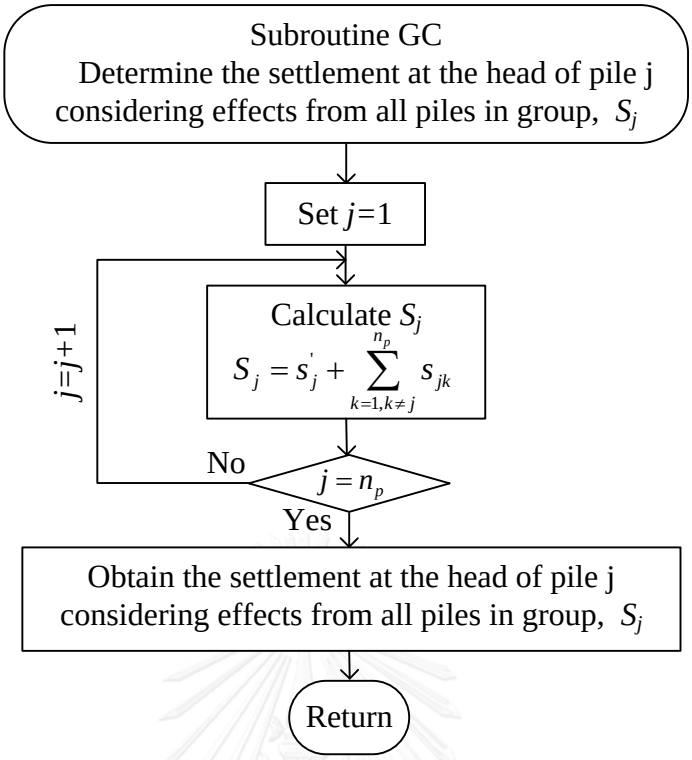

VITA